Model Stickiness in Spray Drying

Petersen, Thomas

Publication date:
2015

Document Version
Publisher's PDF, also known as Version of record

Model of Stickiness in Spray Drying

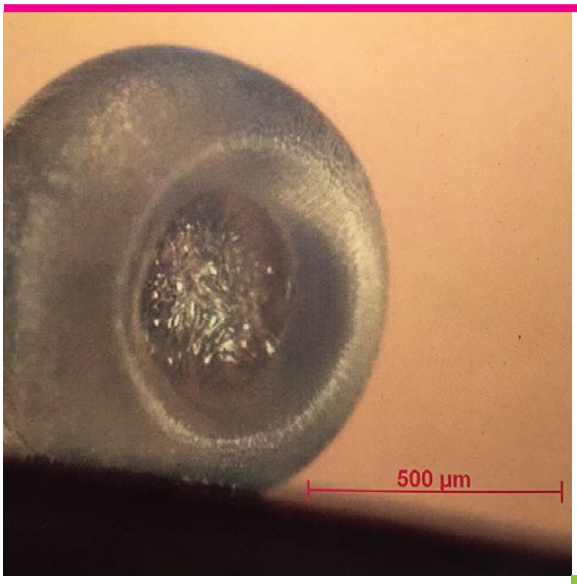

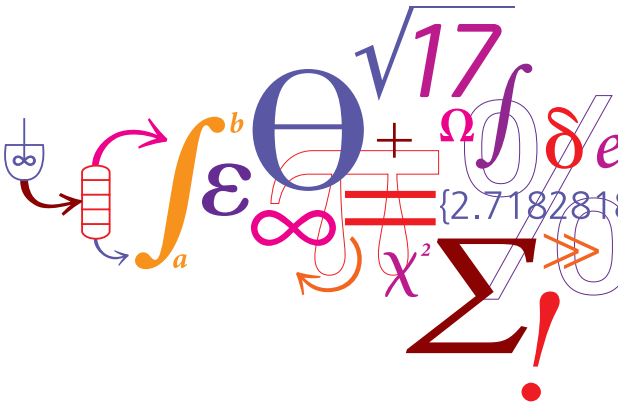

Thomas Petersen

PhD Thesis

August 2015

DTU Chemical Engineering
Department of Chemical and Biochemical Engineering

Technical University of Denmark
Department of Chemical and Biochemical Engineering

Model of Stickiness in Spray Drying

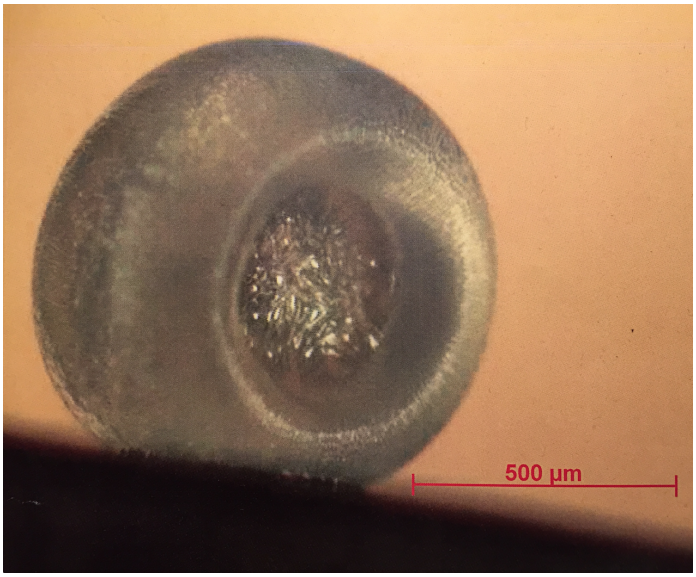

Ph.D. Thesis
2015

Author:
Thomas Petersen

Title Page

Project title:	Model of Stickiness in Spray Drying
Author:	Thomas Petersen

University:	Technical University of Denmark (DTU)
Department:	Department of Chemical and Biochemical Engineering
Address:	Søltofts Plads 227
	2800 Kgs. Lyngby
	Denmark

Company:	GEA Process Engineering A/S
Department:	Research and Development
Address:	Gladsaxevej 305
	2860 Søborg
	Denmark

Start date:	3rd of September 2012
End date:	31st of August 2015

Supervisors:	Professor Ole Hassager
	Jakob Sloth, Ph.D.
	Thorvald Ullum, Ph.D.

Preface

The present thesis was written in accordance with the partial requirements for obtaining a Ph.D. degree at the Technical University of Denmark (DTU). The project was carried out as a collaboration between GEA Process Engineering A/S and the Department of Chemical and Biochemical Engineering at DTU in the period between September 2012 and August 2015. The project was co-funded by GEA Process Engineering A/S and the Innovation Fund Denmark, the latter of which fund research projects carried out in cooperation between universities and industry in Denmark.

During this work I was supervised by Professor Ole Hassager of the Danish Polymer Center, a research group at the Department of Chemical and Biochemical Engineering and Jakob Sloth and Thorvald Ullum, both of the Test and Development Department of GEA Process Engineering A/S. I wish to express my sincerest gratitude to these three for their guidance, supervision and support throughout the project.

I also want to thank the many colleagues and friends I met during my work both at DTU and GEA Process Engineering A/S. These people made my time enjoyable but also served as sources of inspiration and feedback. In this thesis a significant amount of the work will be on a novel measurement technique and I here wish to extent my gratitude to two people not mentioned above who assisted significantly in relation to that setup. First is Anders Brask who build the original levitator setup before I ever started my project and who helped tremendously in modifying it to be able to produce stickiness measurements. Secondly is the technician Michael Bloch who helped me resolve more problems than I care to remember.

During my project I had the fortunate opportunity to spend a short time visiting Professor Gareth H. McKinley and his group at MIT. I wish to express my gratitude to these people as well for making me feel welcome and as a part of the group in spite of the brevity of my stay.

Finally I wish to thank my girlfriend, Naka Mazlom, for her impressive patience with me during this work and my family for their constant and unwavering support.

Abstract

The work presented in this thesis concerns wall deposits encountered in spray drying caused by products that exhibit so-called 'stickiness'. The thesis delves into the understanding of the phenomenon of sticky wall deposits in spray drying and proposes a simple criterion for use in industrial design of spray dryers.

The experimental work centers around a new technique for measuring when, during drying, a particle becomes non-sticky based on a single droplet drying technique used to study drying kinetics. An acoustic levitator is used to dry a levitated droplet in conditions similar to those a droplet would encounter in a spray dryer. The droplet is recorded using a CCD-camera during drying and the subsequent stickiness test. After a user-specified drying time a piston strikes the partially dried particle at a user-specified velocity. After the impact the piston surface is inspected and if the particle was sticky it is seen adhering to the surface, while a clean piston signifies a non-sticky particle. The setup was designed specifically to test the stickiness of a particle produced by drying a droplet of the desired feed - something unlike methods of literature where dry particles have been humidified before tests. The setup allowed for parameter variations in the temperature and humidity of the drying air, impact velocity, piston surface and more.

Results of measuring the stickiness of skim milk is reported for varying impact velocity, drying temperature and relative humidity. It is found that normalizing the critical drying time to get non-sticky particles with the initial diameter squared leads to a single value for a given set of parameters, if the initial diameter is in a limited range. The normalized critical drying time was found to increase linearly when increasing the relative humidity of the drying air. Furthermore, the dependency was the same independently of temperature. The drying time appeared to decrease linearly with increasing temperature, although with a smaller dependence. Measurements with increasing impact velocity showed that the required drying time increased linearly. This finding is opposite of what is typically reported in literature and it is an important part of the hypothesis for stickiness developed here. Finally, measurements with maltodextrin (with dextrose equivalent of 18) are reported for varying relative humidity and impact velocity and the same trends were shown as those found for skim milk.

Replacing the CCD-camera with a high-speed camera allows a user to produce videos of the impact of a sticky particle with a wall in very high temporal resolution. This was done for skim milk powder for varying impact velocity, humidity and piston surface material. The results were mostly qualitative, with a little quantitative analysis where possible. The first observation was that there was very little difference between a particle that just adhered (sticky) and one that just bounced (non-sticky). Both were forced to make some contact with the piston upon impact, deformed only slightly and then typically moved slightly away before either stopping with contact (sticky) or bouncing with no contact (non-sticky). Sticky particles had a large apparent contact angle, similar to what would

be expected for a liquid with poor wetting properties. The velocity did not seem to change this much, although slight deformation was seen when the impact velocity was at the highest used values. The phenomenon did not appear to change noticeable when the droplet was dried in a high relative humidity environment. The qualitative difference observable between Teflon and stainless steel was very limited. On Stainless steel the droplet seemed to wet slightly more after the initial impact while the contact area was constant for Teflon. Modelling work was carried out to help understand the phenomenon, but also to investigate how the impact scaled for particle size. This was done using the Level Set Method implemented in the Finite Element based COMSOL Microfluidics software. Using two level functions allowed for the definition of density and viscosity functions which were different throughout the particle and different from the surrounding air. This was used to model an inhomogeneous droplet which consisted of a skin with high viscosity and a core with lower viscosity. The surrounding air had an even lower viscosity and a lower density. The droplet was modelled without elastic properties. The simulations were initiated with the condition that the droplet was moving towards the wall with a predefined velocity. The simulation was run while individually varying initial droplet velocity, viscosity of skin, core and air, density of droplet and air, surface tension, droplet radius and the radius of the core relative to the droplet. A parameter analogous to the radius of the contact area was defined and the dependency of this parameter upon the ones listed above was mapped. The radius of spreading, normalized with the droplet radius, correlated with the square root of the Reynolds' number (based on material properties of the skin) multiplied with the volume of the droplet divided by the volume of the skin. A simple analytical model was used to show that this dependence on the Reynolds' number could be a result of viscous dissipation of kinetic energy in a zone near the movement of the triple line.

The observations made in the experimental and modelling sections were combined to propose a simple criterion for use in conjunction with other tools for design or possible control of spray dryers. A single droplet drying technique is to be used to obtain a characteristic drying curve for the product of interest. The linear dependencies found is then used to reduce the necessary number of stickiness measurements to as little as three (although more measurements increase accuracy). These data are then used to produce a simple criterion which gives a critical residual moisture content under which a particle must be for it to be non-sticky as depending on the relative humidity in which it is dried, the initial radius of the droplet and the velocity with which it impacts the wall.

Finally, the hypothesis for stickiness that this work leads to is summarized as follows. As a droplet is dried it forms a region near the surface in which the solvent concentration decreases and the viscosity increases. As it impacts a wall in the spray dryer it does so with some kinetic energy. The kinetic energy forces the wet particle to deform and wet the surface, while energy is dissipated in the viscous flow. If the viscosity in the surface region is high enough and the region is large enough the energy is dissipated with very little movement which means the contact area is small. A small contact area means a low

energy of adhesion and the particle is easily removed by other effects. If the energy is not dissipated rapidly enough however a larger contact area is established and the particle will adhere strongly. This hypothesis suggests that the surface properties of the sticky particle are not the only effects that matter and therefore that measuring rehumidified particles is not the same as dried droplets. Furthermore it has the important difference from the established hypothesis that the contact is forced and not spontaneous.

Resume

I denne afhandling præsenteres arbejde med afsætninger i spray tørring som følger af såkaldte "sticky" (klistrede) produkter. Afhandlingen repræsenterer et forsøg på at forstå det underliggende fænomen som giver afsætning og afsluttes med et forslag til et simpelt kriterie til brug i forbindelse med industriel spray tørring.
Det eksperimentelle arbejde omhandler en ny teknik til måling af hvornår en partikel er tørret tilstrækkeligt til at ophøre med at klistre. Teknikken er baseret på teknikker til måling af tørrekinetik for en enkelt dråbe. An akustisk levitator anvendes til at tørre en svævende dråbe i betingelser som hvis den blev tørret i en spray tørrer. Et kamera bruges til at optage dråben under tørring og den efterfølgende "stickiness" test. Når dråben har tørret i en af brugeren specificeret periode bruges et stempel til at slå til den delvist tørrede partikel med en brugerspecificeret hastighed. Efter sammenstødet inspiceres stemplet. Findes en partikel på stemplet regnes partiklen som havende været "sticky", men er stemplet rent regnes partiklen for at have været tør. Opstillingen var designet specifikt til at test partikler produceret ved at tørre dråber, modsat metoder i litteraturen hvor tørre partikler blev befugtet. Opstillingen tillader variation i tørreluftens temperatur og relativ fugtighed samt slaghastighed og stemplets overflademateriale med mere.
Målinger for hvordan "stickiness" af skummetmælk varierer med varierende slaghastighed, lufttemperatur og relativ luftfugtighed rapporteres. Indenfor en begrænset variation i dråbestørrelsen kunne den nødvendige tørretid for at få en partikel til ikke at klistre normaliseres med startdiameteren, hvilket gav en enkelt værdi for hver sæt af parametre. Denne normaliserede, kritiske tørretid steg lineært med stigende relativ luftfugtighed. Denne afhængighed af fugtigheden var konstant med varierende temperatur. Tørretiden så også ud til at variere lineært med temperaturen, men i meget svagere grad. Målinger med stigende slaghastighed viste at den nødvendige tørretid steg lineært. Dette resultat er i modstrid med hvad der typisk rapporteres i litteraturen og det er et vigtigt fund i forhold til hypotesen som præsenteres her. Endeligt blev målinger på maltodextrin (med DE værdi på 18) udført med varierende relativ luftfugtighed og slaghastighed og de samme tendenser som er nævnt ovenfor blev observeret.
Det anvendte kamera blev erstattet af et højhastighedskamera med hvilket optagelser af sammenstødet mellem en klistret partikel og en væg kunne optages med høj tidsopløsning. Dette blev gjort med skummetmælk med varierende slaghastighed, relativ luftfugtighed og stempelmateriale. Resultaterne var primært kvalitative, med kvantitativ analyse hvor det var muligt. Den første observation var at der var meget lidt forskel på en partikel som kun lige sad fast og en som kun lige sprang af. Begge blev tvunget i kontakt med stemplet i sammenstødet, blev deformeret lidt, før de typisk bevægede sig lidt væk fra væggen for så enten at stoppe med kontakt (klistret) eller springe af (ikke klistret). Klistrede partikler så ud til at have en høj kontaktvinkel ligesom en dårligt befugtende væske. Slaghastigheden ændrede ikke meget, men en øget deformering blev observeret ved de højeste værdier

undersøgt. Fænomenet ændrede sig ikke nævneværdigt i et fugtigt miljø. Ved målinger med Teflonstempel i stedet for rustfrit stål var de kvalitative observationer de samme med den lille undtagelse at efter selve sammenstødsdynamikken var afsluttet blev stålstemplet befugtet lidt yderligere, mens dette ikke skete ved Teflon.
Modelleringsarbejde blev udført med henblik på at forstå fænomenet, men også for at forstå hvordan sammenstødsdynamikken skalerede med partikelstørrelse. Modelleringen blev udført med den "Level Set" metode implementeret i det "Finite Element" baserede COMSOL Microfluidics software. To "level set" funktioner blev brugt sammen for at kunne definere densitets- og viskositetsfunktioner som gav forskellige værdier i forskellige dele af modeldomænet. Dette blev brugt til at modellere en inhomogen dråbe med et højviskøst skind og en mere flydende kerne. Den omgivende luft havde endnu lavere viskositet og en lavere densitet. Dråben blev modelleret uden elastiske egenskaber. Simuleringerne blev initieret med en brugerdefineret starthastighed for dråben i retningen af væggen. Simuleringerne blev kørt med varierende starthastighed, viskositet af skind, kerne og luft, densitet af dråbe og luft, overfladespænding, dråberadius og kernens radius relativt til dråbens. En parameter som var analog til radius for kontaktarealet blev defineret og dennes afhængighed af de ovenfor nævnte parametre blev kortlagt. Kontaktarealets radius, normaliseret med dråbens radius, gik som kvadratroden af Reynoldstallet (baseret på skindets materialeparametre) ganget med dråbens volumen divideret med skindets volumen. En simpel analytisk model blev brugt til at vise at denne afhængighed af Reynoldstallet kan opnås ved viskøs dissipering af kinetisk energi i et område nær en tripellinie i bevægelse.
Observationerne fra det eksperimentelle og modelleringsbaserede arbejde blev kombineret til at foreslå et simpelt kriterie som kan bruge i samarbejde med andre værktøjer i forbindelse med design og muligvis kontrol af spraytørrere. En karakteristisk tørrekurve produceres med en passende måleteknik for produktet som skal tørres. De lineære afhængigheder anvendes til at reducere antallet af nødvendige "stickiness"-målinger til tre, selvom flere målinger kan foretages hvis øget præcision er ønsket. Disse data kan bruges til at producere et simpelt kriterie som giver en kritisk restfugt som en partikel skal under for ikke længere at kunne sætte sig på en væg. Den kritiske restfugt afhænger af den relative luftfugtighed dråben er tørret i, dråbens startradius og den hastighed hvormed den rammer væggen.
Endeligt kan den "stickiness" hypotese som dette arbejde leder til opsummeres som følger. Når en dråbe tørres dannes en region nær overfladen hvor opløsningsmidlet falder i koncentration og viskositeten stiger. Når partiklen rammer en væg gør den det med en kinetisk energi. Denne energi tvinger den våde partikel til at deformere og befugte overfladen mens energien dissiperes ved viskøs strømning i partiklen. Hvis viskositeten er høj nok og det omtalte område hvori dissipation foregår er stort nok dissiperes energien ved meget lille deformering og et lille kontaktområde etableres. Dette betyder lav sammenhængskraft og partiklen falder nemt af ved hjælp af andre effekter. Hvis energien ikke dissiperes hurtigt nok dannes et større kontaktområde og partiklen sidder bedre fast. Denne hypotese

betyder at partiklens overfladebetingelser ikke er tilstrækkelige til at bestemme om den sætter sig og derfor at målinger for befugtede partikler og tørrede dråber er forskellige. Derudover er der den vigtige forskel at kontakten er tvungen og ikke spontan.

Contents

Nomenclature List

Latin

d	Diameter
C	VOF function
F	Force
g	Gravitational acceleration vector
k	Gordon & Taylor constant
K	Arbitrary constant
m	Mass
p	Pressure
Q	Heat flow
r	Radius
R	Droplet or particle radius
S	Source term
t	Time
T	Temperature
T_g	Glass transition temperature
v	Linear velocity
V	Volume
$\mathbf{v}$	Velocity vector
w	Weight fraction

Greek

β	Radius of core divided by radius of droplet
γ	Surface tension
θ	Contact angle
η	Viscosity
ρ	Density
τ	Time constant
$\boldsymbol{\tau}$	Viscous stress tensor
ϕ	Level function

General Subscripts

a	air
app	Applied
br	Bridge
c	core
$comp$	Unspecified compound
eff	Effective
g	At glass transition
imp	Impact
l	Liquid
p	Particle
s	Skin
so	Solid
sl	Solid-liquid
spr	Spreading
w	Water

Non-dimensional Parameters

Nu	Nusselt number
Pr	Prandtl number
Re	Reynolds number
Sc	Schmidt number
Sh	Sherwood number

1 Introduction

1.1 Spray Drying

Spray drying is a widely used industrial process. It allows the formation of a dry powder, that can easily be handled, from a liquid feed with dissolved or suspended solids. Drying is used in many processes in order to extend the shelf-life of food and dairy products, to make easier (and cheaper) the transport of goods, to remove solvent from a chemical or for one of several other reasons. Spray drying does this while forming a uniformly sized powder that is readily re-dissolved, it does it rapidly and at temperatures that are not extremely high. The latter means that in many cases even sensitive products can be dried without causing damage to the final product.
In this chapter a brief introduction to some small parts of the rich history of the technique will be given followed by a short description of the technique today. After this a more detailed introduction to drying - both experimental studies and modelling - will be given, as it will be referred to multiple times throughout the thesis.

1.1.1 A Look Back Through Time

The first mention of spray drying seems to be for egg-handling around 1865 ([Mont, 1865]), but typically the first detailed description is credited to Samuel Percy for his patent "Improvements in Drying and Concentrating Liquid Substances by Atomizing". The patent contained no drawings but the description referred to "atomizing" of a "fluid or solid substance" after which it would be dried in a gas ([Percy, 1872]).
While several smaller innovations were described in literature it was only in the 1920's and 1930's that the technique began to see widespread industrial application. Many innovative concepts were suggested around this time making the process conceptually similar to what is in use to this day. The relative lack of in-depth knowledge however meant that operation was far from the economic or stability levels obtainable today.
During the Second World War the need for food that could be easily transported and remain unspoiled for long periods of time lead to an increased use of spray drying - especially for dried milk. The dryers became larger during this period and the process knowledge grew significantly leading to better and cheaper operation.
Following the war many innovations saw the light of day. In the 1960's the innovations included rotary atomizers capable of atomizing abrasive feeds which meant spray drying became widely used in bulk chemicals and mining industries. This decade also saw the introduction of spray dryers with very high inlet temperatures, which made dryer sizes much bigger than those previously used possible. The 1970's saw further innovations in high capacity dryers and it was in this decade the multistage drying was introduced. This concept entailed the separation of the drying process in a spray dryer and fluidized bed dryer which allowed increased capacity, efficiency and new ways of controlling the powder

properties. This was further developed in the 1980's when the fluid bed was moved into the spray dryer room itself. [Masters, 2002]

1.1.2 A Process Description

In the following a very basic description of the actual process itself will be given. Spray drying can in a very simplistic way be divided into the following steps: Atomization of the feed, drying of the droplets and exiting the drying chamber. The description will be made with reference to figure 1.

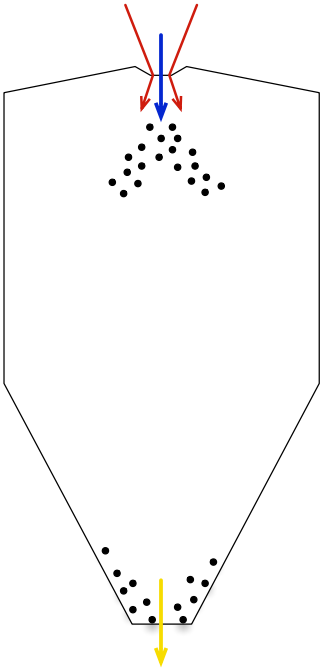

Figure 1: Sketch of spray dryer. The feed is drawn in blue, the drying air inlet in red and the powder exit in yellow. Air outlets can be in many places, here with the powder outlet.

Atomization

The atomization of the feed is vital to the process as hinted at in the historical section. This is what allows for the rapid drying because of the large surface-to-mass ratio of the droplets. Atomization is accomplished as the feed enters the drying chamber and occurs at the top of the chamber (see figure 1).

The mechanism of atomization in spray drying remains a topic of some discussion as it is a very complex mechanical process. The liquid forms a jet shortly after it leaves the atomization device (see below) and is subject to instabilities of different kinds promoted

(a) Rotary **(b) Nozzle**

Figure 2: Examples of atomizers. Copied from GEA Process Engineering A/S advertisement resources.

by the device, both internal and on its' surface, which lead to the jet breaking up into miniscule droplets.
The devices used for atomization vary, but two of the most popular ones will be described briefly here - see figure 2. Figure 2a shows a rotary atomizer. It basically consists of a wheel with holes on its' circumference. The feed enters from the top and the wheel rotates rapidly, hurling the liquid inside it through the holes and into the drying chamber. Figure 2b shows a nozzle atomizer. The feed is pressurized and sprayed from the nozzle. An alternative version is the two-fluid nozzle in which an air current is brought into contact with the feed stream thus causing instabilities leading to atomization. In the two-fluid nozzle the pressure can be much smaller because of the instability from the air current. [Masters, 2002]

Drying

As the feed enters the drying chamber the drying is initiated. The small size of the droplets ensure a large contact area relative to the mass to be dried, allowing for rapid drying. The drying room is designed to the extent possible such that the air currents carry the droplets for long enough for them to be dried to particles. The drying process itself will not be described in detail here, but the topic is covered in more detail in section 1.2. It will be stated here for the sake of clarifying semantics throughout this report that the word 'droplet' are used when the surface is still wet, 'wet particle' is used when the surface is dry enough to appear solid and 'dry particle' refers to a particle that is, as near as makes no difference, dry throughout. These three names help us discuss droplets and particles in drying, but even they are insufficient because the transitions between them are not instantaneous. Keep in mind, always, that a wet droplet changes along a continuum until it finally becomes a completely dry particle.

Exiting the Chamber

The final bit of the process as described here is that the particles have to exit the chamber and be collected. Assuming the droplets dry sufficiently to form particles (often they are still wet at the core) the particles will at some point hit the inside of the drying chamber's walls and roll or fall towards the bottom where there is an outlet. The drying air, now colder and more humid, may exit the chamber in different ways depending on the chamber design, either through outlets on the chamber roof, sides or with the powder at the bottom. No matter which air outlet is employed, some air will escape with the powder and separation must be performed. This is typically done with cyclones or bag filters, but more on this topic can be found elsewhere. [Masters, 2002]

1.2 Drying Kinetics and Modelling

The way a droplet dries is obviously at the very center of understanding spray drying. In this section a description of experimental methods for studying single droplet drying (SDD) will be given after which an overview and discussion of some models for this process will follow. Because spray drying is such a rapid process many studies have shown that inhomogeneities appear. In the following discussion some focus will be on the possibility of describing the solvent concentration profile through the particle as a function of time. This includes the formation of a skin or crust on a wet particle. The reasoning for this focus should also be clear later in this work, when stickiness is discussed in more detail.

1.2.1 Experimental Drying

Drying kinetics have been studied by many researchers and the experimental techniques used are many. The single droplet drying (SDD) systems will be described first and in most detail as these methods are the most popular for studying drying kinetics in spray drying [Fu et al., 2012]. These can be separated into at least three different groups: Free falling droplets, acoustically levitated droplets and droplets suspended on filaments.

The method of observing freely falling droplets allows for controlled drying conditions very similar to that of spray drying, but typically with larger droplets (a trend for all SDD methods). The biggest weakness of the method is the great difficulty in observing the droplet as it dries but the method also requires a very large set-up. The method consists of generating a series of uniformly sized droplets and allowing them to fall through a heated gas in which drying occurs ([Kinzer and Gunn, 1951] [El-Sayed et al., 1990] [Vehring et al., 2007]). The generation of the droplets is typically done by using a pulse controller and a piezoelectric ceramic component (details can be found elsewhere). This way of producing droplets cannot be fitted to the two other SDD methods as they produce a series of similarly sized droplets rather than a singular one. The method has also been fitted with multiple inlets and used in the pharmaceutical industry in which the ability to produce almost perfectly uniformly sized particles is valued while the decreased cost

efficiency is not a big concern ([Amelia et al., 2011] [Wu et al., 2011] [Liu et al., 2011]). It is unsuitable for studying crust formation because the droplet shrinkage and morphology cannot be actively studied as it dries.

The droplet levitator is a prominent technique (a version is described in detail in section 3). This method counts amongst its' advantages that it is non-intrusive and that it is easy to observe the droplet during drying. The disadvantages are that the droplets are typically an order of magnitude larger than the droplets in a spray dryer and the contribution to drying from the ultrasonic waves in the acoustic levitator which lead to discrepancies between experiment and real-world application. The latter can be minimized if the droplet is subjected to convective drying. The setup consists of an ultrasonic actuator and a convex reflector. The actuator produces an ultrasonic wave which is reflected to produce a standing wave. This standing wave produces local pressure nodes. A droplet of a mass in a suitable range can be levitated on such a pressure node against the gravitational pull. The technique of levitating a droplet or sphere on an acoustic wave was theoretically described as early as 1934 ([King, 1934]) and demonstrated experimentally in 1981 ([Leung et al., 1981]). A detailed description of the technique including both theoretical and experimental details are given by Lierke ([Lierke, 2002]). Uses of the technique for drying include those by [Sloth et al., 2006] who modelled the drying of a droplet in a levitator with the specific purpose of predicting drying rates in spray drying. [Kastner et al., 2001] presents the challenge of measuring the mass loss during drying in an acoustic levitator well. They separated the drying into two stages for which the drying rate was evaluated quite differently. In the first stage the droplet shrinks and the shrinkage rate was measured to obtain the drying rate in this stage. In the second stage when the diameter of the wet particle remains fixed the drying rate was estimated from the changes in position in the acoustic field. As the particle dried, the mass would decrease and the particle move up in the field. This is assuming the particle density remains homogeneous, but because of effects like sedimentation this is not always the case. In another attempt to solve this problem Groenewold and co-workers ([Groenewold et al., 2002]) added a dew-point temperature measurement to the outlet gas to determine the actual drying rate more accurately, but such a solution is only effective if the set-up is designed in a specific way in which all drying air exits along the same path (the system can have only one opening and no leaks).

The filament based method has the richest history and is the focus of the review by Fu and co-workers ([Fu et al., 2012]). This method is intrusive and consists of suspending a droplet from a thin filament of capillary tube typically made from glass ([Ranz and Marshall, 1952a] [Ranz and Marshall, 1952b]). It is typically estimated that because of the small size of the filament compared to the droplet the filament's contribution to heating is smaller than 1%. It is uncertain to what degree the intrusive nature of the method affects the morphology and composition of dried particles. This method has the advantage that it quite easily allows for measurement of the droplet mass during drying by connecting the filament or capillary tube to an external micro-balance ([Sano and Keey,

1982]). The well-known Ranz-Marshall equation for heat and mass transfer was found using this particular setup:

$$Nu = 2 + 0.60Re^{\frac{1}{2}}Pr^{\frac{1}{3}} \tag{1}$$

$$Sh = 2 + 0.60Re^{\frac{1}{2}}Sc^{\frac{1}{3}} \tag{2}$$

Later [Lin and Chen, 2002] improved the method, which allowed them to obtain a more accurate relation at high mass transfer fluxes ([Lin and Chen, 2002] [Woo et al., 2011]):

$$Nu = 2.04 + 0.62Re^{\frac{1}{2}}Pr^{\frac{1}{3}} \tag{3}$$

$$Sh = 1.63 + 0.54Re^{\frac{1}{2}}Sc^{\frac{1}{3}} \tag{4}$$

Another improvement was reported by Kwapinski and Tsotsas using a magnetically suspended balance, thus making it less susceptible to disturbances from the drying air ([Kwapinski and Tsotsas, 2006]).
The technique appears to be the most popular SDD method used in the literature, most likely because it is easier and cheaper to set up than the acoustic levitator setup, while still allowing for observation of the droplet during drying.
Many other methods for studying drying behavior exists however these are often less relevant for the study of spray drying. A few however appear interesting specifically when the formation of a skin or crust is to be studied. An example is the microwave drying of milk in Petri dishes in order to study skin formation carried out by Kentish and co-workers ([Kentish et al., 2005]). In their paper they measured the drying rate of various milk formulations while measuring the surface temperature and mass loss of the sample. They found that the diffusion of larger molecules from the surface as water diffused towards the surface was the important factor in the formation of the skin. Skin formed earlier on formulations with less lactose presumably because lactose diffuses more rapidly from the surface compared to the fat and proteins of the milk, thus keeping the droplet more homogeneous. Some researchers have reported that milk powder with higher lactose content is, in general, found to be more sticky and these skin growth effects may be part of an explanation for this. This will be discussed more in section 2.
Another example of a similar method was demonstrated by Shimokawa and coworkers ([Shimokawa et al., 2011]) who studied the skins formed on polymer solutions during solvent evaporation. This method allow the study of the material properties of the skin as well as the time of formation and growth rate of the skin. The skin thickness and properties was studied by placing a blade above a polymer solution after a set drying time and applying a voltage to the blade, thus generating an electric field that pulls at the sample surface. The deformation of the surface is measured by directing a series of lasers towards the surface and measuring the deflection of these.
Finally a review of processing of experimental drying data by numerous authors will be

mentioned ([Kemp et al., 2001]). This review is not an in-depth discussion of the experimental techniques themselves but rather the specific analysis of the data obtained, independently of the method used. The work is notable for a short rundown of interpreting experimental drying data and advise on the topic.

1.2.2 Drying Models

As suggested in a review by Mezhericher and coworkers ([Mezhericher et al., 2010]) drying models can be separated into a few different groups. First the authors suggest separating the models into those for drying of solutions (pure liquid) and those with droplets containing insoluble solids (basically a suspension). This will not be done specifically here as the conceptual description given requires no such thing, but in a more in-depth study this would be an improvement to consider. The models are divided further into the semi-empirical characteristic drying curve (CDC) models ([Langrish and Kockel, 2001] [Strongin and Borde, 1987]), highly deterministic models of mass and energy balances or population balances (the latter is only for models with insoluble solids) ([Sano and Keey, 1982] [Brenn, 2005] [Mezhericher et al., 2007]) and the reaction engineering approach (REA)([Chen and Lin, 2005]). The CDC models basically consist of semi-empirical fits to drying data obtained from SDD experiments. The main advantage of the CDC method is the relative simplicity while the disadvantage is that the models typically extrapolate poorly from the conditions the original measurement was taken at, which means the method demands significant experimental work to model wide parameter spaces (if that is required). The more rigorous deterministic models have the advantage that they are based on real physical phenomena known to occur, thus they can reproduce many physical events to greater accuracy. A problem however is that they typically involve a significant number of parameters (e.g. for materials) which are unknown and difficult to measure, thus requiring fitting. Finally the REA models are fairly recent and resemble the CDC methods in that they are semi-empirical and measurements for each material to be dried must be made for the models to be used. Some publications ([Patel and Chen, 2005]) suggest that these models do better for extrapolating across drying conditions than the CDC models. It appears that the more detailed deterministic models are the strongest tools for understanding when and how the crust forms and how it develops, but in many ways weaker for practical applications. From knowledge obtained with these models it may also be possible to determine identifiers in the simple models that specify when the crust is formed and how it grows. Some care should be taken though as using a model describing the wrong phenomena could easily lead to erroneous results that actually hide the true phenomena. Before delving a little more into examples of the model types listed above, a short mention of a common scaling of drying and when it breaks down. For drying of a droplet of pure solvent, i.e. evaporation, in a still chamber (no convection) the drying rate is proportional to the surface area. This means that under such circumstances the rate of change of the

diameter squared is constant or:

$$\frac{\partial d^2}{\partial t} = constant \tag{5}$$

This allows for very simple scaling of the drying of droplets across different sizes, however, the rule rather easily breaks down. The observation of the relation and its' breakdown has been made by several researchers, including [Law and Binark, 1979], [Law et al., 1986], [Annamalai et al., 1993] and [Renksizbulut and Bussmann, 1993]. Reasons this simple scaling can break down includes convective drying (both forced and natural), other component at the surface of the droplet (condensed water if the solvent is not water or non-volatiles in the droplet) and many other factors. It does however provide a nice and simple way to start, when scaling drying of droplets.

A full analytical solution of a simple formulation of the concentration profile inside a droplet during drying was presented by [Brenn, 2005]. The model consisted of solving the diffusion equation inside a shrinking particle with a constant initial content and a solute that remains in the particle while the solvent evaporates. The solution gave physically feasible results however crust formation - which is considered important here - is not considered explicitly. Brenn's model may still be relevant to this work as it probably described the drying after early precipitation and before crust formation in a way that yield acceptable accuracy for a general understanding of the drying process even if limited quantitative precision.

Mezhericher and co-workers developed an advanced model separating the drying into numerous stages, namely initial heating, drying from the droplet surface and drying of a particle with a porous crust covering a wet core ([Mezhericher et al., 2007]). In the model complex heat transfer phenomena was considered with relatively few explicit considerations for mass flow. This is to say that mass flow is determined by the rate of heat transfer to the position at which evaporation is occurring (depending on the drying stage). In the third stage the diffusion of water vapour through the crust is modelled explicitly. The model is solved numerically and compared with filament SDD experiments perform by Lin and Chen with good results ([Lin and Chen, 2002]). This model appears fairly complicated to solve however it does propose a model that can describe the growth rate of the crust but the appearance of the crust must be determined empirically.

A study of drying in an acoustic levitator and a simple model of drying was reported by Yarin and co-workers ([Yarin et al., 2002]). They too separated the drying into two stages - one in which the droplet shrunk and one in which it retained its' size. They formulated a simple mathematical model for the first stage and suggested that the point separating the two stages was where the crust was formed. This makes sense physically and may suggest that a locking point at which crust is formed can be determined directly from SDD data. A good qualitative description of this is given in Tsotsas ([Tsotsas, 2012]).

Crust formation on polymer films has been studied by [de Gennes, 2002]. A simple qualita-

tive model of the formation of a glassy crust and the thickness of the crust was formulated. The time for formation of a crust is not included however which makes the model less applicable to the problem described in this thesis however a simple expression of the crust thickness was given as. It is not discussed how this thickness compares to experiments This may be a simple way to determine the crust thickness for an arbitrary droplet during drying, however this model has numerous parameters that are not readily available, which again complicates application.
[Okuzono et al., 2006] published a simple model for skin formation during solvent evaporation (drying) of a polymer solution. The model was for a planar geometry and not a spherical droplet and made the assumption that the skin was a gel with a very large diffusion coefficient (i.e. the solvent concentration is constant through the skin) which are both significant deviations from the situation relevant to this particular study. The model contained both analytical derivation of conditions of skin formation and a speed of growth for the skin after formation as well as a numerical model used for validation of the analytical model. The equations derived in the paper are not directly applicable but the general methodology - especially for skin formation - might be applicable. The same group published numerical simulations of higher detail in another paper ([Ozawa et al., 2006]). A recent work by the same group used this knowledge of skin formation to study morphological changes during drying. A model for the formation of cavities inside droplets of polymer solutions during drying has been produced ([Meng et al., 2014]). This model itself is not directly applicable in the problem studied in this thesis but it does show that models for skin and crust can be used to understand other important phenomena in particle formation during drying.

1.2.3 Summary of Drying

The drying of a droplet in a spray dryer is typically separated into a number of steps as follows (some of which are only included in some models):

- Early heating stage. In this stage the droplet is heated with little or no evaporation occuring. Typically this stage is considered to occur very fast and is often omitted in modelling. If the feed is preheated the brevity of the stage is emphasized.

- First drying stage. In this stage drying occurs from the surface of the droplet. Heat and mass is transferred to and from the surface through a boundary layer. This stage ends when the concentration of the product on the surface of the particle becomes so large that a skin or crust can be formed. Describing this phase is relatively easy and the drying rate scales with the droplet diameter squared. Figure 3A visualizes this stage.

- Second drying stage. Once a crust or skin has formed on the droplet it is typically referred to as a wet particle. The actual evaporation is considered to occur on the

boundary between the wet core and the crust in the case of a dry crust. The drying is limited by the rate of vapour diffusion out through the crust. The crust grows throughout this stage, gradually decreasing the drying rate. In the case of a skin, evaporation is still considered to occur from the surface, but is significantly impeded by the large diffusion resistance in the skin thus reducing the availability of solvent on the surface. The second drying stage ends when the core radius reaches zero and the particle is now referred to as a dry particle. Figure 3B visualizes this stage, in the case of a crust.

- Final heating stage. The now dry particle is rapidly heated to a temperature at which the dry particle is in equilibrium with the surrounding air. This is often considered to occur very rapidly as no heat is consumed in evaporation. The final heating is often neglected as it is technically after drying has finished and it is mostly irrelevant here as the particle should be long past the sticky region (see section 2). In the case of slow drying, the heating will also occur during the second drying stage.

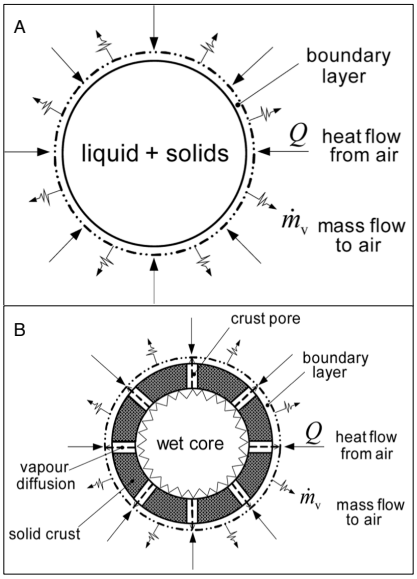

Figure 3: Sketch of the two primary drying stages. A: First drying stage in which evaporation occurs from the surface of the droplet, causing the droplet to shrink. B: Second drying stage in which the solvent evaporates from the core-crust interface and diffuses through the crust. Adapted from [Mezhericher et al., 2007].

Crust is mentioned in most papers and so a hypothesis that it is connected to particles becoming non-sticky is a natural one. Furthermore the observations made by Kentish and co-workers ([Kentish et al., 2005]) that higher levels of lactose in milk delays the formation of a crust coupled with the observations made in numerous studies of stickiness

(e.g. [Paterson et al., 2007], but more in section 2) that it occurs more frequently for products with increased lactose contents lends further credibility to such a hypothesis.

1.3 Wall Deposits

As stated initially, spray drying is a very well-known process with a long history, but some challenges still remains. Discovering the root of a problem in a spray dryer or the phenomena causing it can be very difficult because the system is so complex and measuring on the system without disturbing it is nigh impossible in many cases, which may be the reason the remaining challenges do remain. One such challenge is that of wall deposits ([Masters, 1996]). Two examples of wall deposits are shown in figure 4.

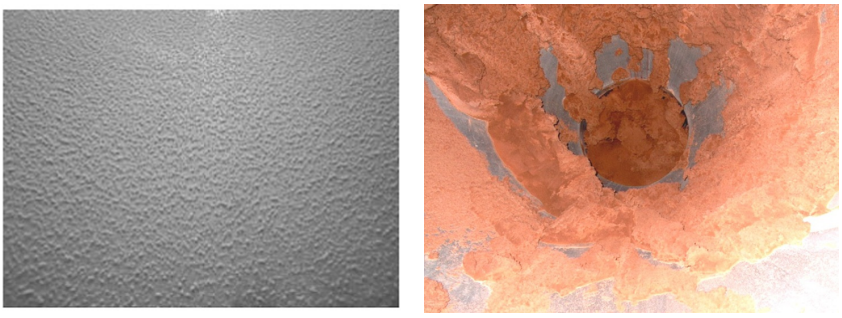

(a) Light deposits, sucrose-maltodextrin mixture. (b) Heavy deposits, tomato pulp.

Figure 4: Examples of wall deposits. The left hand side figure is an example of light deposits of a sucrose-maltodextrin mixture obtained in a pilot scale dryer ([Woo et al., 2008b] and the right is deposits of tomate pulp taken by an employee at GEA Process Engineering A/S (internal source).

Wall deposits can be caused by several phenomena, which will be covered in section 2 but a little will be said here. Both examples of deposits shown in figure 4 show real deposits in spray dryers. Figure 4a show only light deposits and if this is all that adheres to the walls it is likely that production could be continued with no significant issues. If however production is continued and a situation as the one shown in figure 4b results, production must be stopped for cleaning. Thus, wall deposits have a number of negative outcomes. Here, a few reasons why deposits on the chamber walls are undesirable will be discussed. Then the reasons one would not typically be satisfied with the obvious response to wall deposits, namely cleaning, will be discussed.
The products deposited on the walls are inside the drying chamber for significantly longer than they were supposed to, had the particles left the system as planned. This can lead to a number of undesirable effects including (but not limited to) product degradation, crystallization of certain compounds and ignition leading to dust explosions. It is obvious that the two first can lead to subpar products which will hold smaller value to the end-

costumer while the third is a serious risk that can lead to injury to personnel or damage to equipment and should be avoided at all times. It is also easy to imagine that once deposits reach a level comparable to that of figure 4b the outlet hole will plug sooner or later, effectively stopping the production completely.
Should wall deposits appear, an operator is thus likely to want to avoid the scenarios mentioned above and is therefore forced to stop the production to clean the chamber and other equipment that may have been affected. For the duration of shut-down, cleaning and start-up no feed is dried. This down-time is a significant cost because no new product is obtained, incoming feed (if this cannot be stopped) must be scrapped - leading to increased marginal cost of operation unless the feed is free - and of course the cost of cleaning itself. While this does not pose the same safety risk, the cost can be quite considerable which makes these stops extremely undesirable.
It is for these reasons wall deposits must be avoided, however this is not easily achieved. In the historical overview at the start of this chapter conservative operation was mentioned however this becomes quite costly, which makes it a poor choice if it can even be considered a real one. Another path that has been followed is the continual removal of deposits before they build up. This has been done using numerous tools including, but not limited to, pneumatic hammers that automatically, with controlled intervals slam the chamber walls from the outside thus shaking loose deposits or air brooms that move across the inner wall to blow off particles loosely adhered to the wall. These tools however are not great solutions as they cannot remove strongly adhering deposits and because they may disturb the production (as in the case of the air broom).
An alternative to these two options is to design your spray dryer in an optimal way so that it remains cheap but is constantly running on the edge, right before deposition of product is initiated. This however, requires a fundamental understanding of the phenomena leading to wall deposits and thus the topic of this thesis is justified.

2 Stickiness Fundamentals

Having established in the previous chapter that avoiding wall deposits is desirable, understanding these wall deposits is the goal. In this section wall deposits and the phenomena that may lead to it will be discussed. This will start with a description of the types of wall deposits one may encounter during spray drying and it will lead to a discussion of the concept of "stickiness". This concept will then be described in further detail as it appears in literature, including the most important measurement techniques and the current hypothesis used to describe this phenomena.

2.1 Types of Wall Deposits

Wall deposits may appear for a number of different reasons, depending on the product, drying conditions, particle size etc. Among these are a few which will only be mentioned briefly. Effects that are distinctly different from the problem of stickiness is of little interest right here, even if they may in some very unfortunate cases combine with sticky particles to cause great problems for an operator. Such effects include the deposits which would be caused by very wet droplets. Consider a spray nozzle which for some reason is unclean. It may be effectively dysfunctional and spray the droplets almost directly onto a wall, which would lead to deposits, but not caused by what is typically referred to as stickiness. At the other end of the spectrum it is possible that a dry particle which is very light would lay on the wall instead of rolling out simply because the friction between it and the wall dominate the gravity and drag pulling at it to move. This too could be a catalyst for sticky deposits, but is, on its' own, unrelated.
The smallest of droplets dry rapidly, meaning they should be the easiest to handle. In fact this is often used in different ways in spray dryers. In spite of this some of these smallest particles may adhere to the wall even after completed drying. Two different forces that may contribute to this adherence of small, dry particles are Van der Waals' and electrostatic forces.
The so-called Van der Waals' forces or interactions are the sum of forces between molecules - including both attractive and repulsive - not caused by covalent or hydrogen bonding or electrostatic forces. Schubert showed that the attractive force between two rigid, smooth spheres increases with the inverse square of the distance separating them ([Schubert, 1987]). Papadakis and Bahu reported that the attractive Van der Waals' force were twice as large between a sphere and a wall compared to the force between two spheres and that the force was further increased when the two solids were separated by a film of liquid ([Papadakis and Bahu, 1992]).
Friction between particles and equipment wall can charge the particles, which may give rise to electrostatic forces. Such charging is more prevalent when the particle contains insulators such as lactose and glucose ([Jonassen, 1998]). Schubert reviewed equations for calculating the adhesive effects from electrostatic forces based on Coulomb's Law and

found that under realistic conditions electrostatic forces were of less consequence than the Van der Waals' interactions for small particles and that neither mattered for large particles ([Schubert, 1987]). Ozmen and Papadakis have found that grounding the equipment, which should reduce the significance of electrostatic effects, has had little or no effect on the amount of wall deposits ([Ozmen and Langrish, 2003], [Ozmen and Langrish, 2005]). This suggests that electrostatic forces in general are a minor concern. Furthermore particle adhered by electrostatic forces alone are typically easy to remove because the forces are relatively small ([Masters, 1996]).

In general it has been found that the intermolecular and electrostatic forces becomes significant for particles with diameter smaller than 5 microns ([Walton and Mumford, 1999]). This also means that for most spray dried particles it is unlikely that they are the major cause of wall deposits.

Above, types of deposits which may be encountered with wet droplets and dry particles are discussed, however as stated previously there is a transition zone between wet droplets and dry particles, namely wet particles. For these, a different kind of wall deposits may be encountered. In the literature and industry this is referred to as stickiness (the references to this are too numerous to list, but for examples see the reviews by Langrish - [Langrish and Fletcher, 2003] and [Langrish, 2007]). Stickiness occurs with particles that have dried for some time, so they no longer spread on the wall upon impact but retain their shape - as seen in figure 4a.

Stickiness is actually a term used very generally in literature, not just for wall deposits in spray drying. It is an important mechanical property of materials and foods of many various kinds, even if it is at times a rather poorly defined one. Depending on the application it can be either desirable (adhesives, "mouth-feel" of some foods etc.) or undesirable (during processing and packaging) making it a point of interest for researchers of many kinds ([Michalski et al., 1997]).

Numerous reviews have been presented on stickiness in spray drying specifically. Wall deposits and agglomeration have been mentioned as major research areas within spray dryer design and modelling by [Masters, 1996], [Masters, 2002], [Langrish and Fletcher, 2003] and [Langrish, 2007]. Many authors refer to the lecture given by Masters ([Masters, 1996]) where he summarizes the history of spray drying, detailing much of the efforts throughout time to minimize the degree and impact of wall deposits. Herein he also stressed the advantage that detailed understanding could have during design, around which this thesis is centered.

For spray drying both adhesive and cohesive effects can be important in determining the amount of wall deposits. Avoiding the initial deposits by adhesion is important but once these have appeared, cohesion becomes dominant and wet and/or sticky particles will accumulate.

Also of importance when discussing stickiness in spray drying is agglomeration of particles. This occurs when two particles impact and their cohesive properties results in the

two particles sticking to one another. Note once more that agglomeration can be both desirable and undesirable depending on product and application.

2.2 Measurement Techniques

In the following the most important stickiness measurement techniques will be reviewed. Other reviews have been published where many of the following methods are also listed. Good examples of these are [Adhikari et al., 2001], [Boonyai et al., 2003] and [Michalski et al., 1997]. [Peleg, 1977] also included reviews of some characterization methods and while it does not include any of the more recent methods it does contain interesting discussion of older methods. Most methods discussed below are conceptually similar. A sample at controlled conditions is subjected to some form of mechanical stress and the reaction is observed. The conditioning is done in many ways, but as should be clear after reading the review, almost none consist of actually drying liquid droplets. The mechanical stress can take a variety of forms such as shearing, stirring, air blowing or literal impact with a wall. The reaction observed too may be many things e.g. measuring the force required to accomplish something or measuring the weight of material adhered to a surface.

2.2.1 Stirring Method

The first method (chronologically) for measuring stickiness with reference to spray drying may very well be the stirring test. It was first introduced by Lazar and coworkers ([Lazar et al., 1956]) in analysis for drying of tomato pulp and has since been used by other researchers to determine what they called the "sticky point". This is also why it is referred to as the "sticky point method" or even "sticky point temperature method" in some literature. The concept is to keep the sample in a sealed container at a known moisture content keeping the container in a water bath at known, controlled temperature. The sample is stirred by hand and at some point the force required to turn the stirrer would increase sharply and this is what they referred to as the sticky point. Amongst other notable uses of this method are [Downton et al., 1982] who used it to measure the stickiness of mixtures of sucrose and fructose, [Wallack and King, 1988] who used it for measuring maltodextrin/sucrose/fructose mixtures and [Chuy and Labuza, 1994] who used it for dairy powders. Based on this method several authors has suggested a relation between stickiness and viscosity (more on this in section 2.3).
Advancements on the method was added later in the form of mechanical stirring originally introduced by [Brennan et al., 1971] for measuring orange juice and later used for dairy powder by [Hennigs et al., 2001] and [Özkan et al., 2002]. Note that [Özkan et al., 2002] compared skim milk powder and whole milk powder and found skim milk powder to be the most sticky, which corresponds well with the most common findings. [Kudra, 2003] further advanced the technique by changing the setup such that the relative humidity over the sample could be controlled.

2.2.2 Tack Method

The tack or tackmeter method was originally introduced by [Green, 1941] who studied adhesion of different inks and the method resembles extensional rheological techniques somewhat. The basic concept is that a probe is moved to contact the surface of a sample at known conditions. The force required to separate the probe from the sample is measured as well as the time required for separation at a given set of conditions. The word "tack" refers to the area under the curve of a separation force to separation time plot ([Kilcast and Roberts, 1998]). [Saunders et al., 1992] reported that increasing the contact force or contact time both increased the force required for separation, which correspond well with the theory of liquid bridges and findings of others (see section 2.3). In general the tack method has been used primarily for measuring adhesion of semi-solid foods and paste systems, e.g. [Chen and Hoseney, 1995] who measured the stickiness of dough, rather than in relation to spray drying. Many observations suggest that the phenomena observed are related, although not quite the same.

2.2.3 Pneumatic and Fluidization Methods

The first pneumatic test to be mentioned is the so-called blow test devised by [Paterson et al., 2001]. The basic idea was to have a powder at controlled conditions (temperature and moisture content), let it rest for a specified time period and then measure the air flow necessary to blow a channel in the product. The air pipe used to direct the air flow was held close to the powder sample (2-3 mm apart) and near a 45° angle. A sketch can be seen in figure 5 ([Paterson et al., 2005]).

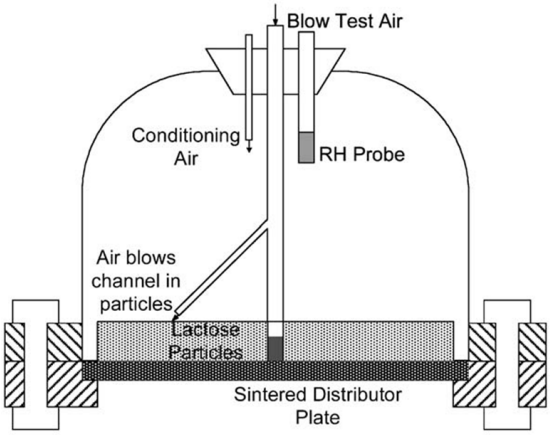

Figure 5: Sketch of the blow test method - from [Paterson et al., 2005].

The purpose was to test the hypothesis that stickiness was caused by flow of the rubbery surface of the amorphous powder to form liquid bridges (this will be described further in

section 2.3). As it turned out, the larger the $(T - T_g)$ value for the sample, the shorter times were required to obtain similarly sticky samples. When time was kept constant, increased $(T - T_g)$ would yield more sticky samples. This was taken to support the hypothesis and support that the concepts presented by [Frenkel, 1945] could be considered valid for stickiness (even if the math was not accurate). That said, the method only investigated relatively long time scales for stickiness (the order of magnitude of minutes), they investigated bulk properties (rather than single-particle interaction) and dealt with a powder that had been conditioned for uniform moisture content and temperature. In fact in a later publication of work using the equipment [Paterson et al., 2005] mentioned that shorter resting times than 30 s could not be accomplished because the setup up required reassembly after the sample had been put in. The same group discussed these considerations thoroughly in a later paper ([Foster et al., 2006]).
[Werner et al., 2006] used the fluidised bed method for determining stickiness depending on the amount of maltodextrin added to a solution. The concept of the method is to have one or more fluidised beds at controlled temperature and air humidity. Increasing the temperature of the sample would at some point result in plugging, meaning the powder could no longer be fluidised. This was then used to determine the sticking temperature of the powder. The fluidised bed method had shorter times than the blow test and might have more accurately measured surface properties, but contact times remain significantly higher than in spray drying.

2.2.4 Particle Gun

The particle gun method has the advantage of having conditions which resembles those found in spray drying more closely than previously described methods in which the stickiness was measured for stationary or slow movement. The technique was first presented by [Paterson et al., 2007] and [Zuo et al., 2007]. In their work samples were entrained in air moving at a velocity of approximately 20 $\frac{\mathrm{m}}{\mathrm{s}}$ towards a stainless steel plate. The particles were dry upon entrainment and the air was controlled to desired temperature and humidity.
In the work by [Zuo et al., 2007] the stickiness point (the temperature and relative humidity (RH) at which stickiness started to occur) obtained using a particle gun was compared to results obtained using a fluidized bed set-up. The results showed that deposits appeared at lower temperature for the same RH and lower RH at the same temperature for the fluidized bed experiment compared to the particle gun. This means particles were more sticky in the fluid bed setup. This can be a result of different factors all of which deal with the difference in dynamics. It is possible that the increased kinetic energy of the particle means that larger adhesive forces are needed to avoid particle bouncing. Another possibility is that the reduced stickiness is a result of fewer contact points (only one for the particle gun). No matter the reason this does suggest that particle stickiness point

will vary depending on the specific spray drying equipment used from plant to plant, if the dynamics changes between these.

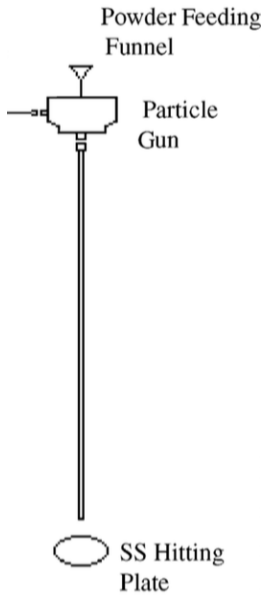

Figure 6: Sketch of the particle gun setup. The air is conditioned before it enters through the access point at the top left and is then directed downwards. The powder is funneled into the air from the top and hits the plate at the bottom - part of a figure from [Zuo et al., 2007]

In the work of [Paterson et al., 2007] they observed similar effects but also made observations that would confirm that it is the amorphous lactose that makes the product sticky, and that increased fat levels makes the product less sticky or has no effect at all.
[Murti et al., 2009] used the particle gun technique to study the changes in the stickiness of skim milk when changing the relative humidity of the ambient air and the initial water activity of the particle powder and found that both had some influence. The dependency upon ambient air relative humidity suggests that the surface of the particle is in fact not quite equilibrated which is a basic assumption of the method. The authors theorize that when the initial particle water activity is increased the particle is less elastic and more viscous, and therefore more sticky. Later the same group ([Murti et al., 2010]) studied the influence of air velocity, impact angle and plate material using the same equipment. The first test of air velocity was performed by comparing stickiness measured using a fluid bed method with that measured using the particle gun method. Typical $(T - T_g)$ at initiation was 10 °C higher for the particle gun method where the velocity was assessed to be two orders of magnitude larger than in the fluid bed. Further tests of air velocity showed that when it was increased the stickiness initiation point increased. This is most likely a result

of shorter contact times and possible also increased elastic effects. No apparent influence of impact angle upon stickiness initiation was observed, but the probability of sticking for a particle after stickiness is initiated was higher when the plate was more perpendicular to the flow direction of the particle.

2.2.5 Pilot Scale Methods

Some work has been published using small scale spray dryers for measuring stickiness under different conditions. These have the advantage that the conditions experienced by the particles match real processing conditions perfectly, but the disadvantages are that particle conditions are not perfectly known upon wall impact and that uncertainties are introduced because you have to work over some finite time periods and average results throughout, which may be especially important as start-up is different from stable operation.
[Woo et al., 2008b] used a pilot scale spray drying set-up to examine the effects of wall properties to stickiness. Several types of deposits were seen and the following is the interpretations of the authors. The experiments at lower temperatures suggested that still wet particles adhered to walls high in the dryer by formation of viscous liquid bridges while dry particles adhered to the lower parts of the dryer room because of intermolecular forces. At higher temperatures formation of immobile liquid bridges were hypothesised because the dry material was expected to have entered a rubbery region. The latter is most likely to be the most relevant because wet deposits are avoided by manipulating the flow and dry fines are easily removed.
[Ozmen and Langrish, 2003] and [Ozmen and Langrish, 2005] also used a pilot scale spray dryer to investigate how different operating conditions and wall properties influence the degree of wall deposition. Their observations were largely similar to those made by [Woo et al., 2008b]. By doing experiments with both a spray dryer that was grounded and one that was not it was found that electrostatic adhesion appeared insignificant. Changing the properties of a wall also had little effect. They also made observations which suggested that particles agglomerate more after depositing on the wall, rather than before, through Scanning Electron Microscopy on final product and wall deposits respectively.
[Gianfrancesco et al., 2009] and [Turchiuli et al., 2011] (of the same group) presented work using a pilot scale spray dryer with a number of air temperature and RH measurement points to try and get a more accurate assessment of conditions. They used this to dry various maltodextrin solutions and made similar observations regarding stickiness and glass transition as other authors mentioned.

2.2.6 Other Methods

A few other methods have been used historically, but are less consequential to stickiness in spray drying and so will only be mentioned briefly here.
The shear cell method can be used for measuring the flowability and as such can be used to

measure the adhesion and cohesion of a powder. The most frequently cited shear cells are the Jenike shear cell introduced by [Jenike, 1964] and the rotational split-level shear cell by [Peschl, 1989]. The basic principle is a cuboid that has been split in two horizontally. Between these two parts a sample is positioned and it is then possible to apply normal and shear stresses to it. Different sources show varying opinions on the applicability of this method for getting accurate results. For example [Adhikari et al., 2001] classified it as one of the better methods in general in their review while [Boonyai et al., 2003] wrote that the method was useful for measuring flow behavior of powders rather than stickiness. No matter what, the method does not seem very appropriate with regards to stickiness in spray drying. [Adhikari et al., 2001], who spoke positively of the method, claimed that it was unsuitable for systems with high temperature or moisture content. Furthermore contact times are much longer than in spray drying and bulk properties may very well dominate over surface effects.

A study on free-flowing powder and the criteria for when the powder became sticky in relation to dryer operation was performed by [Lockemann, 1999]. In this work he devised a novel technique for measuring stickiness optically. A sample is rotated while exposed to a light source. On the opposite side of this light source the optical signal is measured. The sticking point is identified by a significant change in the signal. The method has the advantage that it is relatively fast, easy to use and once the measurement has been initiated, no particular supervision is required. In relation to spray drying however many of the problems remain, namely the long contact times and the possible domination of bulk over surface properties.

[Goula et al., 2007] devised a method using a known centrifugal force to a preconditioned sample. The sample - at known temperature and moisture content - was positioned on a small plate. The angle of this plate to horizontal could be varied and the plate was then spun at an increasing rate. At some point the sample would no longer stick to the plate and, based on the rotational velocity at the time, a force was calculated. From this force a degree of sticking was determined. [Goula et al., 2007] used the method specifically for measuring stickiness of tomato pulp. In general the same trends as found by others was found using this method. The common problem of an impact compared to 'stationary' samples remains and the sample is dry and then subjected to moist conditions rather than the other way around.

[Rennie et al., 1999] presented the unconfined yield test for the use of measuring stickiness of dairy powders as function of powder composition, temperature, moisture content and particle size. The concept is that a sample is laced in a consolidation bank and vibrated so that the powder is packed. The sample is then consolidated using a small weight. After consolidation the cylindrical sample is loaded axially until failure. The larger the load needed before failure occurs, the more sticky the sample is. The method has similar problems as other methods and the consolidation part appears especially strange in relation to spray drying given that particles impact on their own rather than as a consolidated

mass of particles. Something odd that did appear was that they found that whole milk powder was more sticky with their methods than skim milk powder. This difference could be a symptom of the problems with the method in relation to spray drying, namely that the consolidation and contact time means that bulk properties are much more important than surface properties and that the phenomena for adhesion are quite different.
Finally [Michalski et al., 1999] examined adhesion to packaging materials by letting a product flow down a plate and the mass of adhered product was used to assess stickiness. This method has the advantage of simplicity but the consolidation and the long contact times means this is another method with domination bulk conditions and several of the problems listed previously.

2.3 Current Hypothesis

In this section a description of the currently most dominating hypothesis for stickiness found in literature will be given. This will only be concerned with the deposits caused by stickiness and not those caused by other phenomena for wet droplets or dry particles. The section will consist of a short summary of the findings leading to the hypothesis and then a description of the hypothesis.
The primary findings that leads to the hypothesis described here are from the stirring method, the pneumatic methods and the particle gun. As mentioned previously a relation was found between the measured stickiness of several materials and the parameter $(T - T_g)$. [Ozmen and Langrish, 2002] carried out investigations of the stickiness and glass transition temperature and postulated that it occurred virtually the same point but that the measured difference of 14 to 22 °C was caused by the difference in measuring a thermal and a mechanical response.
Other examples of authors publishing work on stickiness and glass transition include [Adhikari et al., 2005] who attempted to predict stickiness using mass and heat balances combined with glass transition theory and [Palzer, 2005] who included it in his work on liquid bridge formation (more on this below). [Paterson et al., 2005] found that stickiness occurred at the same $(T - T_g)$ no matter the specific temperature and moisture content for amorphous lactose and [Foster et al., 2006] found similar trends for other amorphous sugars. In general the specific $(T - T_g)$ for observing stickiness depended on the method for measuring it and ranged from $10 - 60$°C. [Hogan et al., 2010] also studied the glass transition using a technique that can be used for protein and fat-containing powders (making it highly relevant for many dairy products). The method consisted of measuring either gap distance or normal force during a constant heating of a sample.
These findings led researchers to consider the so-called Williams-Landel-Ferry (WLF) equation ([Williams et al., 1955]) which reads as follows:

$$\log\left(\frac{\eta}{\eta_g}\right) = \frac{K_1\,(T - T_g)}{K_2 + (T - T_g)} \tag{6}$$

The parameter $(T - T_g)$ appears explicitly in this equation. A short introduction to the topic of glass transition where the WLF equation appears will be given to explore the significance of the findings however the topic is much too big for a comprehensive description.

Glass transition is a phenomenon where a material moves from a rubbery, free-flowing to a glassy, rigid state. This occurs across a temperature region, but typically this is only referred to by the onset temperature or the temperature in the middle of the region (this differs between authors, but a description covering all of the is given by [Angell, 2002]). This temperature is known as the glass transition temperature T_g. Note that the material is rubbery above T_g and glassy below. Mixing different substances gives another glass transition temperature depending on the composition and compounds in the mixture. For instance a sugar or polymer mixture with water will typically have a lower T_g than the pure compound because water has a very low T_g (the glass transition of water is a complicated research topic, as discussed by [Angell, 2002]). Materials used to lower T_g this way are typically referred to as plasticizers. Frequently the Gordon and Taylor equation ([Gordon and Taylor, 1952]) is used to predict the glass transition temperature for such mixtures including ones where water is a component. The equation looks as follows:

$$T_g = \frac{w_w T_{g,w} + k w_s T_{g,comp}}{w_w + k w_c omp} \tag{7}$$

This leads us back to the WLF equation. The equation was used to describe the mechanical and electrical relaxation times of polymers, polymer solutions, organic glass-forming liquids and inorganic glasses. The relevant equation is shown above (equation (6)) and describes the dependence of viscosity upon temperature and glass transition temperature. It was found by [Williams et al., 1955] that values for K_1 and K_2 of 17.4 and 51.6 K respectively gave good results for most materials. The equation is empirical and only valid in the region of T_g to $T_g + 100°\mathrm{C}$. All reportings suggest that stickiness occurs somewhere in this region but above it typically an Arrhenius type equation can be used.

The transitions occurring for amorphous food substances was investigated by [Roos and Karel, 1991] who also discussed the stickiness in relation to plasticization of said foods. They found that stickiness of foods depended on moisture content and temperature in the same manner that glass transition did. They and others have attempted to explain the phenomena of stickiness based on the changes in viscosity that occur above a substance's glass transition because of such findings.

This leads us to the hypothesis itself: The cause for particle deposits caused by stickiness is formation of a liquid bridge between the flowing surface material of a particle and the wall it deposits on. The concept of liquid bridge formation and relevant topics will be discussed. First liquid bridges will be discussed in general. Than two other phenomena that are relevant in this topic will be discussed, namely sintering and wetting.

2.3.1 Liquid Bridges

In this section and the next discussion of 'bridges' will be given but first a few words on what is meant by a bridge. A bridge is basically material binding two particles together or a particle to a wall. This material can be either solid or liquid and can take different forms although typically the sides are concave when they are static. Some sketches with examples can be seen in figure 7.

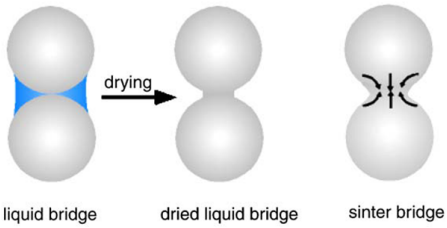

Figure 7: Sketch of different forms of bridges - copied and adapted from figure by [Palzer, 2005].

In this section only liquid bridges will be discussed while sintering and solid bridges will be discussed in the next section. Liquid bridges can be formed when surfaces are close enough that a liquid film on the surface can flow from one surface to the other or film from the two can flow together and combine. The strength of a liquid bridge will thus be the force required to pull the two objects apart such that the liquid bridge breaks.
The list of researchers who have made observations that lead to the connection between liquid bridges and stickiness include: [Downton et al., 1982], [Lockemann, 1999], [Paterson et al., 2001], [Paterson et al., 2005], [Foster et al., 2006], [Paterson et al., 2007], [Woo et al., 2008a], [Murti et al., 2009], [Hamawand, 2011] and [Turchiuli et al., 2011].
Because the formation and break up is governed by fluid flow a liquid bridge can be described using continuum fluid mechanics. Typically this is done by solving the equations of mass and momentum conservation ([Bird et al., 2007]):

$$\frac{\partial \rho}{\partial t} + \nabla \cdot \rho \mathbf{v} = 0 \tag{8}$$

$$\left(\frac{\partial}{\partial t} + \mathbf{v} \cdot \nabla\right)(\rho \mathbf{v}) = -\nabla p - (\nabla \cdot \boldsymbol{\tau}) + \rho \mathbf{g} + S \tag{9}$$

, in which S is a source term. In the subject of liquid bridges these are typically associated with surface tension. For incompressible, Newtonian fluids these equations can be simplified further, but it is unclear from literature whether this assumption always holds. For non-Newtonian fluids, details on mathematical description can be found in the book by [Bird et al., 1987]. Because liquid bridges in this field are typically small the phenomena of surface tension can become important because the associated forces may

become comparable in scale to the relevant body forces. This will usually be incorporated as boundary conditions or approximated with a body force (source term) only appearing very near the edges.

Because the geometry of liquid bridges is usually somewhat complex, problems are often difficult to solve analytically. In the following some attempts at this will be described while numerical options will be considered later.

Theory for the formation of a liquid bridge driven by surface tension and viscous forces has been dealt with by a number of people. [Frenkel, 1945] developed equations for the calculation of time for viscous flow under the influence of surface tension to form a liquid bridge between two particles with a given bridge diameter compared to particle diameter. [Rumpf et al., 1976] elaborated on this to include an applied force. [Palzer, 2005] added the well-known WLF equation ([Williams et al., 1955]) as a way to express the viscosity as a function of temperature and glass transition temperature. The result ends up as follows:

$$t = \left(\frac{5d^2\pi}{4\gamma d\pi + 2F_{app}}\right)\mu_g \left(\frac{d_{br}}{d}\right)^2 10^{\frac{K_1(T-T_g)}{K_2+(T-T_g)}} \tag{10}$$

This was derived in relation to general agglomeration and typically slower processes - e.g. storage or fluidised bed operations - than the impact between particle and wall during spray drying. Practically it was actually used to determine $(T - T_g)$ required to build a strong liquid bridge for a given contact time. In his work he chose that a 'strong' bridge would be one with a bridge diameter of one tenth of the particle diameter as inspired by the work of [Wallack and King, 1988] who inspected adhesion as a function of bridge thickness. He was able to produce good predictions for a wide range of applications, but it was unclear how he actually predicted F_{app} and the choice of bridge diameter d_{br} and contact time t was based on somewhat uncertain assumptions. [Murti et al., 2010] used this equation in their work and compared it with results obtained for both the fluidised bed and particle gun method (see 2.2.3 and 2.2.4 respectively) and found that without better ways to calculate F_{app}, d_{br} and t the equation gave wrong quantitative results and even qualitative results as well. It should also be noted that elastic effects might be important and since this is not included in any of these models that might be another reason why they become inaccurate at higher impact velocities.

Another approach was shown by [Mu and Su, 2007] where the rupture energy of bridge between two spherical particles was compared to their volume. In this analysis they found that surface tension dominated viscous effects significantly for bridge rupture. Their analysis however was carried out only for very low Capillary numbers ($Ca = \frac{v\mu}{\gamma} \approx 0.0001$) which might not be accurate during the formation and break-up of bridges during spray drying, where it is likely that both velocity and viscosity are significantly larger.

It should be noted that in literature a liquid bridge also appears in relation to extensional

shear and extensional rheology. This means that significant amounts of work are available for this which can be used for modelling or understanding the break up of liquid bridges. For now references will simply be made to two publications as examples of modelling. [Yildirim and Basaran, 2001] gives a good review of other work on extensional flow of both Newtonian and shear-thinning fluids and describes both one- and two-dimensional models for describing them. [Balmforth et al., 2010] solves a model for viscoplastic fluids and compares them with experimental measurements. This type of liquid bridges are formed differently so it cannot be used for understanding formation but it is comparable for break-up.
Finally a few examples of papers working with liquid bridges in a slightly different way will be mentioned. [Rabinovich et al., 2005] modeled the capillary forces in bridges formed by the spontaneous condensation of liquid on spherical particles, which is a significantly different case compared to the liquid bridges formed by stickiness, but the humid environments in which they worked makes it a interesting case to look at. [Men et al., 2009] showed results of using atomic force microscopy to investigate the formation and rupture of liquid bridges. They found that associated energy barriers could lead to hysteresis. It is unclear however whether these are relevant effects to the problem of stickiness or a phenomena primarily important in atomic force microscopy.

2.3.2 Solid Bridges and Sintering

Solid bridges will typically be the result of further drying of a liquid bridge (see the middle of figure 7). As such wall deposits observed during spray drying may be a result of initial liquid bridges that are dried further and so actually held on by solid bridges. Because solid bridges are usually formed from drying of liquid bridges there are not much theory on solid bridges as such but a little is available.
Some researchers have looked into sintering in relation to cohesion. This is often interesting in relation to agglomeration but it might also be relevant for wall deposits, given that a layer of particles is often established on the equipment wall no matter the conditions, after which cohesion becomes important. [Rumpf et al., 1976] carried out an analysis of various effects for particle cohesion, including sintering. They found that during short contact times viscoelastic effects seemed more important, but for long contact times sintering dominates. It is not immediately apparent that this might occur during spray drying due to short contact times as discussed previously, however if a particle is stuck with weak cohesive forces this may be enough to establish the contact time necessary for sintering to form a very strong solid bridge. [Palzer, 2005] found that sintering did not appear to be the phenomenon that causes deposits initially but it may still play a small role. [Leaper et al., 2012] reported on the growth of bridges between dry particles, using atomic force microscopy and from this study it is confirmed that the solid bridge formation for dry particles is a very slow process compared to other phenomena.

2.3.3 Wetting and Thermodynamic Adsorption

Something else that can affect adhesion is the concept of wettability. If a fluid material has high wettability i.e. large mutual affinity with the surface it will spread making the chance of adhesion greater. Conversely, if the wettability is low the fluid will be more likely to form droplets on the surface and even small forces can separate the two. A fluid will have high wettability if the surface it is wetting has higher surface energy than the fluid ([Saunders et al., 1992]). This is why some materials can sometimes be used to avoid adhesion because they have very low surface energy. An example is teflon which has a very low surface energy. The relevant forces are typically calculated based on the surface tension of the solid and liquid and the solid-liquid interfacial tension as well as the liquid contact angle at the solid/liquid/gas triple point. Based on the Young's force equation presented by [Fowkes, 1964] and work discussed in the review by [Michalski et al., 1997] the following equations can be used for calculating the work of adhesion:

$$\gamma_{so} = \gamma_l cos\left(\theta\right) + \gamma_{sl} \tag{11}$$

$$W_{adh} = \gamma_{so} + \gamma_l - \gamma_{sl} \tag{12}$$

Generally it has been found that the force calculated this way is much smaller than actual adhesive forces which meant that for a long time this theory was doubted. It has later been found that the higher force was actually a result of other contributions, most importantly viscoelastic effects in the solids ([Michalski et al., 1997]).
[Woo et al., 2008b] investigated the changes in wall depositions occurring at different temperatures with different wall materials. They found that different types of deposits occurred faster for teflon at the top of the spray dryer while occurring slower with teflon at the lower parts. They also found that typical sticky deposits occurred more rapidly and more easily on stainless steel but that the difference was very small. [Murti et al., 2010] also investigated various wall materials including teflon, stainless steel and silicone rubber using the particle gun method (see section 2.2.4) and found no significant differences in the stickiness initiation point. It was however observed that particles tended to move towards the edges of the target plate for teflon. [Ozmen and Langrish, 2003] also found that using Teflon or adhesive tape instead of stainless steel gave no significant increase or reduction in wall deposits during experiments in a pilot scale spray dryer. The same authors published more work with similar results later ([Ozmen and Langrish, 2005]).
From these it is unclear whether changing the wall material contributes anything to limiting wall deposits because but even when some contributions are observed they appear very limited.

Summary of Mechanistic Hypothesis

A very brief summary of the hypothesis in literature will be given here. The concept is that the stickiness of the particle is largely, if not purely, a surface phenomenon. The surface of the particle is in a condition where it can flow as a viscous and rubbery material. As it is brought into contact with another material (a wall in the case of deposits) the surface flows to form a liquid bridge between the particle and the other material. It seems that it is hypothesized that this formation of the bridge is caused by spontaneous wetting although this fails to explain the experiments that show that surface energies are of little significance. Whether the particle then adheres is a matter of the size of the bridge established in the time of contact between the sticky surface and the other material. Furthermore, it is hypothesized that only the surface conditions are of importance and not the inside of the particle.

3 Stickiness Measurement Setup

3.1 Introduction

As was described in section 2.2 many stickiness measurement techniques have been developed over the years. None however has consisted of drying a single droplet in a controlled manner and then bringing it into contact with a wall as would be the case inside of a spray dryer. Because of this it was desired to develop a new stickiness measurement setup as a part of the present work.
The goal of this setup is stated somewhat implicitly above. Have a single droplet dried for a user-determined amount of time under controlled conditions similar to those a droplet would encounter inside of a spray dryer. After this set amount of time the now dried droplet is to be brought into contact with a wall that for all intents and purpose is comparable to the inside walls of a spray dryer. After this point it should be possible to evaluate whether the particle adhered (i.e. it is sticky) or whether it bounced from the wall (i.e. the particle is non-sticky).
Unlike some methods in the literature it is not of primary interest to quantify how adhesive the material is (as e.g. the Tack Test did (section 2.2.2)) as it matters little how strongly the particle is adhered so long as it is in fact adhesive enough to remain attached.
In this chapter the setup will be described including the data acquisition procedure and the type of data resulting from the setup. The setup itself will be described in two sections, namely the droplet levitator and the particle impactor. The procedure for obtaining data will be discussed and finally examples of results will be shown.

3.2 Setup Description

3.2.1 Droplet Levitator

The droplet levitator is based on an experimental setup used to study drying kinetics and particle morphology during spray drying ([Brask et al., 2007]). The levitator setup is also referred to under the trademark DRYING KINETICS ANALYZER^{TM}. A description of the modified setup as used for the stickiness measurements will be given in the following. The levitator setup belongs to the single droplet drying (SDD) group of drying kinetics analysis methods ([Fu et al., 2012]) and consists of 4 separate parts some of which is shown in figure 8):

1. An ultrasonic horn and a concave reflector.
2. An optical system consisting of a diffuse light source and a CCD camera and lens.
3. A gas conditioning system used to control the gas temperature and humidity of the drying environment as well as the air flow velocity.
4. A droplet injection system.

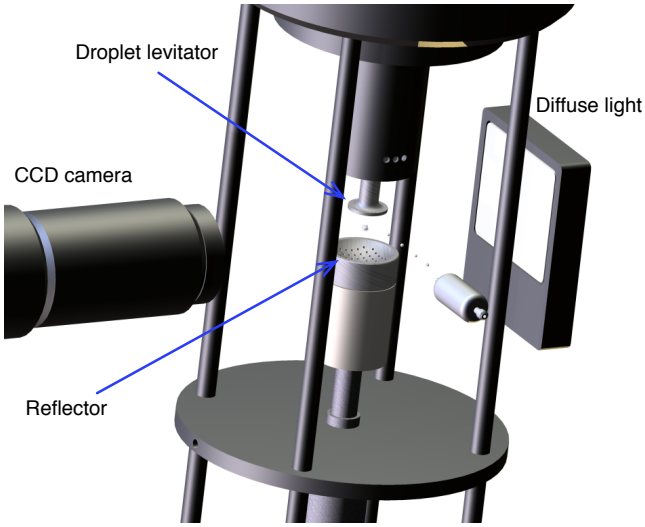

Figure 8: Sketch of levitator setup.

References to descriptions of the method in literature are given in section 1.2 about single droplet drying techniques.
The 58kHz levitator itself consists of an ultrasonic horn and a reflector. The horn produces an ultrasonic wave that propagates downwards and as it reaches the reflector the wave is reflected upwards. The ultrasonic horn is positioned $^5/_2$ wavelengths above the reflector in such a way that 5 pressure nodes are produced. Because the speed of sound in air depends on the temperature and composition of the air the exact separation of the horn and reflector must be adjusted depending on the specific conditions being tested. A droplet in the size range of $d_p = 50 - 2000$ μm can be levitated in each of these nodes ([Lierke, 2002] [Brask et al., 2007]).
A very important part of this setup is the visual recording of the droplet as it dries. This is also vital in evaluating whether the particle has adhered. The droplet is recorded using an optical system of a CCD camera and a diffuse light source. The light source is used to illuminate the droplet from behind. The droplet scatters light in such a way that the otherwise transparent droplet becomes black anywhere but at the center (see figure 11a). This provides a sharp silhouette, which is advantageous in the image analysis vital for the practical operation. Calibrating the length scale is done using a glass filament of accurately known diameter such that the temporal change in diameter of the droplet, as it dries, can be measured.
In order to make the drying similar to the drying a droplet is exposed to during spray drying, the reflector contains a multitude of holes through which a pre-conditioned drying air can be blown. The relative humidity and temperature of the drying gas are accurately

controlled by mixing heated nitrogen and evaporated water. Furthermore a double-walled chamber is heated by a hot air to reduce influence from the surroundings (not shown in figure 8). Computational fluid dynamics (CFD) have been used in determining the velocity of the air relative to the droplet to (unpublished, internal work at GEA Process Engineering A/S) and it is set to $0.4\frac{\mathrm{m}}{\mathrm{s}}$ although it can be changed.
The direction of this flow was found to be a little unstable, which effectively meant that the particle would move rapidly around the acoustic field. This, in many cases, lead to the particle falling out of the spot in which it was supposed to levitate. In such cases, stickiness measurement is of course impossible, because the particle could not be dried long enough for the impact to be relevant. The fact that it was the drying air causing this was not immediately apparent during early tests, but in looking for the cause it became clear that the disturbances disappeared when the air was shut off. The instability was solved by putting a small, curled up piece of a very thin napkin underneath the reflector (just below the sensor which says $T_{reflector}$ in figure 9). This served as a source of pressure drop, which might help distribute the flow equally through the reflectors capillaries, but it also reduced the space under the reflector in which eddies could potentially appear. This resolved the problem satisfactorily. The air flow control included both valve and controller, so it is impossible for the small piece of napkin to reduce the overall air flow through the system, but merely ensured that it would flow evenly.
The actual temperature of the chamber is measured with multiple sensors, albeit it is impossible to place one exactly where the droplet levitates (it would disturb the acoustic field, but it would also be moved or possible destroyed the first time the piston is activated). Three thermal sensors are used to obtain the highest certainty possible that the drying temperature is as desired. One is placed just below the reflector, to ensure that the drying air itself is the correct temperature. The temperature measured here will be referred to as the "reflector temperature". A second sensor is positioned just outside the path of the impactor, in an attempt to get the best approximation for the temperature at the droplet's position. The temperature measured by this sensor is referred to as the "jet temperature". Finally, a sensor is kept inside the drying chamber, but further away from the acoustic field and closer to the chamber wall - measuring the temperature referred to as "chamber temperature". A simple sketch of these sensors is shown in figure 9. It would be desirable for all these to be equal to the drying temperature at which measurement is being carried out, but it turned out that in order to keep the reflector and jet temperatures equal, the chamber temperature had to be kept slightly higher. This is most likely because there is heat loss to the surroundings, such that an excess of heat must be kept in the parts of the chamber outside of the position where the droplet is dried. The final component of the levitator system is the droplet release mechanism (not shown in figure 8). This particular part of the system has been developed by GEA Process Engineering A/S and is kept confidential and as such divulging further details is impossible. For the sake of evaluation results it will be said that droplets were inserted quickly so that very little

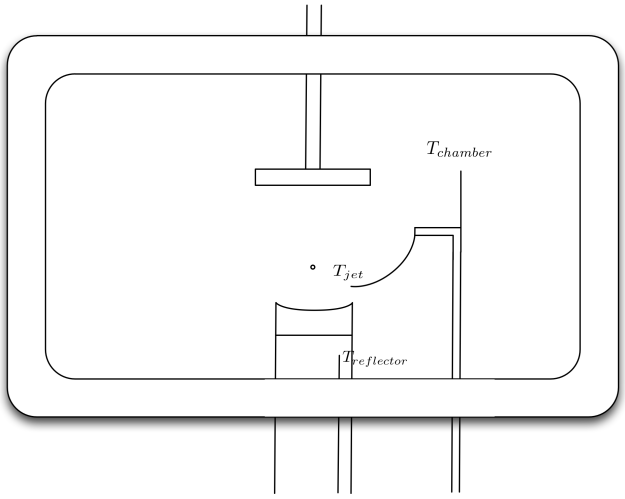

Figure 9: Sketch of thermal sensor positions as it would be seen from the position of the CCD-camera.

drying can occur prior to the controlled drying inside the acoustic levitator and that the droplets produced this way are larger than the ones obtained in a spray dryer atomizer. Typically 800 μm is the lower limit in this setup.

3.2.2 Particle Impactor

The particle impactor is the novel innovation to the levitator setup to allow for a measurement of stickiness. The impactor is a linear DC-servomotor attached in such a way that upon activation a piston will move forward and strike the particle from the side as recorded by the CCD-camera seen in figure 8. This is visualized in figure 10. The speed of the piston upon impact can be set by the user up to a maximum speed of $v_{imp} = 6.4\,\frac{\mathrm{m}}{\mathrm{s}}$. The equipment has no lower limit of importance but speeds below $v_{imp} = 0.5\,\frac{\mathrm{m}}{\mathrm{s}}$ should be used with care as the piston may disturb the ultrasonic field carrying the droplet. If this happens results become unclear because the droplet could either be non-sticky or it may have fallen before impact, both results leading to a clean piston. After the droplet has dried for a time period predefined by the operator the movement of the impactor is initiated. Until then the piston will be in a waiting position (figure 10a) to the right of the levitated droplet. Upon initiation the piston starts moving towards the left at an accelerating speed until it reaches the speed set by the operator. It reaches the point where the levitated droplet is located - defined as the zero position, see figure 10b - and continues towards the left. From here the piston decelerates until it stops to the far left in figure 10c. The piston then returns to the zero position such that the surface of the piston can be observed with the CCD-camera (figure 10d). After staying in this position for a short

time the piston returns to the waiting position. It is from the observations made while the piston is stationary at the zero position that it is evaluated whether the particle was sticky or non-sticky.

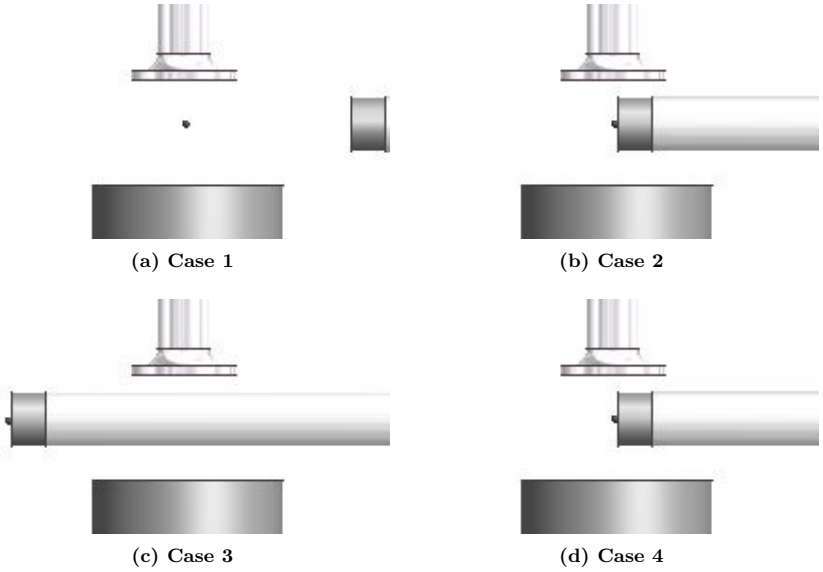

(a) Case 1 (b) Case 2

(c) Case 3 (d) Case 4

Figure 10: Sketch of impactor from the perspective of the CCD-camera with the piston in four different positions. The images represent: (a) Waiting position, before impact, (b) impact, (c) final extension after impact and (d) zero-position after impact.

3.3 Experimental Procedure

The experimental procedure will be describe including feed preparation and storage, the methodology of the measurement itself and the clean-up required after a measurement.
The feed for the experiment is prepared by dissolving a solid form of the desired product in a solvent of choice - typically, but not necessarily, water. The solid content of the feed - later referred to as 'initial solid content' - is assessed by drying a small sample of the feed and comparing the mass loss to the initial mass of the sample. Note that this assumes that the product and all components of it are non-volatile, but since the solid form of the product is often obtained by spray or freeze drying the original product, any volatile compounds would already have escaped the sample, so the assumption should hold in all relevant cases. If the desired solid content is above the saturation point, so it cannot be fully dissolved, heating can be used to increase the saturation point, but this will influence the end results, so it should be done consistently if at all. In most cases later a heated feed was used, both to ensure that all products were dissolved, but also to mimic the feed used in a spray dryer, which is typically preheated. If the same feed is used over

an extended time period, smaller samples should be extracted so that the remaining feed may be refrigerated. To avoid product degradation however no feed was used more than five days after its' original mixing.
The heating of the chamber may take time but a homogeneous temperature distribution is a necessity to ensure that the drying conditions are exactly as desired. When the thermal sensors show the required temperature to obtain the right drying conditions and remain unchanged for a few minutes measurements may start.
A droplet is inserted into the chamber using the injection devise described above. As stressed it is important to be swift here as you want the recording to start immediately as the drying is initiated and not several seconds later. From this point until the impactor is initiated the only work the operator has to do is observe the droplet while controlling the sound pressure level to ensure the droplet remains stable.
When an operator-chosen drying time has been reached, the piston is activated. As described above the piston will impact the wet particle and return to show the result in the view of the camera. Here the operator must document whether the particle adhered (i.e. is sticky) or whether the piston is clean (i.e. the particle was non-sticky). After 30 seconds in this position the piston moves away and after 5 further seconds the camera will stop recording. At this time the measurement has ended and the piston can be cleaned (using demineralised water and a cotton bud) as needed. When the system temperatures described previously have been stable at the desired drying temperatures for half a minute or more the next measurement may commence.

3.4 High-Speed Recording

This specific setup allows for a form of examination that other methods (this includes all methods described in the literature) do not in the same way. Because a singular, wet particle impacts the wall (piston), it is rather easy to observe the impact itself given a camera that can record images rapidly enough. This can be done using a high-speed camera capable of obtaining sufficiently high frame rates. The results will be discussed in the next chapter but a little time will be spent here describing the setup specifically for recording videos of with high frame rate.
A few things were slightly different, but overall the setup described above is very similar to the one used to produce slow-motion recordings. The camera is, obviously, changed. The Mini UX100 is used with a framerate of 20,000 fps and a resolution of 1280x248 pixels. Because of the rapid movement of the piston and therefore droplets, the images were very blurry if a shutter speed of 1/20,000 seconds was used. Therefore it was reduced even further to 1/160,000 seconds which gave much sharper images. A recording and shutter speed such as this requires a more intensive light source than the one used during the regular impactor tests. A simple, but more powerful LED source replaced the diffuse light source normally used.

This new camera did not feed the recorded image directly into the same computer as usual (the problem was a technicality) but it means the automatic droplet insertion mechanism was disabled. This means operation is slightly more complicated, but manual insertion remained possible. Apart from these changes, the setup remained unchanged. The resulting recordings will be described in the latter parts of the results section (see section 4).

4 Results

4.1 Raw Results

4.1.1 Single Droplet

In the description of the impactor in the previous chapter the method of evaluation is hinted at to some extent. In this section the procedure will be described in more detail. Figure 11 shows different snapshots taken from the video captured with the CCD-camera. The first image (figure 11a) is not an image for evaluating stickiness, but rather the image of a levitated droplet early in its' drying. The sharp silhouette of the droplet described in section 3.2.1 can be seen clearly in this image (as well as figure 11b and 11c technically). The remaining three snapshots (figure 11b-d) will be used to describe the different observations that can be obtained with the impactor and what these can be interpreted to mean.

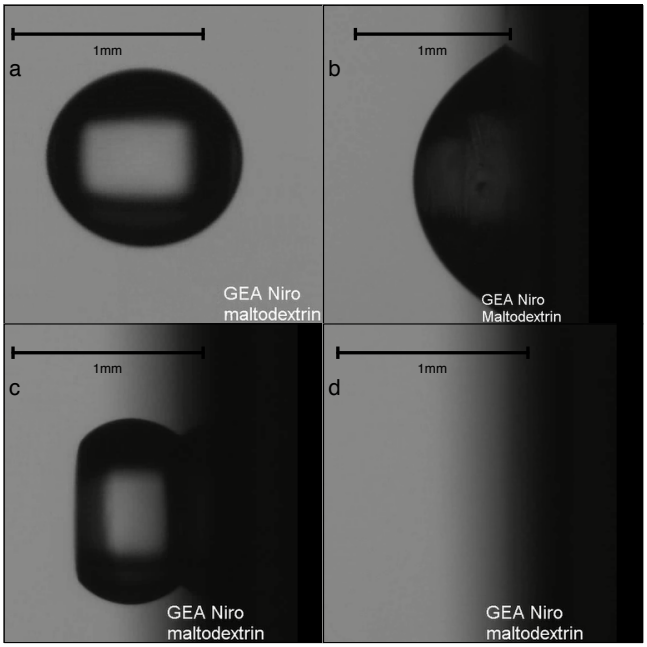

Figure 11: Snapshots of droplets during drying (a) and after impact (b,c,d). a) Before impact. b) Wet droplet, post-impact. c) Sticky particle, post-impact. d) Clean piston, post-impact.

Figure 11b is a droplet that spreads widely across the surface, similar to a droplet of water on a metal surface (i.e. a hydrophilic surface). This suggests a wet droplet which has not yet developed anything resembling a skin or crust on the surface. This observation is typically made for droplets that have only dried for short durations of time (compared to the other observations) or for droplets of pure solvent (i.e. water). This makes reasonable

the interpretation that a wet droplet spreading on the surface is observed.
Allowing the droplet to dry for a longer duration leads to observations as the one shown in figure 11c. The first important change is the different, apparent contact angle between the droplet or particle and the wall. This contact angle resembles the contact point between a water droplet and a hydrophobic surface. The piston tip is not a low-energy surface though and the dried skim milk is not an especially high-energy material, so this is an unlikely explanation. It seems more likely that the particle simple has become so dry that the surface is very resistant to movement. The surface is therefore most likely a very viscous, thick liquid or a solid, rigid crust. Such a surface would mean the droplet is either close to becoming or has become what is referred to as a wet particle, although the transition is poorly defined. Whether a viscous skin adhered to the wall or a broken crust with a liquid core underneath is more likely will be addressed later on. Note that further drying of the particle often lead to slight changes in morphology of the particle rather than just shrinking which further solidifies the interpretation that the surface is very resistant to movement.
The final snapshot seen in figure 11d appears comparatively uninteresting. The piston can be seen to be empty, with no adhered droplet or particle. This means that the droplet must have dried to a point of being a wet particle and continued until a point at which it is non-sticky. This does not necessarily suggest that the particle contains no solvent anymore, but rather that the wet particle has become sufficiently dry that the surface is not adhesive or the crust is dense and thick enough that the impact could not break through.
This yields the information on whether a singular droplet was dried enough or not. It does not however inform in any way how much more drying would make a sticky particle non-sticky or how far past the critical drying time a non-sticky particle was. This question will be addressed in the following.

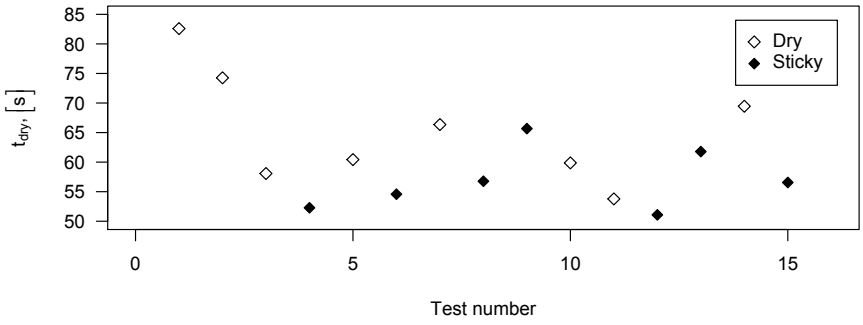

Figure 12: Raw data of test number plotted against drying time for skim milk with initial solid content of 30 w% dried at $T = 75°$C and 0%RH and then impacted at 3000 $\frac{mm}{s}$.

4.1.2 Critical Drying Time

The title of this section suggests that a critical drying time exists but no argument for its' existence have been presented. It may well be that there is a transitory region in which the chance of adhesion decreases from 100% to 0% in some way. In this section we will search for the transition between adhesive and non-adhesive particle in a manner that presumes nothing about the transition.
Consider measurements of numerous particles in the manner described in section 3 with observations as described above. These particles will be dried for differing duration and some will adhere while others will not. This may be plotted as is done in figure 12. It appears that for these data no clear trend is observed. This suggest one of multiple things:

- The zone in which a wet particle transitions from adhesive to non-adhesive is very broad.
- Some currently undescribed factor or factors are not reflected in this way of plotting the data.

Rather than discarding this as useless results or going back to the laboratory to take measurements over a much wider range of drying time, a moment of deliberation for the second item above should be taken. The results shown in figure 12 does not list anything about the sizes of the droplet. It is obvious that a larger droplet needs to be dried for longer compared to a smaller one, but the degree is not necessarily obvious. For an early estimate the so-called d_d^2-law (see section 1.2) will be used to account for the different sizes. Figure 13 shows the result of this for the same data as shown in figure 12.

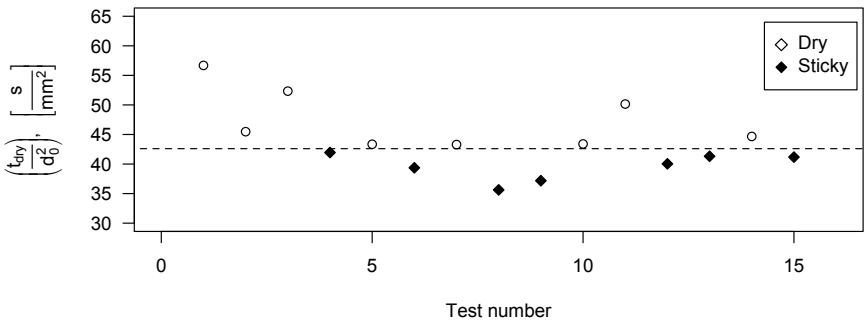

Figure 13: Raw data of test number plotted against drying time normalized with the initial diameter squared, for skim milk with initial solid content of 30 w% dried at $T = 75^oC$ and 0%RH and then impacted at 3000 $\frac{mm}{s}$.

This new way of plotting the data reveals something entirely different. Suddenly the data align itself in a very meaningful manner suggesting that there is a critical drying time or

narrow transition zone that separates the adhesive particles from those that are not. Note that this scaling is of the drying time, but does not take into account any other effects of size. This will be considered in section 5.

Now, in the following we will consider a way of expressing the uncertainty of this critical drying time based on the raw data obtained. This may either be an expression of the width of the transition zone or the confidence interval of the critical drying time.

Consider now the scaled drying time as a continuum from 0 to infinity (as it basically is). We will divide the continuum into small intervals and for each interval consider the empirical likelihood of a non-sticky particle. As an example, consider in figure 13 particles that have dried between 41 and 44 $\frac{s}{mm^2}$. Here we find that the chance of the particle **not** adhering is about 0.57. It should be apparent that changing the size of these intervals will influence the exact chance of adhesion and if there are too few measurements to get an assessment of the chance in a given interval (either because the data misrepresents the actual chance or because there are simply no measurements) it too represents a problem. The problem of interval size will be dealt with by reducing the size of the intervals, while examining how this affects the results. This exacerbates the problem of data availability in any given interval, because they become smaller, therefore requiring more overall data points to ensure sufficient data in each interval. This problem is reduced by interpolating the value in intervals without data to values in intervals near it that does have data points. This does not directly solve the problem occurring when there is not enough data available, but it allows us to inspect the data anyway. Using this technique any problems become apparent, when the data actually suggests a problem.

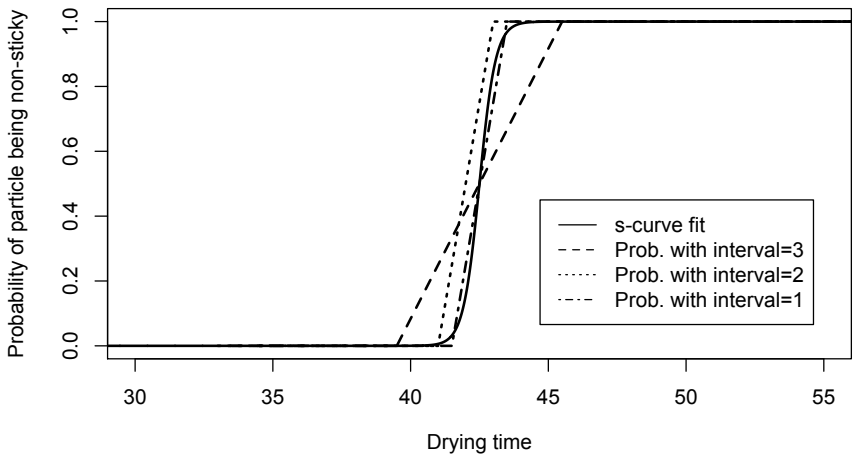

Figure 14: Example of s-curve fit to the probability of a particle being non-sticky depending on duration of drying.

In the remaining plots of data an error bar of sorts will be plotted to give an assessment of the internal agreement of any given stickiness measurement. The lower and upper bounds are found by determining the drying times corresponding to 0.05 and 0.95 in the s-curve fitted to the data in a given point. This is a very simple way of getting an impression of the internal agreement, but it does not account for any consistent error in a given data point, as for example would occur if the drying room was slightly warmer or colder than expected.
In future discussion the transition will be described as a critical drying time (always scaled for droplet size) with a given uncertainty attached to it, but it should always be kept in mind that it might represent a transitory region as well, given any number unknown parameters that may be stochastic in nature (e.g. surface roughness of wall or irregularity of particle shape).

4.2 Varying Parameters

Now that a critical drying time has been defined we are ready to investigate how it changes with varying parameters. Below a number of parameters will be varied, with discussion of each of these.

4.2.1 Drying Conditions

The first parameters to be examined will be the drying conditions. Many conditions may be considered included in this subset of conditions such as temperature and humidity of the surround atmosphere and the velocity of the air movement relative to the particle (effectively changing the convective contribution to drying). Here the focus will be on changing the atmospheric temperature and humidity. The humidity here will be expressed as relative humidity, which is a well-known function of temperature and absolute humidity. This decision was made because the driving force for drying is differences in relative humidity (or vapor pressure), but going from one expression of humidity to the other is very easy, should it be necessary.
A series of experiments were run, with the purpose of determining the critical drying point at each set of conditions where particles become non-sticky. This was done for skim milk powder (SMP) dissolved in demineralised water, with a constant initial solid content, constant impact velocity and the same piston material. These conditions are as shown in table 1. A few comments about these conditions will be given here. SMP was chosen

Table 1: Constant parameters during experiments with varied drying air conditions

Feed Material	Initial Solid Content	Impact Velocity	Piston Material
SMP	$0.3\frac{\mathrm{w}}{\mathrm{w}}\%$	$3000\frac{\mathrm{mm}}{\mathrm{s}}$	Stainless Steel

because the product is industrially well-known - GEA produces many dryers for customers who dry skim milk powder - and the drying kinetics have been measured before (a drying

curve is shown in section 6). The solid content is lower than the one typically used in spray drying (internal GEA Process Engineering sources), which is done because of the challenge of creating a droplet in the levitator setup compared to a spray nozzle discussed previously.

The impact velocity was chosen as a value considered reasonable for the impacting velocity inside a spray dryer. This value is very difficult to obtain. [Murti et al., 2010] varied the impact velocity in the range of $10 - 30 \frac{\mathrm{m}}{\mathrm{s}}$ but gave no reasoning for that choice.

Consider a wet particle moving with the air flow towards a wall. In such a case the air flow would change direction and the particle would feel the drag and move with it. The inertia of the particle means that it would not follow the wind perfectly and if the air flow turns sharply enough the droplet can hit the wall. In such a case the droplet will impact with some velocity lower than the velocity of the air flow. CFD simulations internally at GEA Process Engineering suggested that particle impact with velocities in the range of just above 0 to as high as $30 \frac{\mathrm{m}}{\mathrm{s}}$. A random walk model is used in conjunction with deterministic models however, to model the particle motion, which means a particle very close to the wall can impact at a unrealistically high velocity if it random walks into it. Therefore the higher results in those simulations should most likely be neglected. Alternatively the terminal velocity of a droplet in stagnant air might be considered reasonable because this is a result of the combination of drag and gravity, however the drag in stagnant air is very different from the drag experienced inside a spray dryer. A spherical water droplet with diameter of 1 mm would have a terminal velocity of approximately $0.3 \frac{\mathrm{m}}{\mathrm{s}}$ in stagnant air ([Gunn and Kinzer, 1949]). The velocity chosen was thought to be a compromise, while the piston mechanics did set an upper limit to the velocities reachable. Those were examined using a high-speed camera, where the actual velocity of the piston could be tested simply by tracking the position from frame to frame.

Finally, the piston tip material was chosen to be stainless steel as that is the material most dryers are made from (a simply search on the internet will confirm that this is the industry standard), but a Teflon tip was also produced, which was used as part of the high-speed recordings discussed later.

The temperature was ranged from 75^oC to 85^oC and the relative humidity was ranged from 0 to 20%RH. These ranges easily cover the traditional operating window for drying of skim milk (internal sources). For each combination of a temperature and relative humidity a number of droplets were dried and a plot similar to the one shown in figure 13 produced. This leads to a plot as the following.

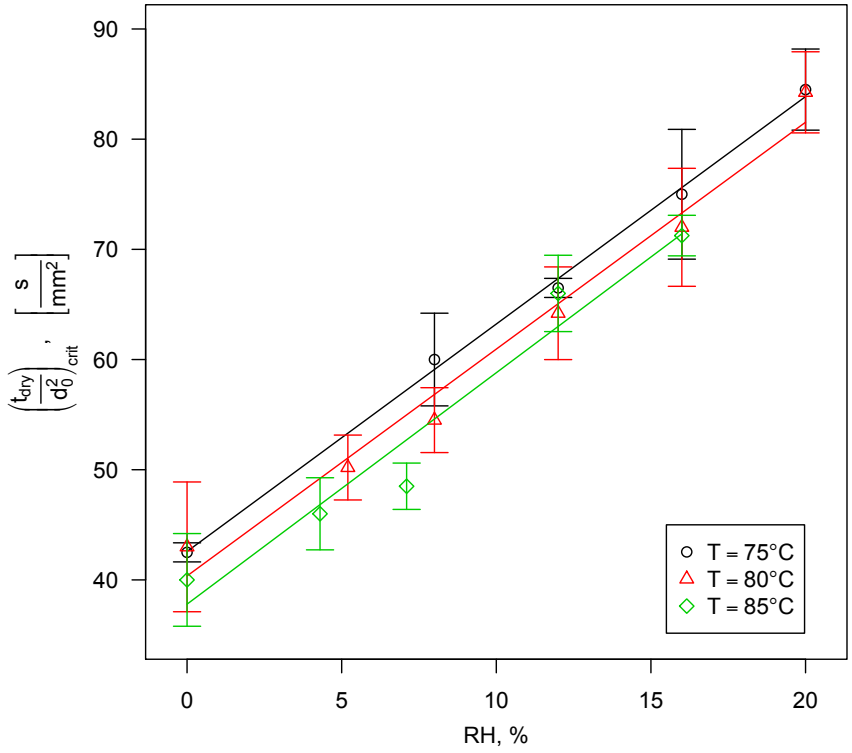

Figure 15: Critical drying time for varying drying conditions for skim milk droplets with initial solid content of 30 $\frac{w}{w}\%$ and impact velocity of 3000 $\frac{mm}{s}$. The straight lines are linear regressions to each set of temperature data.

This plot invites a few observations. First off it is very noteworthy that temperature dependency is significantly smaller than the humidity dependency. Given that heat transfer is required for drying to occur it may be surprising that temperature affects the results so little, but further consideration can make some sense of it. Increasing the temperature in the surrounding air by 5°C increases the driving force by relatively little - i.e. increasing the temperature difference by about 17% for 80°C and 12%RH. Changing the relative humidity 5 percentage points changes the relative pressure of water in the gas. This leads to a change in the surface temperature of the particle in the phase of drying where this is constant (i.e. when water is freely available on the surface). Going from 8 to 12%RH decreases the surface temperature in this phase almost 10°C, thereby increasing the temperature difference by double the amount a change of 5°C in the surrounding air would.
A second interesting observation is that the critical drying time appears to correlate linearly with the relative humidity of the drying air. Other types of regression was attempted

but gave no higher accuracy across all temperatures. At this point this fact remains mysterious, but an explanation might exist. The observations made in this plot will be used later on in a more general, practically applicable stickiness criteria. Note also that the distance between the line for 75°C and 80°C is very similar to the distance between 80°C and 85°C suggesting a linear correlation here as well.
This plot may be done differently, by placing the two parameters of drying on the two axes and making a contour plot, where the contours cover different drying times. A plot like that looks as follows.

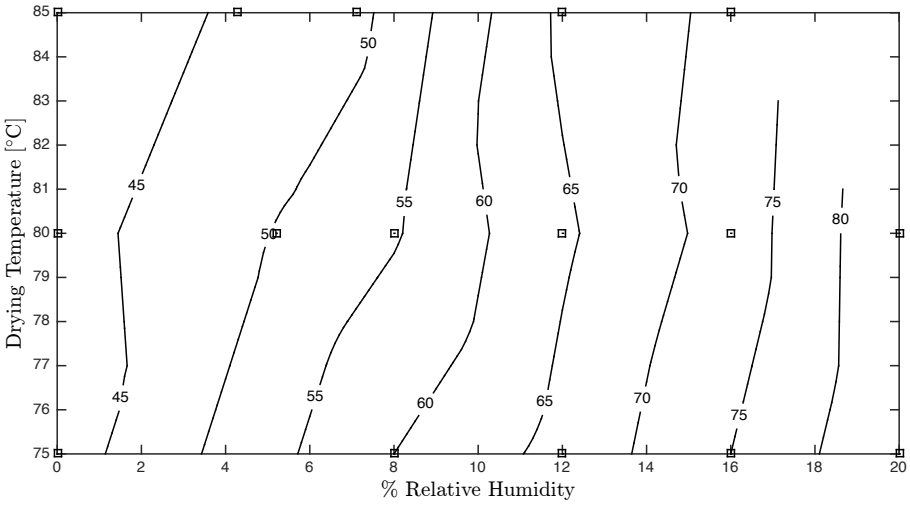

Figure 16: Contour map of critical drying time with varying drying conditions. Squares mark positions with a datapoint.

This figure basically allows for similar observations as the previous as the lines are almost vertical and for most of the chart they are equidistant. This chart then contributes little new to the observations listed above, but it can be applied slightly differently. Such a chart could help an operator keep a production stable. This can of course only be done if the chart is accurate.
An operator cannot realistically change the residence time of her dryer, because it is impossible to change the design or size. From a practical perspective she can only change the outlet temperature and humidity. This is done by regulating the temperature of the drying air as well as the amount of both drying air and feed fed to the system. Lets imagine now that the operator knows the typical average residence time of a plant, for initial particle diameter of 100 μm, is 700 ms. Usually the outlet air conditions at this plant are 77^{o}C and 14%RH. On one unfortunate day, the humidity in the area is increased so that the relative humidity of the outlet air increases to 16.5%RH, which means the required residence time for particles to become non-sticky increases to approximately 750

ms. The unfortunate operator now starts to manipulate the parameters available for control and reduces the amount of feed put into the dryer, thereby reducing the total amount of water released in the drying, and increases the amount of drying air slightly, which reduces the fraction of the outlet air which is vapour. This effectively reduces the outlet humidity and the problem has been solved. If the operator attempted to solve the problem by increasing the inlet temperature, thereby increasing the outlet temperature, it is clear from the chart that it would require a very significant increase. This could have very unfortunate local effects in the dryer, effectively compromising the product, so the approach of reduced throughput is most likely preferred.

4.2.2 Different Substance

In the following results for varying humidity with a different product will be shown. This is of course to show that the trends observed are more general and while that does not necessarily ensure generality, it does offer up additional certainty of the conclusions. Maltodextrin is a product which is very easy to handle and industrially well-known. In the present case a maltodextrin with a dextrose equivalent (DE) value of 18 has been used as it is the standard dextrin used by GEA. This will be used as a model material here and one that was expected to be slightly less sticky than skim milk, although that was by no means completely certain.
Because it was already shown that humidity is the primary parameter once the drying temperature was significantly above the temperature that leads to a vapor pressure equal to the partial pressure in the air, only this will be investigated here. The really interesting part here is whether the trend observed from skimmed milk is replicated, i.e. does the dependence seem linear and is the slope comparable? The resulting data are shown in figure 17.
The first observation must be that a linear regression does not perform nearly as well here. This begs a reminder; the uncertainty shown in the figure is very dependent on the specific data obtained for a set of conditions. It does not reflect any consistent error which may have occurred (say the room was slightly more humid one day). That said, the general trend of increased humidity increasing the required drying time remains - anything else would be very surprising. Two different regression lines appear in the chart. The dashed one is a simple linear regression to the specific measurement points, with no accounting for the uncertainties, while the full one has been modified to increase the error further when outside the errorbars. The two are fairly close, but clearly a small difference does appear. One interesting point of observation is that the slope of the dashed line (regular linear regression) is quite close to the slopes of the three linear regression lines in figure 15. The parameters for these four regression lines are shown in table 2 for the equation form $y = ax + x_0$.

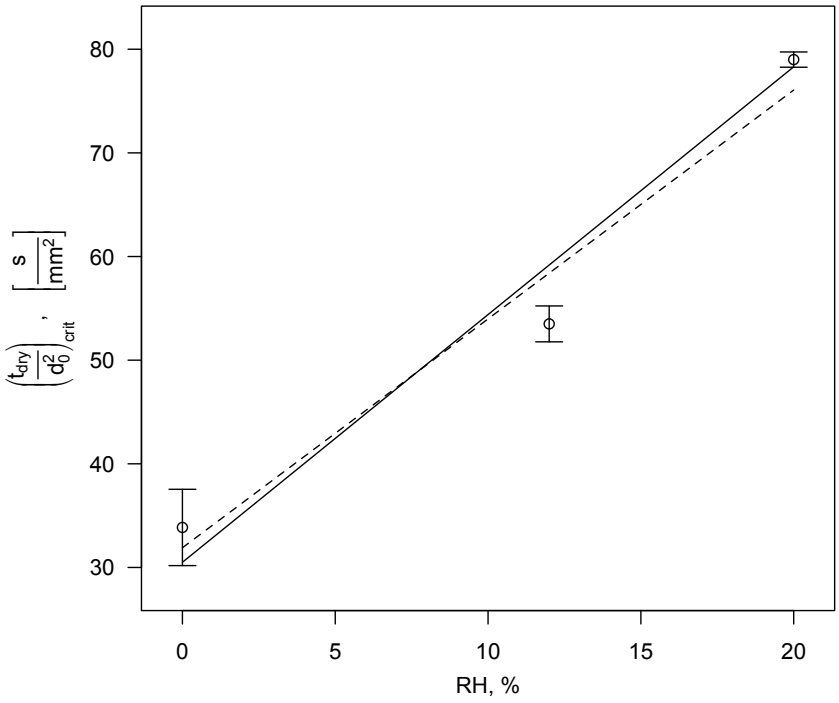

Figure 17: Critical drying time for varying drying conditions for maltodextrin DE18 droplets with initial solid content of 30 $\frac{w}{w}\%$ and impact velocity of 3000 $\frac{mm}{s}$. The straight lines are two different linear regressions which are explained further in the text below.

Table 2: Parameters for the linear regressions to humidity dependency.

	a	$\mathbf{x_0}$
SMP, 75°C	2.06	42.6
SMP, 80°C	2.06	40.4
SMP, 85°C	2.10	37.8
DE18, regular fit	2.21	31.9
DE18, fit w. uncertainty	2.39	30.5

First notice that the three lines for skim milk powder have slopes that are very close. Furthermore the difference in x_0 seen when the drying temperature is increased 5°C appears to be almost constant, which was also indicated previously. For the two lines for DE18 the regular fit is quite close as well, which is to be expected from figure 17. The fit that does not account at all for the uncertainties also has a slope quite close to that of the skim milk powder, which might indicate generality, but this will remain a hypothesis until many more products have been investigated.

4.2.3 Impact Velocity

The primary impact parameter which can easily be manipulated in the setup is the impact velocity. In the following the results of experiments to determine the critical drying time for different impact velocities are shown. This too was done for both skim milk powder and maltodextrin (DE18) dissolved in water to obtain feeds with 30 $\frac{w}{w}\%$ initial solid content. The piston material too was unchanged and the drying conditions were set to 80°C and 12%RH. The impact velocity was varied from 1000 to 5000 $\frac{mm}{s}$, which is about as big of a difference as can be obtained with the impactor setup. This span is considered good, because it is more than half an order of magnitude. While extrapolation should always be done with care, a wide parameter space minimizes the extrapolation needed at a later point. The results of these tests are shown in figure 18.

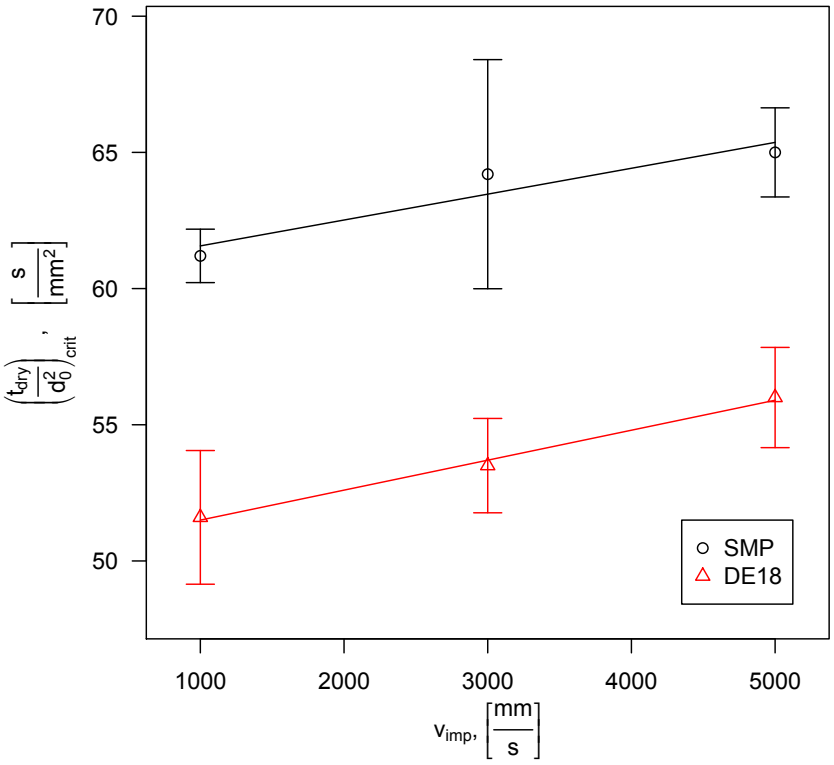

Figure 18: Critical drying time for varying impact velocity for both SMP and DE18. The lines are linear regressions to the two sets of data.

These results show that the dependence of the point of transition for these particles on

impact velocity is not very strong (at least compared to the relative humidity dependence observed earlier). The trend however is fairly clear; increasing impact velocity increases the time required for a particle to become non-sticky. The uncertainty in the middle point for skim milk powder makes the linear observation a little unclear, but it is noteworthy that the DE18 results show such a good linear regression and that the regression to the skim milk data - while worse - has a slope that resembles the other quite closely. Once more this might suggest a common trend although generality is uncertain still. In an attempt to explain this effect the impact will be examined more in section 5.
Note that this is the opposite of the velocity dependence reported in literature on measuring stickiness using both the blow test and the particle gun (see section 2.2). This may very well be a result of the difference that particles measured here were droplets that were dried, whereas the particles measured in literature were rehumidified, dry particles. It suggests that stickiness is not, in fact, purely a surface phenomenon as it is otherwise considered in some literature. More on these thoughts will be discussed in section 5.

4.3 Summary

Before proceeding to describe the results of the high-speed recordings made with the setup (as eluded to in section 3.4) a brief summary of the results obtained so far will be given. In this section the type of results obtained with the new setup was introduced and the way these are used to make general conclusions about critical drying times described. This included the assessment of a critical time, scaled for particle size, as inspired by the d^2-law seen in the drying of a single droplet of water. Furthermore it included a simplistic method for assessing the deviation of the results for a given set of conditions, purely based on the results available.
The levitator-impactor setup was used to measure the required drying time of single droplets of dissolved skim milk powder and DE18 maltodextrin respectively. For skim milk an elaborate drying map was produced with varying drying temperature and humidity (i.e. the relative humidity of the drying air). According to these results there was a linear relationship between the required drying time for particles to become non-sticky and both temperature and relative humidity respectively, although the latter appeared much more important than the former. This difference in importance can be understood from considerations of drying and the driving force for this process. The maltodextrin critical drying time was only measured for varying humidity because of the clear domination of this parameter and while the linear regression was less impressive in this case, the line obtained had a slope curiously close to those for skim milk.
Both products were also examined for varying velocity. It was found that increasing velocity, increased the time required for stickiness to cease. Once more a linear regression was found, which in this case was especially strong for DE18. This effect in particular will be investigated further in section 5.

4.4 High-Speed Recordings

As described in section 3, the setup can also be used with a high-speed camera. In this section the resulting high-speed recordings of partially dried particles impacting with the piston will be shown. The important part of this section is to observe how the impact itself appears, while furthering the understanding of the phenomena.
This section will start with a general introduction of the type of results obtained with the high-speed camera. These general recordings will also serve as example of how a closer inspection revealed a few interesting factors. This will be followed up with results for widely varying impact velocity. Then a few results for impacts with a different piston tip, namely a Teflon tip - i.e. a low-energy surface - will be shown.

4.4.1 General Results

All results from the high-speed recordings were obtained with the same skim milk feed that was used for the normal measurements, namely one with an initial solid content of 0.3 $\frac{w}{w}\%$ and initial temperature of 50 ^{o}C. Controlling the time a droplet spends in the dryer is significantly more difficult because the software used to automatically detect the droplet and measure its' size could not, for practical reasons, be used with the new camera. A manually controlled stop watch was used to control drying time to some degree but this is a major source of uncertainty, which should be kept in mind when comparing results.
The observations made are to a large degree qualitative. Later a few quantitative analyses will be attempted. The qualitative observations made are based on visual inspection of the videos recorded. Here, selected frames will be shown instead, which hopefully will give an intuitive understanding of what a video would look like. The first example, figure 19, shows a recording obtained with a droplet dried until it was close to non-sticky before being impacted at 3000 $\frac{mm}{s}$.
All figures like this one will have the first frame showing the droplet freely hanging and the last frame showing something shortly before the piston surface leaves the image area. The frames in between will be chosen with the aim of giving the best possible view of what happens in the movie. The wet particle is shaped as something in between a torus or an ellipsoid. Think of an ellipsoid which curves inwards at the middle, but without actually forming a hole. As the piston makes contact with the particle it starts to change alignment. This can be seen in frames 2 through 4 in figure 19. As the flatter surface of the particle aligns with the piston, the particle feels the full force of the impact, causing it to accelerate to the velocity of the wall. The particle then starts to move slightly more rapidly than the wall, resulting in a surface area that decreases. This can be seen in frame 4 through 6 of figure 19. Finally as the initial impact is finished the particle appears to move slightly closer to the wall, which is a sort of wetting happening slowly.

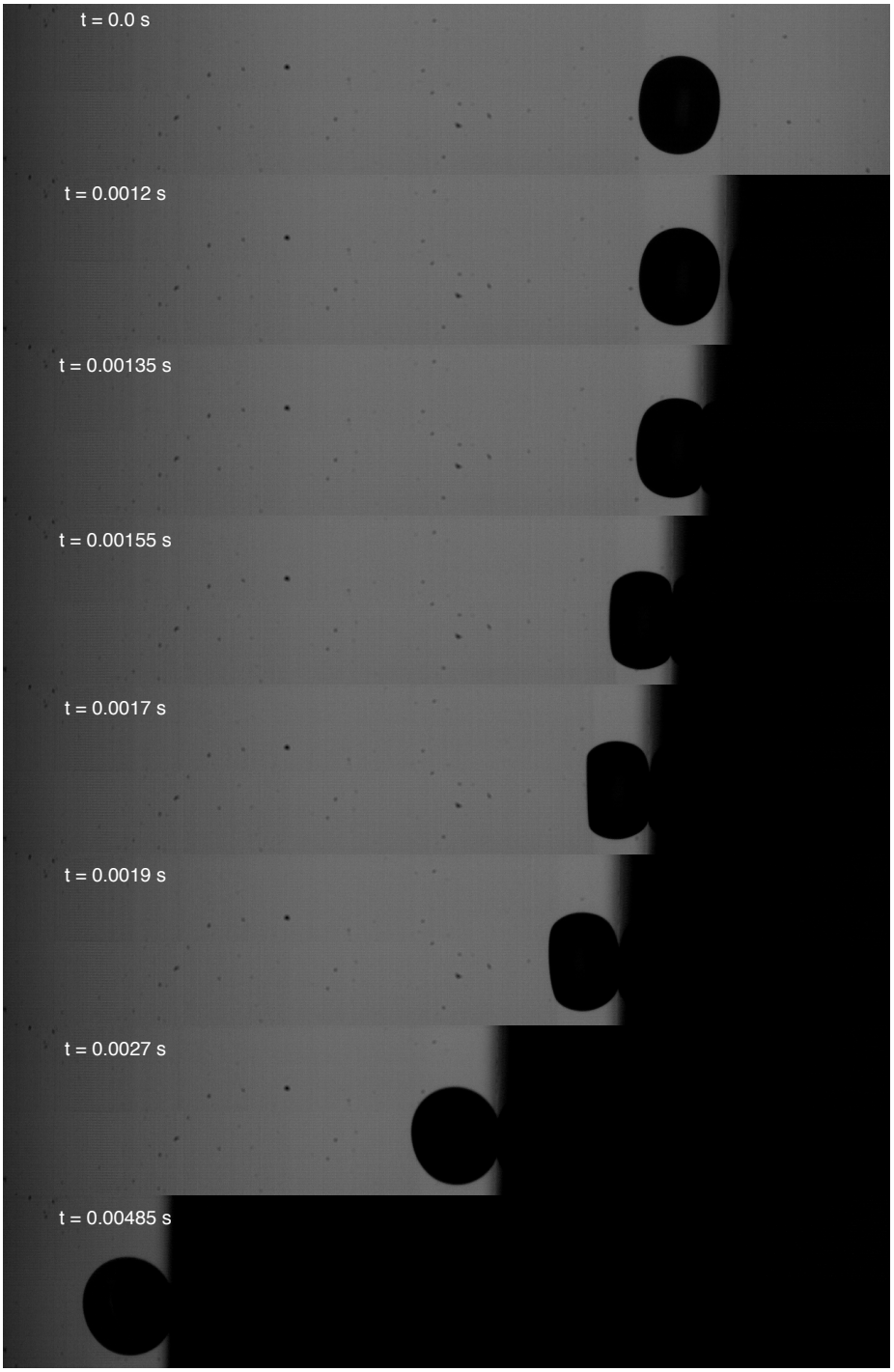

Figure 19: Different frames from a high-speed recording of a sticky SMP particle. The time for each frame is written in the figure.

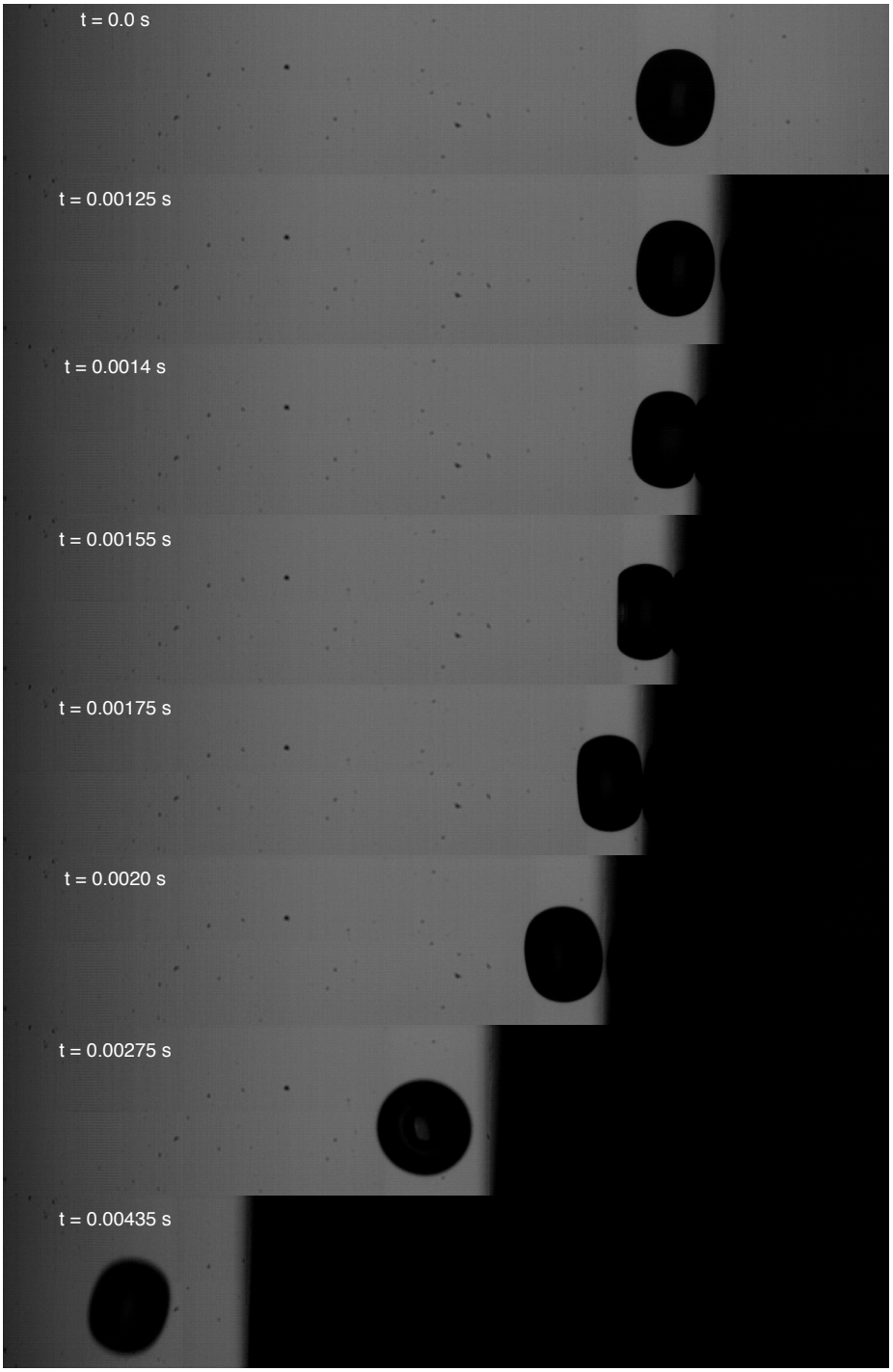

Figure 20: Different frames from a high-speed recording of a non-sticky SMP particle. The time for each frame is written in the figure.

Consider the same event, but in a coordinate system that moved with the piston, rather than being stationary in space. This would look as the event occurring when a moving particle hits a wall in a spray dryer. In this case the particle would hit the wall and be aligned for maximum contact. It would then be decelerated because the wall is practically immovable. A very slight elastic effect would cause it to move slightly from the wall but not enough to overcome the adhesive force established in the contact between the particle and the wall.

Note that the particle is barely deformed at all - which matches the expectations for a sticky particle, but not a traditionally wet droplet. The apparent contact angle at the wall is very large, but decreases slightly after the initial impact. The low deformation coupled with this changing contact angle suggests that the surface is an extremely viscous liquid. This matches poorly with a hypothesis of a rigid shell covering a liquid core, but better with a highly viscous skin, with a gradual transition to a core of a less viscous liquid. From this video it is difficult to assess whether it is slight elastic effects causing the particle to move a little in the direction away from the piston or whether the piston slows down after the initial impact. It is known that this will happen eventually as the piston halts its' movements, but determining the degree to which it happens in this image requires further analysis.

Figure 20 shows a similar set of frames for a particle dried slightly longer before being impacted. Notice that the particles in the first frame of figures 19 and 20 look very similar. As this particle comes into contact with the piston it too rotates to align the flat of its' surface with the piston. It too begins to accelerate in the direction of the movement of the piston. As the velocity increases the contact area decreases until finally the particle and piston separates as seen in frame 6 of figure 20. At this point it moves faster than the piston and so the space between the two increases. Because the initial point of contact between the particle and the piston was in front of the center of mass of the particle it spins while moving from the piston. Furthermore it appears that gravity pulls the particle down as it is closer to the bottom in the final frame.

It is difficult to conclude much about the phenomena happening during the impact in this particular video, but comparing it to the video with a sticky particle it is noteworthy that up until the fifth frame, the last frame shown here with contact, it is impossible to tell whether the particle will adhere or not. This suggests that the difference between a particle that adheres and one that does not, is small.

As mentioned above, it requires more detailed analysis to determine whether the particle is elastic or not. If, in fact, the piston has started slowing down in the later part of the video, then that might be enough to cause the particle to move faster than the piston, but if this is not the case the effect must be on of elasticity. Image analysis has been used to locate the approximate center of mass of the particle and the surface of the piston respectively. Tracking the movement of each from frame to frame gives an approximate velocity profile.

This has been done for all figures, and examples are shown in figure 21. All of these are for 4000 $\frac{\text{mm}}{\text{s}}$, with different drying times. The jumps up and down are most likely not real, but rather an expression of the relatively poor resolution of the video, which means tracking the object consistently is difficult. In all cases it can be seen that the particle only starts moving after a number of frames, which corresponds to the time when the piston hits the particle. The top one is for a particle which stuck to the wall. After the particle accelerates the velocity of it remains very close to the velocity of the piston. This obviously should be the case if the particle has actually adhered to the wall. The middle and lower part are for particles which bounced from the wall. In both cases the full line remained slightly above the pistons. In all cases the piston moved at a pace which appears constant, with no apparent slowing down. This means the particle speeding ahead of the piston is in fact a result of slight elasticity. Given how small the difference between the velocity of the piston and the particle it is clear that the viscous dissipation is still significantly higher than the elastic effects.
Several attempts were made to interpret the results further for quantitative analysis. It turned out that the most successful was to track the length of the contact line in each frame. The contact line is assumed to be the projection of a circular contact area and as such the length of that contact line is halved to obtain the radius of the contact area r_{spr}. In order to compare different size droplets, the radius of spreading is divided by the radius of the droplet. This radius is assumed to be half the average of the longest and shortest line between two points on the surface of the particle and through the middle. Because of the low resolution of the image, the results are quite scattered (even more so than the velocity data shown above) and so a simple filter was used to smoothe the data. An example of the result can be seen in figure 22.
As the particle impacts, the radius of the contact area increases rapidly and then stays approximately constant for a while. Then as time progresses, the radius starts to increase slowly as the droplet wets the wall more. This corresponds well to the qualitative observations made above.

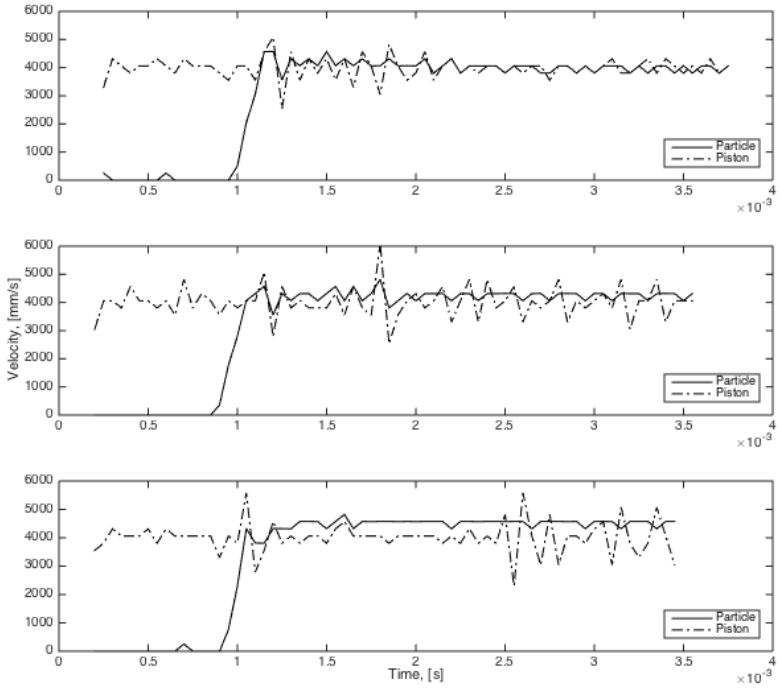

Figure 21: Plots of the velocity of the piston and the particle respectively determined through visual tracking in three different high-speed recordings. All three experiments were with skim milk impacted at $4000\ \frac{\text{mm}}{\text{s}}$ after drying. The top one was sticky, while the two lower ones were non-sticky.

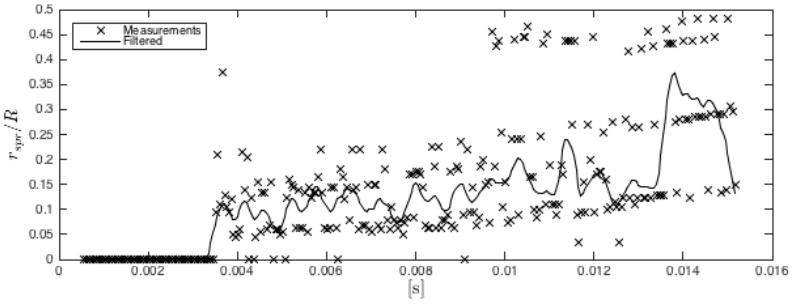

Figure 22: Plot of $\frac{r_{spr}}{R}$ as a function of time for a sticky particle impacted at $1000\ \frac{\text{mm}}{\text{s}}$. The filter was used in an attempt to smoothe the data.

Figure 23 shows similar qualitative results with an early jump upon impact, maybe with

a slight overshoot in this case, after which slower wetting increases the contact area. The decrease at the end is most likely caused by errors in the tracking of the contact line as that part of the frame was dark in the associated video (this lighting issue can be seen in figure 19). The scatter in the data from the low resolution coupled with the general uncertainty in the drying time meant there was no strong relationship between impact velocity and the quantitative value of $\frac{r_{spr}}{R}$ to observe in the data. There was no clear trend to observe for a constant minimum spreading for adhering particles either, which may also be a result of uncertainty in drying time and low image resolution.

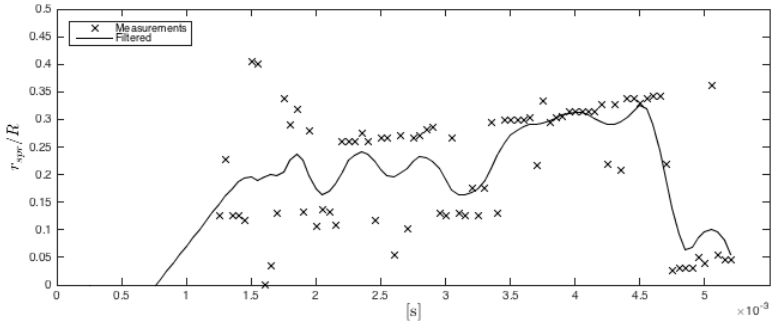

Figure 23: Plot of $\frac{r_{spr}}{R}$ as a function of time for a sticky particle impacted at 3000 $\frac{\text{mm}}{\text{s}}$. The filter was used in an attempt to smoothe the data.

4.4.2 Varying Impact Velocity

Velocity and drying time are the parameters most easily varied with importance for the impact. As stated previously, the drying time is difficult to control properly here, so several experiments were carried out with varying accurately for these recordings. In general the impact looks quite similar throughout as the result in figure 19, but with some difference which will be discussed here. Figure 24 shows a frame shortly after the initial contact for different velocities ranging from 500 to 6000 $\frac{\text{mm}}{\text{s}}$. The maximum here is the highest velocity obtainable with the piston used. Velocities lower than the lowest value listed resulted in the droplet falling from its' position before the piston actually hits the particle, because the piston disturbs the acoustic field. The velocities written in the figure are the settings used, but tracking the piston position from frame to frame confirms that it is close to accurate, although with slight variations.

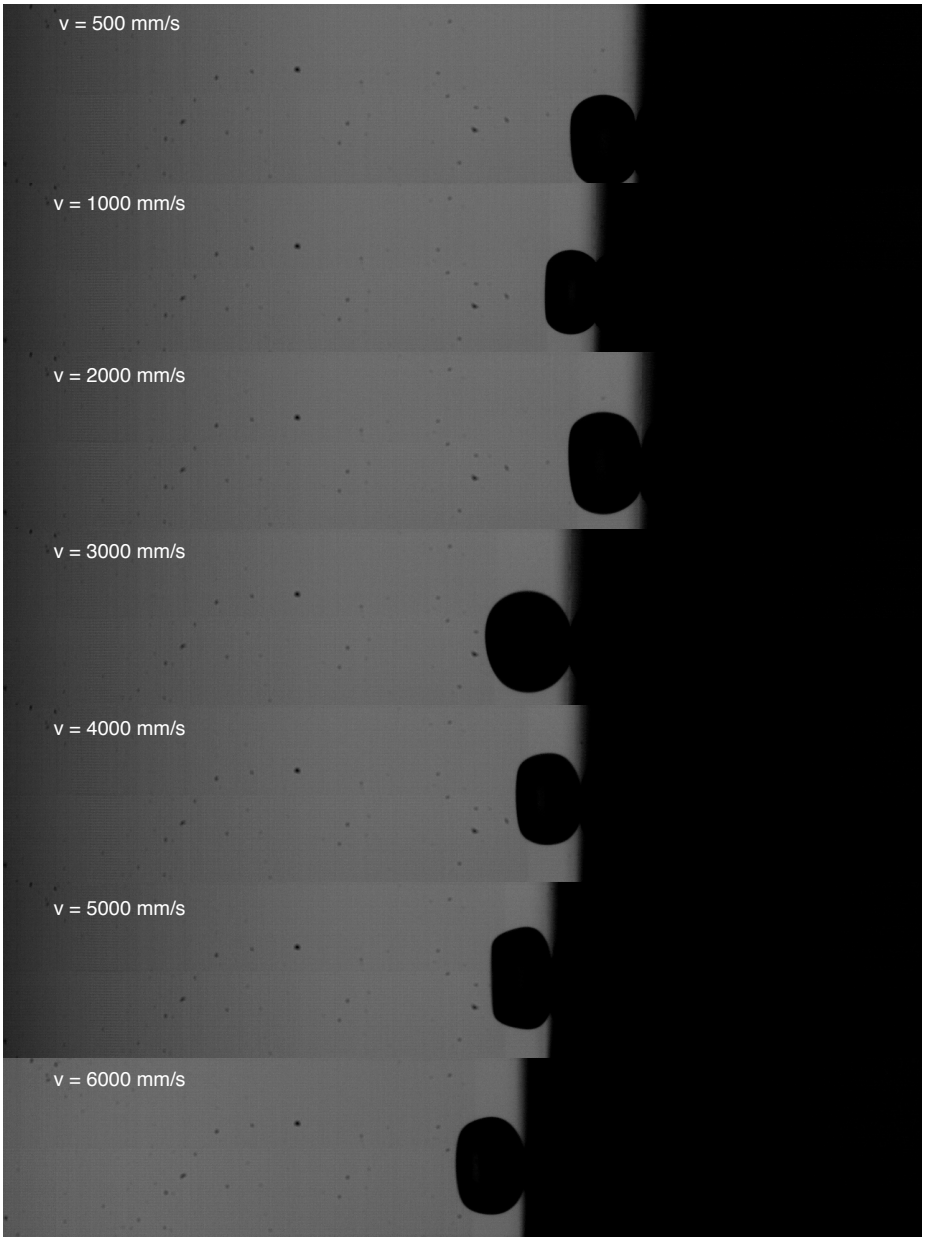

Figure 24: Frames from different high-speed recordings of sticky particles impacted at different velocities. Velocities are listed in each frame.

Notice the particle for 500 $\frac{\text{mm}}{\text{s}}$ is much lower in the image than most of the other particles shown. This is because it started falling before the piston reached it. For the highest

velocities it can be seen that the particle is deformed in a slightly different way, than the particle impacted at very low velocity. The increased kinetic energy of the impact thus deforms the particle more, leading to a more visually observable change in the symmetry of the morphology. Figure 25 shows similar frames for a few recordings that led to bouncing particles. The top frame shows a very early part of the impact, which shows that the particle symmetry is unaffected. It is already seen to be falling out of the view of the camera. The lower frame shows that the particle has deformed to a non-symmetric one, in spite of it not adhering. This particular frame specifically, was chosen because it was as late as possible where the asymmetry was clear. The rotation caused by the impact means that when it is clear that the particle is free of contact with the piston it is no longer obvious that the particle is asymmetric.

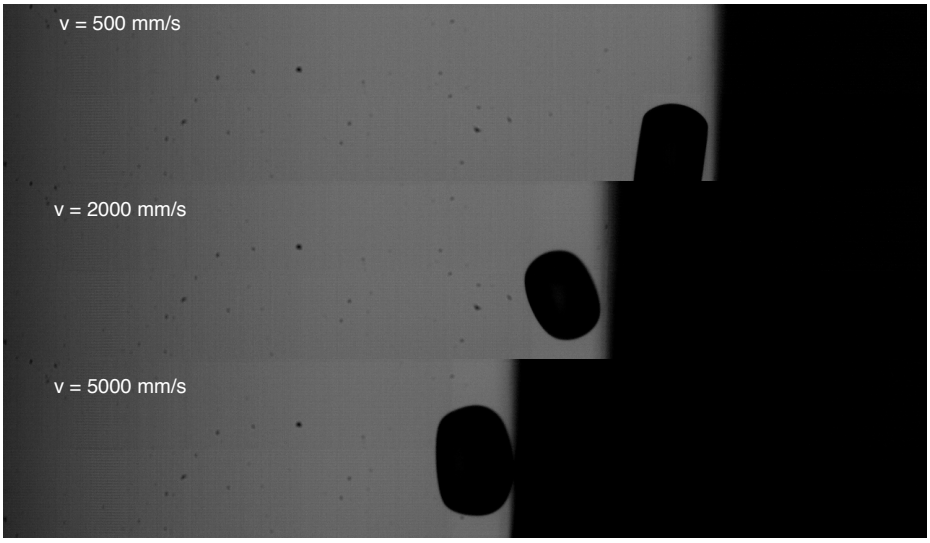

Figure 25: Frames from different high-speed recordings of non-sticky particles impacted at different velocities. Velocities are listed for each frame.

4.4.3 Different Relative Humidity

Drying a particle in a more humid environment means that it will take longer to dry simply because evaporation is slowed. This obviously means - as has also been shown previously - that it must be dried for longer time before it becomes non-sticky. In the interest of determining whether the impact is actually different, a few particles were dried at much higher humidity (16%RH) before being recording with the high-speed camera during impact at a velocity of 2000 $\frac{\text{mm}}{\text{s}}$. The recording with a sticky particle as close to the point where it would stop sticking is shown in figure 26.

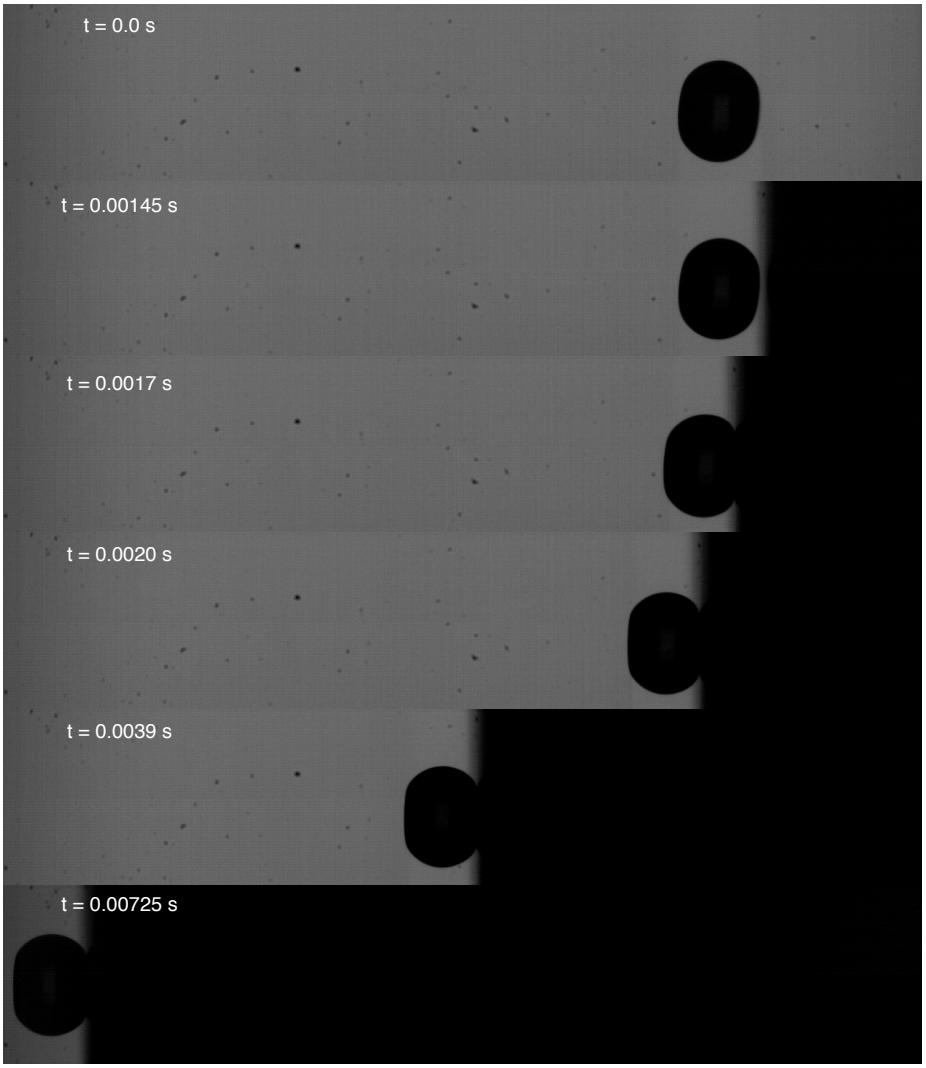

Figure 26: Different frames from a high-speed recording of a sticky droplet which was dried with humid air with 16%RH. The time of each frame is written in the figure.

Because the focus of the experiments with the high speed camera were made with varying velocity, this one is not nearly as close to the point of becoming non-sticky as the one shown in figure 19. A comparison between the first frames suggests that the morphology is the same, but upon impact the particle does not seem to require as much rotation to align with the surface. The surface might also be slightly softer, which would lead to a similar result. Since some alignment is still seen it is proposed that the difference is mostly attributable to the different morphology that arises during slower drying. A droplet that is dried slower

will have less inhomogeneities and therefore it can dry further before deforming from a spherical shape, which means less deformation even after complete drying. The particle also does not move away from the wall as observed previously, which suggests stronger adhesion than previously seen. This is most likely a result of the particle being further from the critical drying time. The droplet does show the important features of only minor deformation and the large contact angle near the triple-line. The measurements made here is scarce evidence, however it appears that there is little difference in the phenomena of the impact between a wall and a particle dried slowly and one dried quickly.

4.4.4 Low-Energy Wall Material

As part of the experiments with the high-speed camera a few particles were impacted using a Teflon tip. Similarly to the tests with humid drying air, these were carried out with an impact speed of 2000 $\frac{\text{mm}}{\text{s}}$. Furthermore relatively few of these tests were performed. This, coupled with the uncertainty of the duration of drying, means that the sticky particles obtained were not as close to the point of becoming non-sticky as the one shown in figure 19. Figure 28 shows the one closest to that point. That said, the impact observed with a Teflon tip is remarkable similar to the impact observed with the stainless steel tip. As the particle impacts it rotates to align with the surface and then moves slightly away from the wall before stopping. The apparent contact angle at the triple-line is very large, which is similar to the observations made for the stainless steel tip. It is difficult to tell from the sparse measurements with this piston tip whether the particle spreads upon the surface after the initial impact, as it did for the stainless steel tip, but it also does not seem to pull further away.
The $\frac{r_{spr}}{R}$ data for the Teflon experiments for sticky particles had a higher degree of coverage than those shown previously and held more constant after that, rather than spreading upon the surface. This can be seen in figure 27. It is unclear whether this was a result of the particles flowing a little more easily than the ones impacted with stainless steel or whether it is an actual effect, but given the magnitude of the difference it is very possible that the effect is real. It makes sense that the particle does not spread further after the initial impact given that the surface is less prone to be wetted. The higher initial coverage may be a result of decreased friction at the triple line.

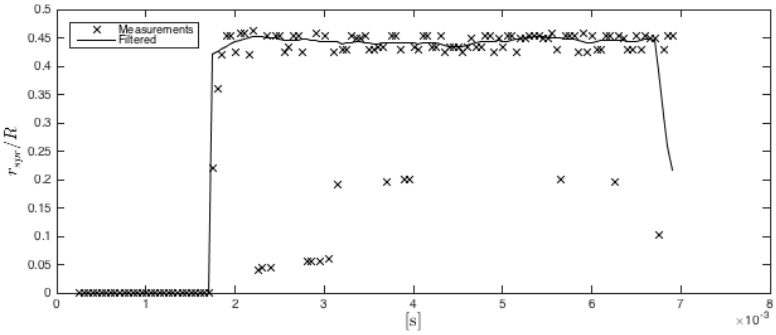

Figure 27: Plot of $\frac{r_{spr}}{R}$ as a function of time for a sticky particle impacted with a Teflon tipped piston.

Given the results in literature (see section 2.3.3) it is not surprising that there is little difference when a low-energy surface is used. A low-energy surface will have a different equilibrium wetting, but if force is applied it is still possible to wet it in spite of the changed thermodynamic equilibrium. This finding suggests that the force of the impact is what causes the initial spreading of the droplet upon the wall, not thermodynamic wetting.

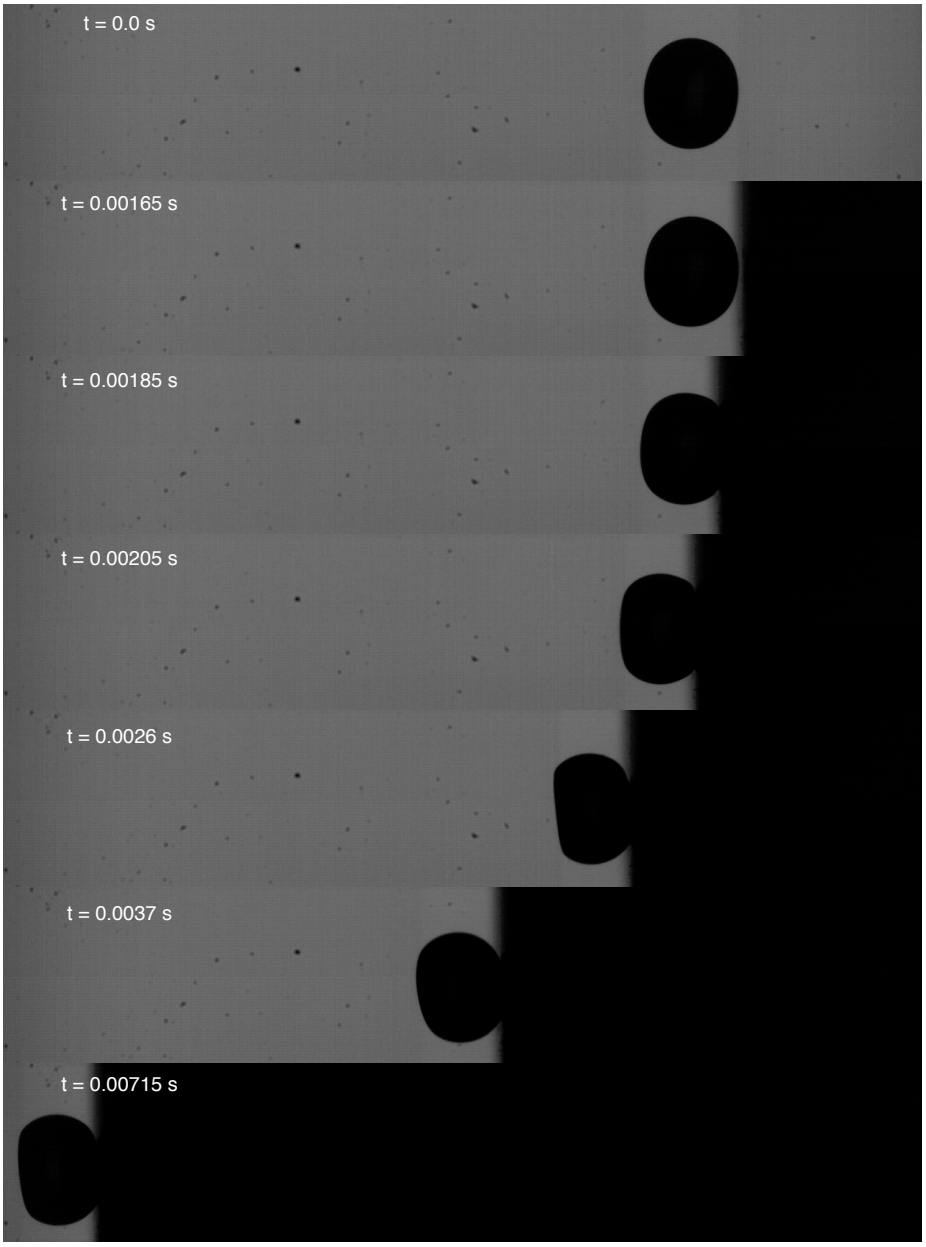

Figure 28: Different frames from a high-speed recording of a sticky droplet which was impacted with a teflon tip on the piston. The time for each frame is written in the figure.

5 Particle Impact

In this chapter the impact between a wet particle and a wall will be considered. The modelling work done to understand the impact covers a couple of different topics. Modelling includes a Finite Element Method (FEM) model developed using the COMSOL microfluidics package. Observations were made from the resulting simulations, which lead to analytical modelling done to understand those results. The ultimate purpose of this chapter is to understand the observations made in the experiments and provide scaling arguments specifically for a stickiness criteria as industry might use it.
Studies of droplet(s) impacting a surface, often a wall, are plenty and span both experimental and modelling work. A comprehensive literature survey of this will not be given here, because none are directly relevant to the topic of stickiness. [Yarin, 2006] gives a review of drop impact dynamics which include discussion of numerous attempts at modelling the phenomena involved. A few other representative examples would include a model of water droplets rebounding upon collision by [Foote, 1974], modelling of adherence and bounce of liquid droplets impacting a dry surface by [Caviezel et al., 2008] and the impact of liquid drops upon various solids of different wettability by [Sprittles and Shikhmurzaev, 2012].
It is because the literature on the topic of partially dried particles, inhomogeneous droplets or another suitable analogue, impacting a wall does not exist that a modelling study was performed as part of this work. The following is the result of that study.

5.1 Introduction to Method

Finite Element Methods are often used to solve equations used to model flow or transport problems. The topic of FEM is huge and it is unreasonable and unnecessary to cover in detail here. In the following a short introduction will be given. The method basically consists of dividing the geometry in which you work into a number of smaller segments. The model equations to be solved are discretized into many equations which are simpler to solve. Each equation in the original model gives one equation per segment after discretization. Typically these equations are algebraic for a steady state model, while being ordinary differential equations for transient problems. This produces a large system of equations which may be solved numerically by any number of methods appropriate for the particular type of equations obtained. Note that the mesh (basically the way the domain is divided into segments) can be constructed in many ways, with more segments typically leading to more accurate solutions. More detailed introductions may be found in the books by [Desai, 2001], [Brenner and Scott, 2007] or [Johnson, 2009].
Problems solved with Finite Element methods include problems of flow in the formation and break-up of liquid bridges. These problems however have the added complexity of multiple fluids and interfaces between these, which will also be the case in the problems of stickiness. As an example consider the simulation of a droplet moving in a gas. One

fluid will be the viscous droplet and the other the fluid is the air around the droplet. Depending on the method, you might describe the particle itself as a multi-fluid system, e.g. a highly viscous skin over a core with a lower viscosity (as will be the case here). Usual finite element methods are unable to handle this but additional tools have been developed to work with standard FEM which allows it to handle the free surface problems relevant here. The basics of some of these will be described below.
Lagrangian methods can be used to model some flow problems with multiple fluids while including surface tension, but the moving meshes cause problems when topology changes are involved, such as those occurring during drop coalescence and break-up of liquid bridges. At the onset it was impossible to know whether any form of break-up might occur but the contact with the wall may also cause problems, so the Lagrangian methods are not optimal for the study of stickiness. In the case of a core/skin-divided particle it is also conceivable that the skin might thin and break, which would also cause problems with a Lagrangian approach.
Some Eulerian methods have been developed as well and because of the way they have been designed they handle topology changes naturally, although some cases require fine meshing near interfaces. The two most common methods will be mentioned here and for both these methods surface tension is treated as a body force which is only included in cells near the interface. This additional force is easy to calculate and handle using the algorithms already available for finite element methods although attention must sometimes be directed at their accuracy as is elaborated upon in the following.

Volume of Fluid Method
The volume of fluid (VOF) method was introduced by [Hirt and Nichols, 1981] and uses a so-called VOF function to track the fluid interface in the system. The VOF function (C) is a volume fraction made up by fluid 1. As such it can be expressed as follows:

$$C_i = \begin{cases} 1 & \text{if cell } i \text{ is in fluid 1} \\ 0 & \text{if cell } i \text{ is in fluid 2} \end{cases} \tag{13}$$

For cells that are not entirely in one or the other fluid phase the VOF function is between 0 and 1. The exact value is defined by the fraction of fluid 1 in the specific cell. A sketch of this can be seen in figure 29.

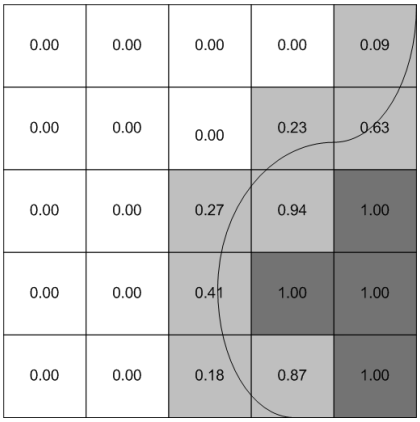

Figure 29: Sketch of VOF fluid interface tracking, with estimated values. Note that dark grey cells is one fluid (fluid 1 e.g. liquid), white cells are another fluid (fluid 2 e.g. gas) and light gray areas are cells in which the interface runs - redrawn from [Egholm, 2008].

Calculating the surface tension at a given position requires the local curvature of the interface. The local curvature is calculated based on the derivative of the normal vector along the interface. The very simplest approximation is when the interface is kept parallel to the cell walls which gives a very crude interface representation. A slightly more complex but still computationally fast approximation is obtained by drawing a linear representation in each cell with a normal vector calculated from the value of C in the neighboring cells. Both of these are fairly simple and more advanced schemes may be applied in order to obtain more accurate normal vectors, which again may help in the determination of surface curvature necessary to calculate surface tension forces.
The general solution procedure for a problem using the VOF method requires moving the interface, which is effectively done using a convection equation as follows:

$$\frac{\partial C}{\partial t} + \mathbf{v} \cdot \nabla C = 0 \tag{14}$$

, in which $\mathbf{v}$ is the velocity field.
Basically the procedure is as follows after the problem has been initialized:

- Solve the transport equations relevant for the problem, including the momentum balance.
- Convect the VOF function using the velocity field obtained from the previous step.
- Produce a new interface approximation using whatever algorithm has been chosen.
- Move to the next time step and repeat until the final time step has been reached.

The VOF method has the distinct advantage that the mass of each fluid respectively is conserved excellently. This however is counteracted by a disadvantage the method has in

the difficulty in calculating surface curvature, which is required to model surface tension accurately. Several authors have suggested various methods to mitigate or solve this problem. These have been compared by [Gerlach et al., 2006] and it showed that for most applications the Combined Level Set and Volume of Fluid (CLSVOF) method is accurate and computationally the fastest. This is basically a mixture of the two main methods described in this section, so for more elaboration see below.
Because of the relative weakness of the method in regards to surface tension there are not that many highly relevant published examples of application but one can be found by [Nikolopoulos et al., 2009] who modelled droplet collisions.

Level Set Method

The level set method (LSM) was first introduced by [Osher and Sethian, 1988] in which they used a basic version of the LSM that we know today to model curvature dependent movement. At this point it was not directly linked with surface tension, but rather flame propagation and crystal growth. This ability to include curvature dependent effects is the strength of the LSM and also what makes it suitable for stickiness modelling in case those effects are of importance. The method was later refined to the method used today by [Sussman et al., 1994].
The general idea is that you have a level set function, typically signified as ϕ, which is the distance to the interface. The function is positive in one fluid and negative in the other. As such the 0 level of this function ($\phi = 0$) is the position of the interface between the two fluids. Both fluids can then be modelled using a single motion equation and continuity equation where density and viscosity properties can be included as functions of the level function ϕ. To avoid discontinuities these are made as smooth transitions across a few cells near the boundary. The concept of the level function is sketched in figure 30.

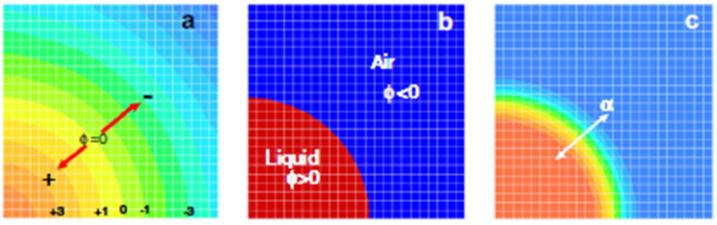

Figure 30: Sketch of the LSM fluid interface tracking. a shows the level function, b shows the interface and c shows the narrow region across which fluid properties transitions - adapted from [Deganello et al., 2011b].

As with the VOF function in the previous method the level function is moved using a convection equation typically written as follows:

$$\frac{\partial \phi}{\partial t} + \mathbf{v} \cdot \nabla \phi = 0 \tag{15}$$

This equation is obviously similar to the equation used to convect the VOF function, which is because both are just regular convection equations. While this equation moves the interface as desired it does not preserve ϕ as a function describing the distance to the interface and as such it must be reinitialized between each time step. It also follows from the equation that ϕ is only moved after the motion and continuity equations have been solved to obtain $\mathbf{v}$ for the next time step, which means the solution procedure is also similar to the VOF method with only small changes. For good measure the solution procedure is summarized below:

- Solve the transport equations relevant for the problem, including the momentum equation.
- Convect the level function using the velocity vector obtained from the previous step.
- Reinitialize the level function so that it once again becomes a distance function to the interface.
- Move to the next time step and repeat until the final time step has been reached.

Many interesting studies have been published using the LSM. [Shepel and Smith, 2008] gives a review of surface tension modelling using the level set method and includes a number of examples. In his work [Balabel, 2012] modelled collision of droplets in two dimensions with various outcomes. Some of the more advanced work includes the study by [Zhao et al., 1996] in which multiple level functions were used to model more than 2 phases in flow problems, the work with surfactants made by [Xu et al., 2006] and the introduction of force based model for dynamic contact angles at the point where two fluids and a wall intersect given by [Deganello et al., 2011a]. This method was applied to a more relevant case by the same authors ([Deganello et al., 2011b]) in which stretching of a liquid bridge was modelled. Work has not yet been published showing if the method can handle initial contact or break-up where one fluid completely leaves the solid surface.
Something that users of this method must always be aware of in spite of its elegance in describing interfaces is that the method does not always accurately conserve the mass of each individual fluid. As such it has the opposite problem of the VOF method. Some attempts at reducing the problem of mass conservation that sometimes appear with the LSM have been published. [Wang et al., 2008] has published a comparison between the so-called Particle Level Set (PLS) and the CLSVOF methods. The basic concept of both methods is to use tools to recalculate the level function right after it has been convected. In the PLS method a band of imagined particles are initiated along the interface. Just like the level function these are convected and the particles through which the level function no longer passes are used to correct the level function after the convection. The level function is then reinitialized and corrected once more. The particles then have their radii readjusted such that they only just touch the interface and they are redistributed so the

interface is covered well. It is then time for the next time step. In the CLSVOF method the interface is tracked using the VOF function introduced in the previous section and the normal vector determined using the level function. Based on these two methods the interface is reconstructed and the level function is reinitialized as a distance function. These two steps basically make up the CLSVOF method. The re-distancing of the level function is comparable to what was seen in the pure LSM but the interface reconstruction is different. The purpose is to locate the interface based on the discrete VOF and level functions which serve to achieve mass conservation.
[Wang et al., 2008] concluded that both methods were far superior to the conventional LSM in mass conservation. They also found that for standard tests the PLS method was better but that for applied flow problems the CLSVOF method showed more realistic results than the PLS method. They also found that the PLS method was easier to implement when compared to the CLSVOF method but computationally slower for three dimensional problems.

5.2 Setup

The introduction to methods above mention several complicated methods, but a larger study of numerics was not the objective here, so these were not implemented specifically. The simulation software COMSOL however has an implementation of the level set method with some of the numerical tools for minimizing mass conservation problems (i.e. a version of the CLSVOF method).
The COMSOL software is a tool for solving multiphysics problems using FEM models. For this specific problem tools from the standard COMSOL Multiphysics package as well as their Microfluidics module is used. The latter allows us to use the Level Set Method mentioned above. Because of COMSOL's modular structure, it is possible to use multiple level set functions at once, thereby allowing us to simulate more than two phases. This will be used to simulate the impact between a viscous wet particle with two different phases and a solid wall. The three fluid phases relevant in that scenario are the two phases inside the particle itself and the air around it. The handling of the solid wall will be discussed later. The setup in general will be described in the following, including description of the handling of the two level set functions and how they are applied in the modelling of the material functions of the different phases.
A brief aside; the model mentioned earlier which was developed by [Zhao et al., 1996] was not used here because it is much more complex than is necessary. The model they presented is a comprehensive numerical model, which for the sake of robustness is quite complicated. Here, a very limited case is to be studied, so this same robustness is not necessary and we have no need for explicit options for more than three fluids. Because of this and to save time, the method was not implemented and instead the COMSOL option was pursued.

5.2.1 Geometry and Mesh

A simplified geometry was used. We saw in the experimental section that the droplets could take different geometries during drying, the most predominant one being a shape which was somewhere in between a torus and an ellipsoid. Here - for simplicity's sake - spherical droplets were modelled. This made the model much simpler because axisymmetry could be applied. The domain was a rectangle, with two concentric semi-circle. This is shown in figure 31.

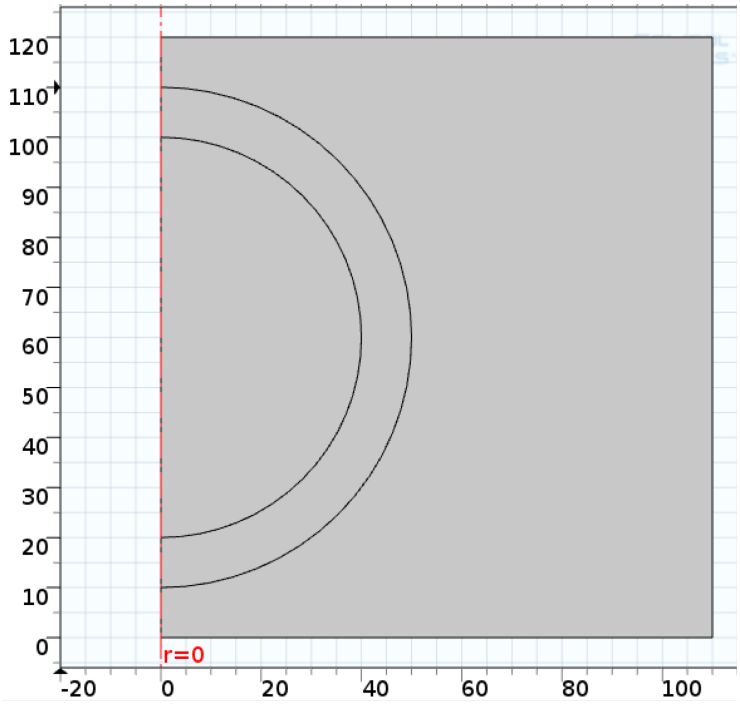

Figure 31: Print of geometry from COMSOL. Axis annotations are in micrometers and the vertical axis is the center of the axi-symmetry.

This covers all three relevant zones in the model. The inner-most semi-circle is the wet core of the particle (low viscosity liquid), the semi-circle around this one is the skin (high viscosity liquid) and the rest is the surrounding air (a gas). The specific parameters are all controlled from a central tab, where R, β, ρ_a and ρ_l and the three different viscosities η_c, η_s and η_a (core, skin and gas respectively) are defined. If R is changed, the width and height of the rectangle, the radius of the core and the distance from the particle to the wall are all corrected so that they remain correlated in the same way. Thus, if β is changed, only the core radius is changed.
For the meshing, COMSOL's standard methods were used. The "Physics-controlled mesh"

option pre-programmed was used with different element sizes (to ensure the solutions weren't significantly dependent on the mesh), with the default option used here being "Finer". Furthermore, in an attempt to increase accuracy while keeping calculation time reasonable, "Adaptive mesh refinement" (also pre-programmed) was used. This refines the mesh in the vicinity of the different interfaces in the system. This automatically includes both the gas-skin and skin-core interfaces in the system. The initial mesh is shown in figure 32, where a second, adapted mesh is shown, simply to show how it changes.

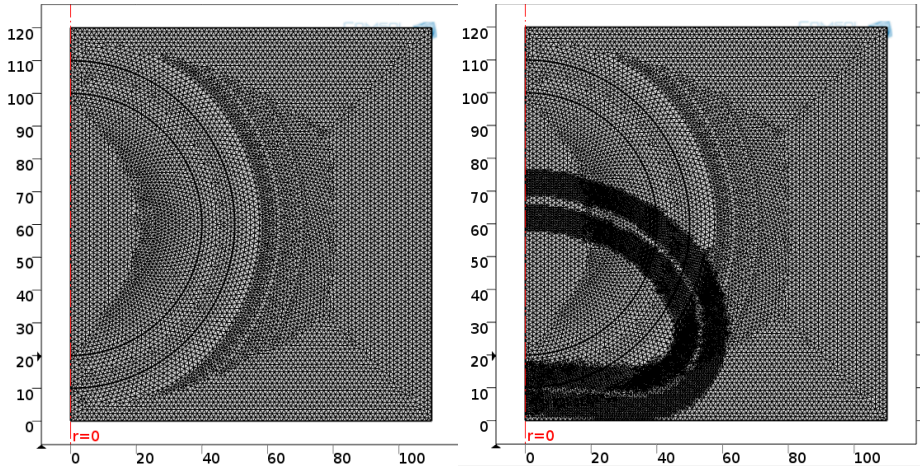

Figure 32: Print of 2 different meshes from COMSOL, used to solve the problem. Axis annotations are in micrometers and the vertical axis is the center of the axi-symmetry. The second mesh is adapted, with mesh refinement around the two interfaces in the system.

The original mesh (shown left in figure 32) contains 17770 triangular elements, while the adapted (shown right in figure 32) contains 29391.

5.2.2 Parameters and Parameter Space

Here the parameter space will be described. This includes brief description of the parameters, listing the parameter space and detailed information about the way the level set functions were used to produce global density and viscosity functions, which were locally accurate.

The system was described with geometric parameters, initial conditions and material parameters. The geometric parameters of relevance are the radius R of the particle, the radius of the core relative to the radius of the particle β, the distance from the center of the particle to the wall and the height and width of the rectangular domain. In all cases the particle's center was $1.2R$ from the wall and the height and width of the domain was $2.4R$ and $2.2R$ respectively. For $R = 50$ μm this leads to the geometry shown in figure 31. The only initial condition needed in this setup was the initial velocity v_{imp}, which was

used to describe how the particle met the wall, and was always in the direction of the wall along the symmetry-axis.
The material parameters were viscosity, density and surface properties. The latter will be adressed later in this paragraph. The viscosity was different in all of the phases modelled, namely particle core, particle skin and the surrounding air. These were named η_c, η_s and η_a respectively. The density inside the particle was set constant as a simplification, while the density of the surrounding air was given a separate value. The names of these were ρ_l and ρ_a for the droplet and air respectively.
Normally in the level set method implemented in COMSOL the user is assisted in assigning the correct parameters to each phase, but because this model uses the framework to model three phases this is no longer an option. The program is not setup for this, so it does not contain an algorithm to determine the material parameters in each phase based on two different level set functions. Instead this is introduced manually. This means that where normally the user inputs the density and viscosity of each fluid in different places, here we input the same parameters for both fluids in both modules, but make sure those parameters are functions of the level functions, such that the correct density and viscosity values result.
In order to do this properly, it is necessary to know how the level set functions are defined specifically in COMSOL. We are working with two different functions named ϕ_1 and ϕ_2, which are the level functions of the two different modules respectively. The first one is 0 inside the particle (the two semi-circles in figure 31) and 1 outside, in the air. The second one is 0 inside the core of the particle (the inner semi-circle in figure 31) and 1 in the skin and air. This means they can be expressed as follows:

$$\phi_1 = \begin{cases} 0 & \text{in particle core and skin} \\ 1 & \text{in surround air} \end{cases} \tag{16}$$

$$\phi_2 = \begin{cases} 0 & \text{in particle core} \\ 1 & \text{in particle skin and surrounding air} \end{cases} \tag{17}$$

Note that in the vicinity of the interfaces where either functions changes from 0 to 1 (or vice versa), the equation above is wrong, because the functions change continuously from one value to the other. The width of this transition zone is mesh dependent.
Having defined ϕ_1 and ϕ_2 we can proceed to define the two material properties that depend on these. The viscosity function is slightly more complicated than for usual level set methods, because both level set functions are needed. The function used to obtain the results discussed later were obtained with the following expression:

$$\eta = \eta_c + \phi_1 (\eta_a - \eta_s) + \phi_2 (\eta_s - \eta_c) \tag{18}$$

This expression is linear and satisfies the requirements for this problem. During early testing a non-linear function was used instead and did not appear to cause any problems, but because this is a simpler expression and because the results appeared the same, the linear function is recommended for future use.
When $\phi_1 = 0$ and $\phi_2 = 0$ the viscosity of the core is used. Moving outwards, into the skin, ϕ_1 remains equal to 0 while ϕ_2 changes to 1. Thus η_c is cancelled out and the viscosity becomes equal to η_s. Moving further out into the air ϕ_1 changes to 1 as well and the viscosity becomes equal to η_a.
The density function was defined as follows:

$$\rho = \rho_l + \phi_1 (\rho_a - \rho_l) \tag{19}$$

This equation can be see to be simpler than the one used for viscosity which is because it is chosen to keep density constant throughout the particle (this is justified below). It is linear and is seen to be equal to ρ_l inside the droplet and ρ_a in the surrounding air and so is considered to satisfy all requirements.
Throughout this it has not been addressed what happens when $\phi_1 = 1$ and $\phi_2 = 0$. This is unaddressed in the equations used and this was a worry during early testing, but it turns out that during none of the simulations carried out, this was ever close to occurring. It is unclear whether it is numerically possible for it to happen, but it cannot easily be ruled out completely. It is concluded that it was not an actual problem in this specific model.
Finally the surface tension of the interfaces in the system must be chosen. There is no actual, physical surface inside the particle and so the surface tension is neglected in level set module 2, but module 1 contains the interface between the skin and the surrounding air and here a surface tension γ was used. This is simply specified in the module, under interface options.
The simulations were run with a set of default parameters, and to obtain results a single parameter was varied at a time. The default parameters were as shown in table 3.
A few notes will be made about these parameters. The density of water was used in the droplet. This particular value was chosen because skim milk density is only slightly higher than water (commonly available values are in the range of $1020 - 1050\ \frac{\text{kg}}{\text{m}^3}$ - [EngineeringToolbox, 2015a] is one example of a source). The density of the dry powder is a bit more difficult to assess because it depends on powder packing, but it is in the same order of magnitude (see for example [Sharma et al., 2012]). Because so little difference is seen it is just set to a simple value and then varied as part of the parameter investigation later. The density of the surrounding air was chosen approximately equal to the density of air ([EngineeringToolbox, 2015b]).
The radius corresponds well with those of spray dried droplets. They vary significantly, but this one is in the range of industrial scale dryers ([Masters, 2002]). β is completely unknown, because - as stated earlier - no drying model has been sufficiently verified to be

able to predict internal composition without fitting a number of parameters. The impact velocity is based on a fairly rough estimate made using CFD simulations of spray dryers (discussed in the section on choice of parameters for the impactor experiments, see section 4), but once more this value falls somewhere in the middle of the expected region.

Table 3: Default parameters for the COMSOL simulation of a two-phase particle impacting a solid wall.

Parameter	Value
R	$50\,\mu$m
β	0.8
v_{imp}	$3\,\frac{\mathrm{m}}{\mathrm{s}}$
ρ_a	$1\,\frac{\mathrm{kg}}{\mathrm{m}^3}$
ρ_l	$10^3\,\frac{\mathrm{kg}}{\mathrm{m}^3}$
η_a	10^{-5} Pas
η_c	10^{-3} Pas
η_s	10^{0} Pas
γ	$4 \cdot 10^{-3}\,\frac{\mathrm{N}}{\mathrm{m}}$
θ	0.7π

The surface tension was chosen as a value close to the real value of surface tension for milks ([Bertsch, 1983] and [Mukherjee et al., 2005]). The contact angle was chosen at random, but as will be discussed later it turned out to be inconsequential. The viscosities of the fluids in the droplet were the parameters furthest from real, known values (β not included) and this was for practical reasons. The viscosity of surrounding air represents a fair estimate in the area of interest, which is closer to $2 \cdot 10^{-5}$ Pas ([EngineeringToolbox, 2015b]). The viscosity in the core was much higher than that of skim milk ([Bakshi and Smith, 1983]). This was chosen with consideration of numerical issues occuring if the change in viscosity was too high. Finally the viscosity of the skin. This value was once again chosen to be much lower than the cited values of particle in the sticky region (many authors working with stickiness refer to [Downton et al., 1982] for viscosity values of $10^6 - 10^8$ Pas and in the model by [Palzer, 2005] discussed in the literature section values of $10^8 - 10^9$ Pas was used with reference to [Sperling, 1986]), which again was because of a worry about numerical stability. These will be discussed more in the results section later.

5.2.3 Other Implementation Details

Having described the setup of geometry, mesh and the parameters included there are still a few more items to address. These will be done in no particular order, except for a brief mention of the actual execution at the end. The movement of the droplet towards the wall is only driven by initial motion. The initial condition is the flow-field, which will be v_{imp} in the direction of the wall for cells that are within the particle and 0 in the air around the

particle. The velocity of the droplet is assumed homogeneous before coming into contact with the wall and while the air flow is not actually stagnant in the real system, it could not be expected to be systematic. The air however, is not expected to have a significant impact on the droplet in the form of drag or similar, so it is not expected that this particular initial flow pattern will lead to any significant errors. The specific implementation is to make the flow-field as follows in the entire domain:

$$v = v_{imp}\,(1 - \phi_1\phi_2) \tag{20}$$

This is a non-linear equation, but since this equation is not part of the system of equations to be solved later it has no implications for the numerical work of solving the model.
Note that in this case the direction of the initial velocity is always directly towards the wall. In case of a larger study of velocity effects the perpendicular direction would be the obvious base case, but here it is also a direct consequence of the axi-symmetry approximation. Consider the case where the angle of approach is anything different from perpendicular. It cannot be done in a two-dimensional, axi-symmetrical system. That flow field would be such that in the three-dimensional system all points would move in the direction of or from the symmetry axis, which by no means reflects the expected flow pattern. Thus, it would increase the numerical complexity greatly to investigate other directions. A few thoughts to the effects of a different angle of approach will be given in the discussion.
Any external boundaries that are not wall or symmetry axes are considered outlets in the COMSOL setup. In effect this is the upper and right most external boundaries seen in figure 31. In COMSOL, outlets can be defined in a number of different ways. In this system it is rather unimportant what happens at these boundaries so long as no problems arise as a result of how they are defined. The options in COMSOL are "Pressure", "Velocity" and "Laminar flow" and since nothing is well-defined and quantitative is known about the flow at the outlets, the "Pressure" option is used. The specific pressure is inconsequential, so a value of 0 is set. During early testing it was found that while it did not matter much, simulations were slightly more stable with the "Suppress backflow" option checked.
The topic of gravity has not been addressed in the description of the setup and it is not in fact included. It is not expected that gravity has a significant effect in the physical phenomena, because the time scale is so small. Furthermore, even if gravity was important, it would increase the complexity significantly to properly implement it. Consider the walls shown in the rough sketch in figure 1. The direction and therefore effect of gravity relative to the wall is very different depending on whether the particle is hitting the cone of the cylinder region of the dryer wall. In none of these situations the gravity would act perpendicular to the wall - neither towards nor away from. This means that beside introducing at least one new parameter to vary (the direction and to some degree the magnitude of the gravitational effects) the model would have to be changed into a

three dimensional space - similarly to non-perpendicular initial velocities. Instead, just a few minor thoughts on the topic will be given. Because the gravitational effects would never be directly, although in some cases partially, towards the wall it is doubtful that gravity will significantly increase the contact area between droplet and wall. Rather, in many cases gravity is one of the two primary reasons a particle would fall (the other, and probably dominant one being drag) after initial impact. Therefore, it is not considered a flaw in the model presented here that gravity is not included.
The program is now ready to compute when the desired simulation time is put in. Simulations were completed when they had reached $2.5 \cdot 10^{-4}$ s for results here, which was significantly past the initial impact phenomenon. Computation took approximately 4 to 6 hours on a computer with a 8 GB ram.

5.3 Results

5.3.1 General Results

The results of the COMSOL simulations will be separated into a number of sections. This first one will describe the results in a general fashion, which will include qualitative description of the observations made for the simulations and the method for determining the spreading parameter r_{spr} which will be used to compare results during parameter variations. After this general description of results a smaller section for each parameter varied will follow.
First, the results obtained. For all the parameter variations tested the general, qualitative observations were the same. That is to say; the description given in the following was seen in all cases, while quantitative differences (i.e. the amount of spreading and specific duration of impact motion) did appear. Figures 33 and 34 show different snapshots from a visualization of the droplet during the impact. The function displayed does not represent anything physical other than how the phases are distributed. Red colour signifies the core, yellow the skin of the particle and the blue is the air around it.

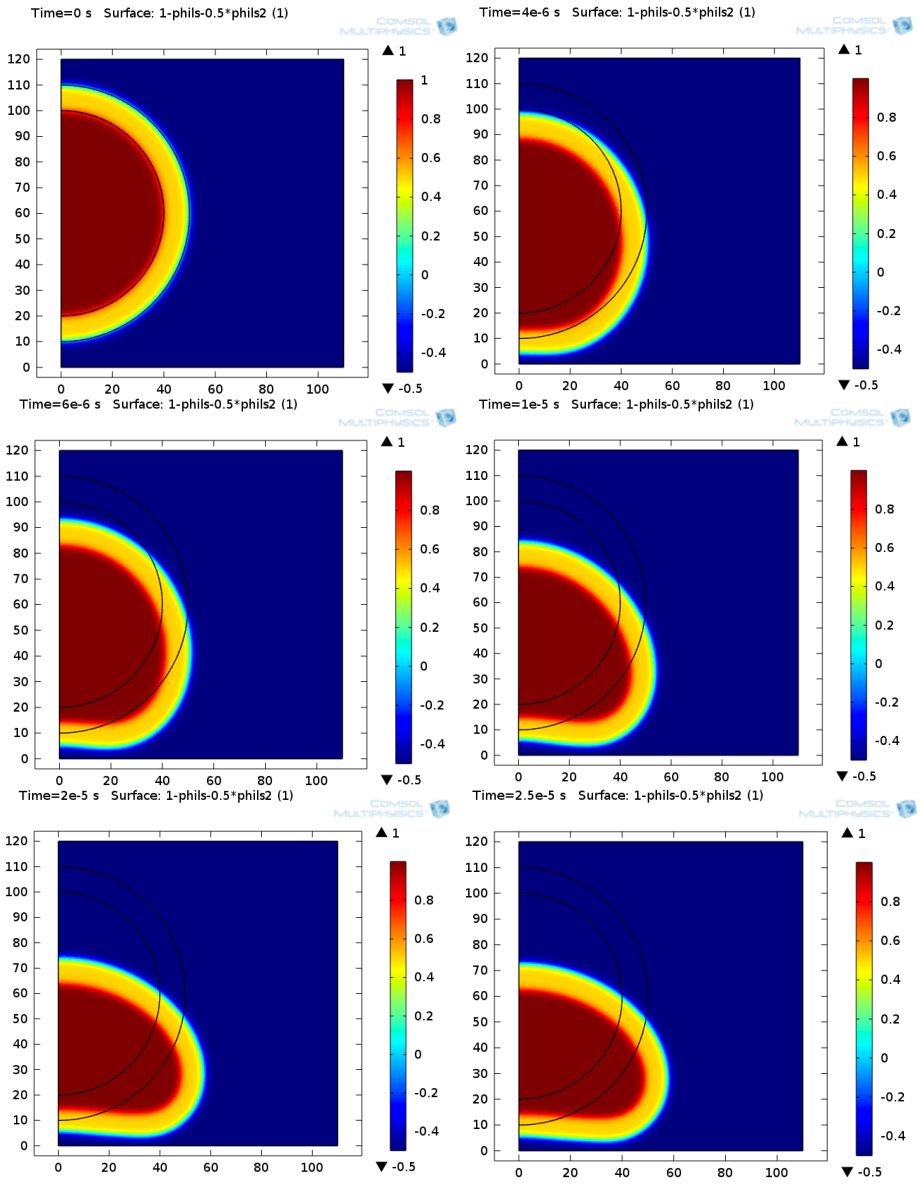

Figure 33: Frames from different times showing the phase distribution resulting from the COMSOL simulation. Times are displayed with each frame. Red is the core, yellow the skin and blue the air.

The first snapshot - in which the droplet is perfectly spherical - is the initial condition as visualized with this representation. After this, the position and shape of the droplet is shown at different times. As the droplet closes to the wall it starts to deform, slightly

at first but then more so. Early in the impact the part of the droplet near the symmetry axis, on the bottom stagnates and stops moving while the rest continues. This leads to the bottom of the droplet flattening at first and then curving slightly the opposite way. The point closest to the wall (the bottom boundary) thus moves further from the symmetry axis until a point when the droplet stops moving entirely.

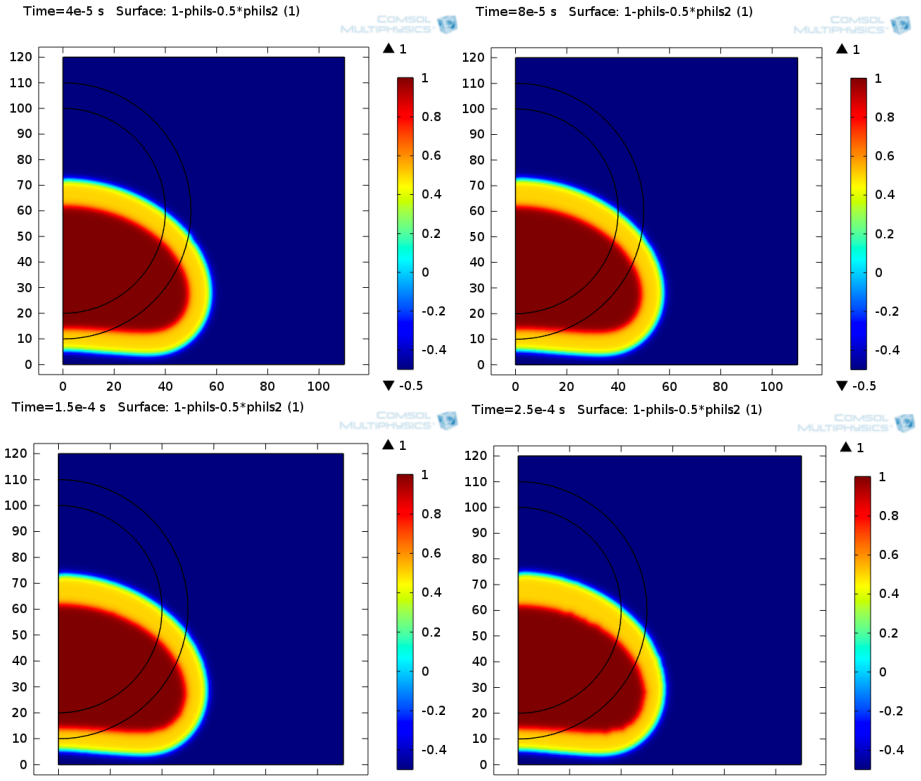

Figure 34: Frames from different times showing the phase distribution resulting from the COMSOL simulation. Times are displayed with each frame. Red is the core, yellow the skin and blue the air.

After some time the droplet would start to move slightly again, with the parts furthest from the symmetry axis moving the most, while the parts closest to the axis moving much less. This second motion is most likely because, at this point, nothing else is happening and so the effects of surface tension begin to become apparent, whereas when there were other events happening, the surface tension effects were negligible. The tension in the droplet surface is highest when the particle is deformed and so to minimize the energy, the droplet moves so as to minimize the surface curvature, which is lowest when the shape is fully spherical. Because the model contains no explicit elasticity this restoring effect of surface tension is the only effect resembling elasticity and this combined with the lack

of gravity is the reason why the particle remains near the wall after impact. some slight numerical instabilities can be seen in the last frame of figure 34, but these were of no consequence in general.
It is clear here that the droplet does not actually come into contact with the wall. This will be addressed at the end of the discussion section.
Notice that throughout the entire impact the skin thins only very slightly, to the point where it is barely visible to the naked eye. This was the case for all simulations produced in general. In no cases did it ever appear that the skin was even remotely approaching a breaking point. As such, these simulations are in strong opposition to a hypothesis of a breaking skin revealing a very wet core that then adheres to the wall.

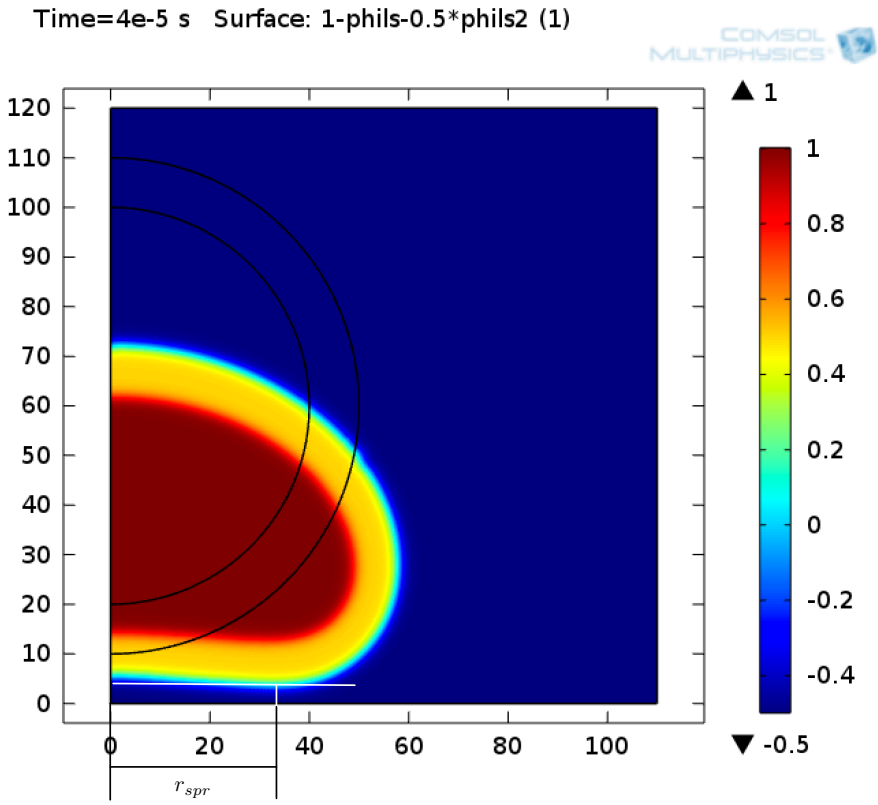

Figure 35: Screenshot from COMSOL simulation results showing how r_{spr} is defined. Units on axes are in μm.

In the interest of more quantitative investigation of the results a spreading parameter was chosen. A parameter similar to the radius of the contact area used in the analysis of the high-speed recordings will be used. It will be defined as the distance from the symmetry

axis to the point on the surface of the particle closest to the wall, at the point in time where the droplets' approach towards the wall stops. This is visualized in figure 35.
This parameter will be referred to as r_{spr} throughout even though it is not quite the same as in the high-speed recordings. Furthermore it will be scaled with the radius of the droplet at the start of the simulation, R, to correct for size differences.

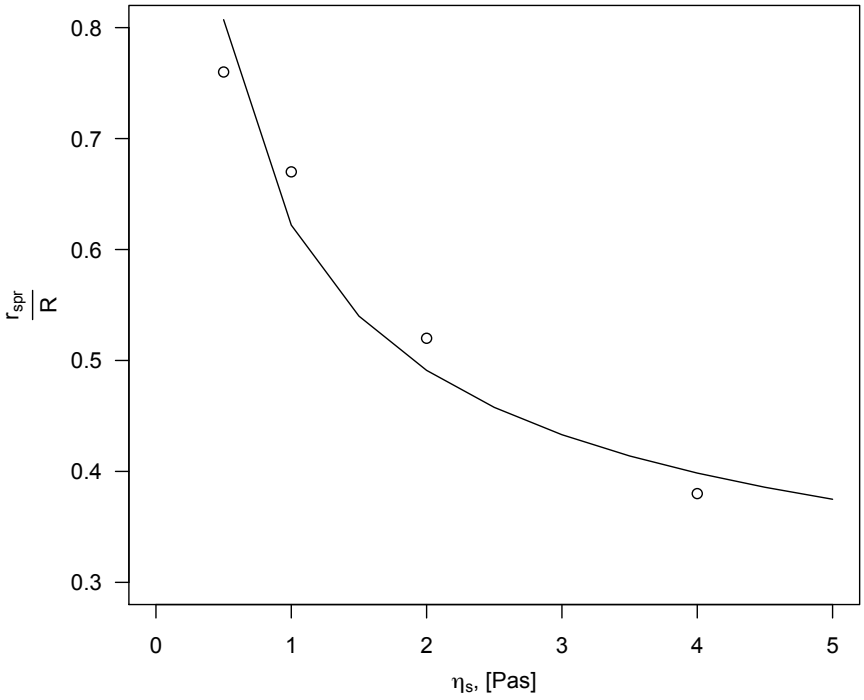

Figure 36: The deformation parameter $\frac{r_{spr}}{R}$ as a function of the skin viscosity η_s. The fit shows that $\frac{r_{spr}}{R} \propto \frac{1}{\sqrt{\eta_s}}$.

5.3.2 Varying Viscosity

The three viscosity parameters had very different effects. Variations in the viscosity of the air by an order of magnitude in either direction showed absolutely no effect on the results. Variations in the core viscosity only began to have an effect when it was increased a hundredfold, becoming a tenth of the viscosity of the skin. Here it is likely that the effect becomes comparable to a situation with a thicker skin. In the case of $\eta_c = 0.1\eta_s$ the spreading parameter $\frac{r_{spr}}{R}$ only decreased by 13.4%.
As could probably have been expected the most interesting of these three parameters turned out to be the viscosity of the skin. Significant effects were seen when varying it.

Figure 36 shows a plot of how $\frac{r_{spr}}{R}$ changes with changing skin viscosity.
The line drawn was a fit that resulted from trial an error but shows that there is a decent fit for a proportionality between the spreading parameter r_{spr} and one over the square root of the viscosity of the skin. This will be used in the discussion but for now it will also be added that increased skin viscosity shows a decrease in spreading and deformation. This is to be expected as a increased viscosity means that the same amount of energy can be dissipated with less deformation. Once more, this will be elaborated upon in the discussion.

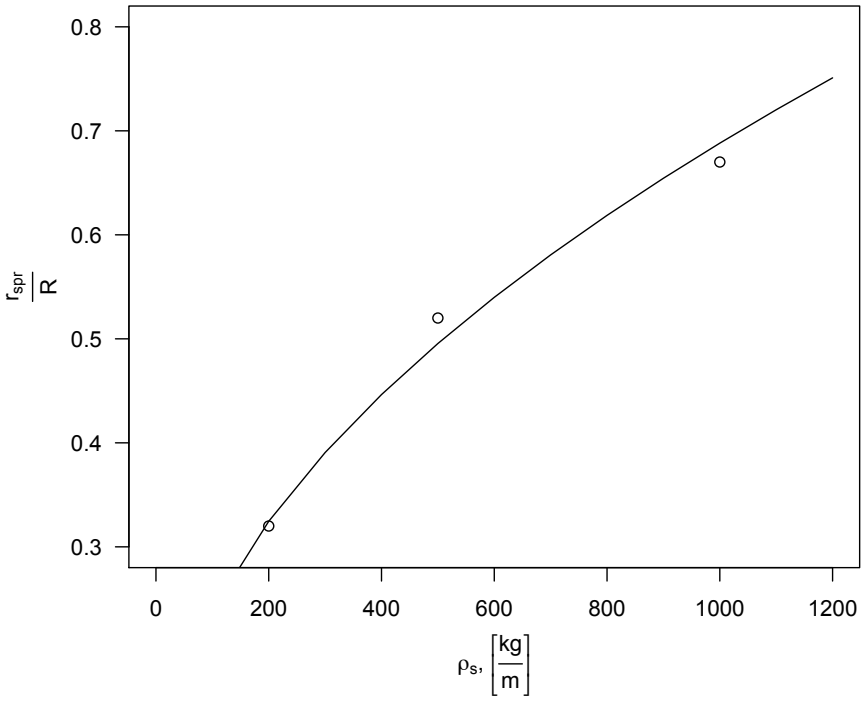

Figure 37: The deformation parameter $\frac{r_{spr}}{R}$ as a function of the droplet density ρ_l. The fit shows that $\frac{r_{spr}}{R} \propto \sqrt{\rho_l}$.

5.3.3 Varying Density

Varying the density of the air ρ_a showed no difference in results at all. This supports the hypotheses mentioned in this thesis and in the literature that it is the conditions (and flow) in the particle that matter and not the surroundings.
The differences observed with varying droplet density were significant and can be seen in figure 37.

It is seen that increasing the density of the droplet leads to more spreading and deformation. This leads to the natural suggestion that kinetic energy is the driver for spreading since there is no gravity in this model. A fit involving a square root is seen once more, however this time it is understandable if a critical reader were to suggest that a linear fit would also do very well here. For reasons seen later, this square root proportionality turns out to be very convenient.

5.3.4 Varying Impact Velocity

The initial velocity of the particle - referred to as the impact velocity - is quite literally the driving force behind the deformation of the droplet seen in the model and therefore it is expected that increasing the velocity leads to more spreading and vice versa. The actual results may be seen in figure 38.

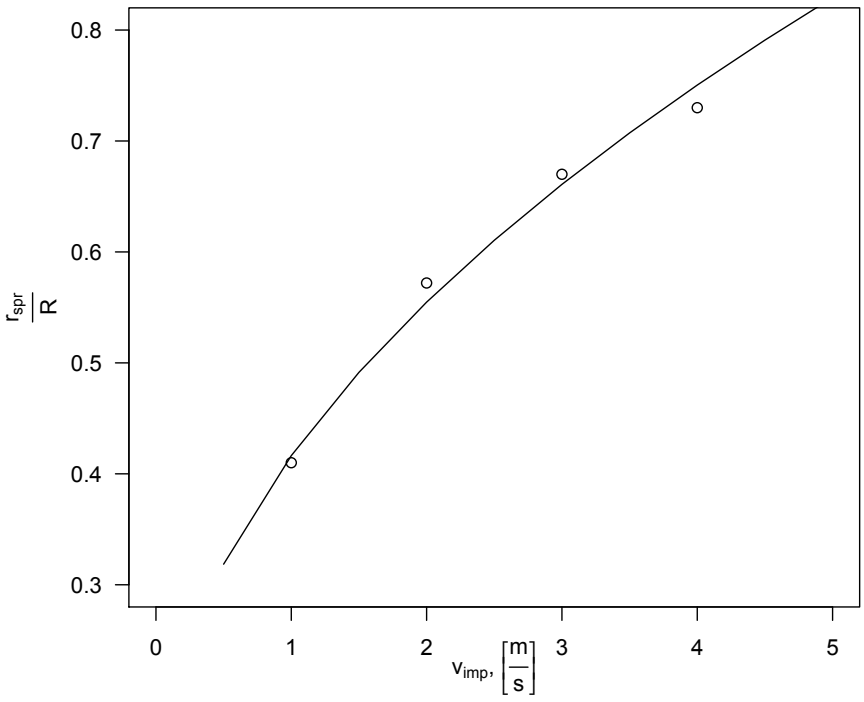

Figure 38: The deformation parameter $\frac{r_{spr}}{R}$ as a function of the impact velocity v_{imp}. The fit shows that $\frac{r_{spr}}{R} \propto \sqrt{v_{imp}}$.

As was fully expected, it is seen that increased impact leads to increased spreading. This is once more a good indicator that the important reason for spreading - and therefore, as

is hypothesized; sticking - is kinetic energy. This will be addressed in the discussion.

5.3.5 Varying Particle Size

The particle size is of utmost importance in the results, because the size is not the same in a spray dryer as in the single droplet dryer method used in this work. Thus, this model is meant to help scale the findings in the experiment so that they are applicable in relation to spray drying. Also, unlike velocity and to an extent density and viscosity, it seems non-trivial to predict how the problem changes with size. Remember here that β is kept constant so the actual skin thickness also changes in the problem, making it even more difficult to predict the outcome.

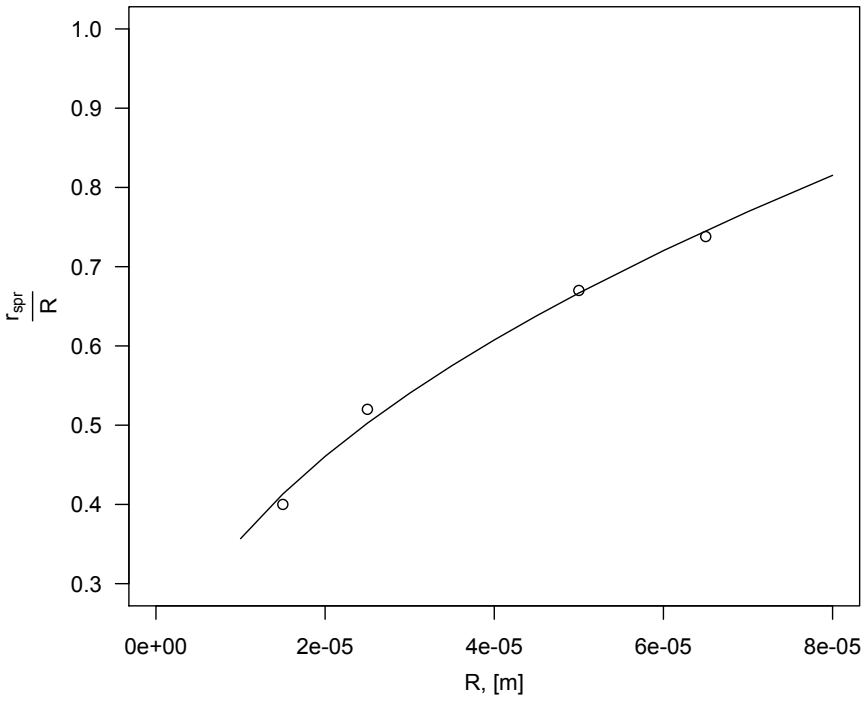

Figure 39: The deformation parameter $\frac{r_{spr}}{R}$ as a function of the droplet radius R. The fit shows that $\frac{r_{spr}}{R} \propto \sqrt{R}$.

Figure 39 shows the results of these simulations. Here it will once again be mentioned that both $\frac{r_{spr}}{R}$ and β are defined relative to the droplet size, which means an increase in droplet size with constant $\frac{r_{spr}}{R}$ and β also means an absolute thicker skin and an absolute larger spreading. Not only that, it turns out that $\frac{r_{spr}}{R}$ also increases which means the radius of

the circle of contact increases a lot when the droplet grows in size.
The square-root dependence shows up once more. This fit adds to the pattern that is emerging here and this proportionality is quite satisfactory.

5.3.6 Varying β

Finally the relative thickness of the skin will be investigated. This parameter returns us to the somewhat predictable because the larger the region of the droplet that has a high viscosity, the more easily energy should be dissipated in the impact. Thus; it is fully expected that decreasing β leads to decreasing r_{spr} - remember that β is the core radius relative to the particle radius, so decreasing it increases skin thickness. Exactly how the parameters correlate is much more difficult to predict. The results are shown in figure 40.

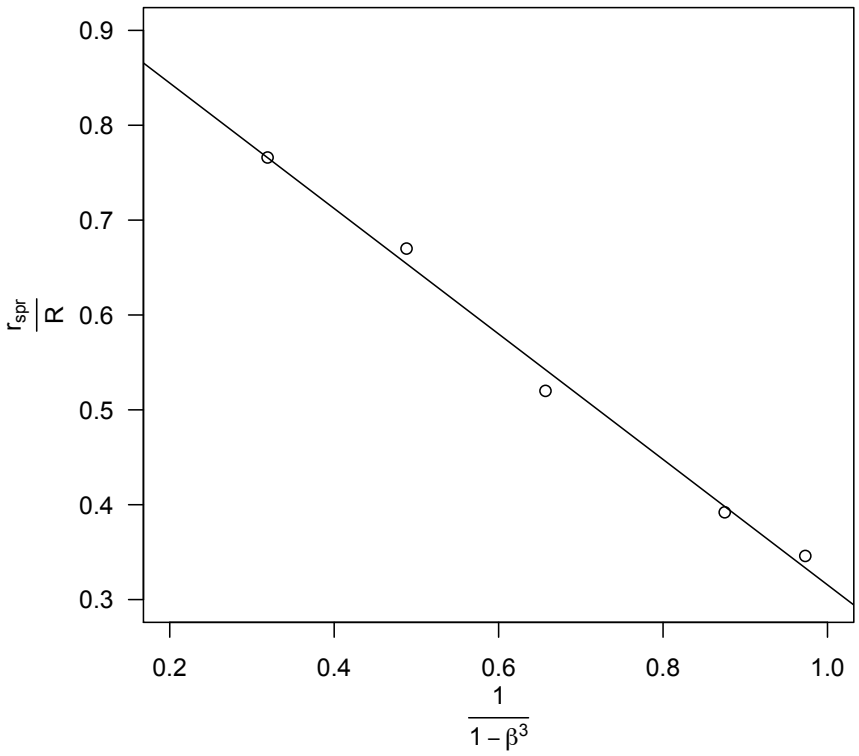

Figure 40: The deformation parameter $\frac{r_{spr}}{R}$ as a function $\frac{1}{1-\beta^3}$ in which β is the relative thickness of the skin. The fit shows that $\frac{r_{spr}}{R} \propto \frac{1}{(1-\beta^3)}$.

As expected these results show an increase in β leads to increased $\frac{r_{spr}}{R}$. As stated this

makes perfect sense. It turns out through some experimenting that $\frac{r_{spr}}{R}$ approximately moves with $\frac{1}{(1-\beta^3)}$. This means that during drying, just after the skin is formed a small change in thickness leads to big differences in potential spreading, which seems sensible. As the skin grows thicker, it takes a bigger difference in thickness to make a substantial change in the potential spreading.

5.4 Discussion

In this section an attempt will be made to combine the different findings from above and a discussion of them will be given with the purpose of understanding the results and with thoughts to how the findings may be used. The discusson will conclude with an analytical analysis with the purpose of furthering the understanding.

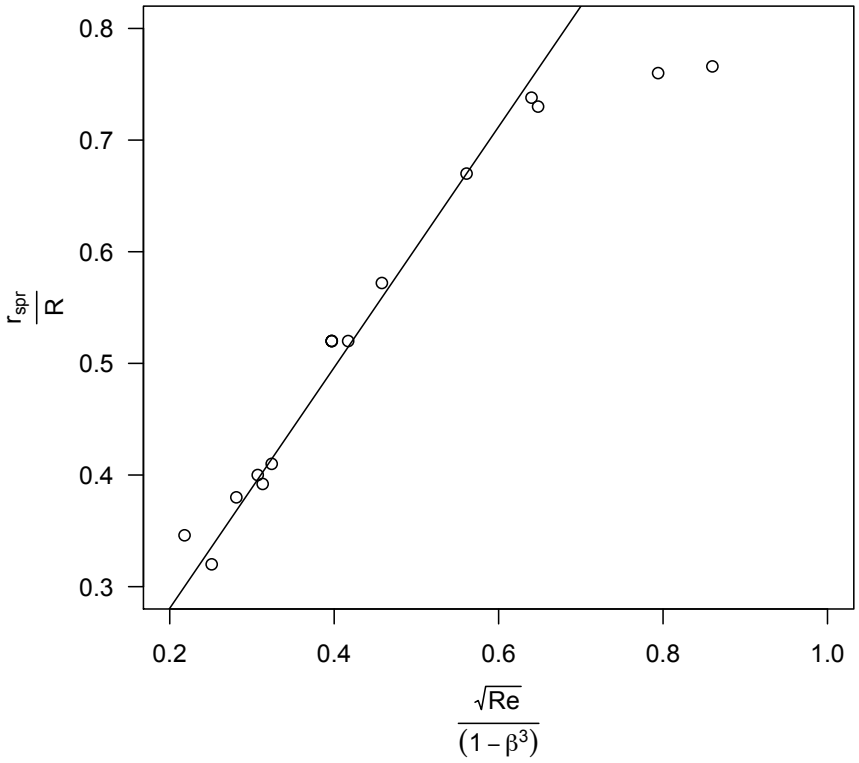

Figure 41: A plot showing the proportionality expressed in equation 22.

First off, an equation will be shown, which combines the proportionalities found in the

results section. This basically looks as follows:

$$\frac{r_{spr}}{R} \propto \frac{\sqrt{\rho_l}\sqrt{R}\sqrt{v_{imp}}}{\sqrt{\eta_s}\,(1-\beta^3)} \tag{21}$$

Notice that all the parameters in the nominator and the viscosity in the denominator show an important point. All of them are square-rooted and the combination of them in this way is the Reynolds number (if it is based on the parameters of the skin and the impact velocity of the particle). Thus, the relation becomes:

$$\frac{r_{spr}}{R} \propto \frac{\sqrt{Re}}{(1-\beta^3)} \tag{22}$$

This resulting proportionality is shown plotted in figure 41.
Apart from the two datapoints at the top that lead to a fit that is less convincing the fit is quite strong. This suggests that the resulting fit might become weak as the Reynolds' number increases, but examination of that region would be necessary to further understand it. The skin viscosity chosen however was actually smaller than the viscosity cited in literature, so the low-Reynolds' number region is the most interesting.
It seems reasonable that the most important parameters are those of the skin, and not the core or surroundings. Furthermore it seems quite reasonable that the Reynolds number is important, given that the only energy put into the system is the kinetic energy (since gravity or similar field forces are neglected) and the way the energy is consumed can practically only be through viscous dissipation. The only way energy could be stored - given that there is no elasticity in the bulk material - is in the surface. Surface tension tends to restore a spherical shape to a droplet, which means the surface 'stores' energy upon deformation which is regained when the particle reforms to a spherical shape. This effect could have mattered, but changing the surface tension γ showed that the effect is much too small for the relevant parameter space to have any significant effect. This point is only made more clear when considering the fact that in the real system the viscosities in the skin and possible core are expected to be even higher, leading to greater dissipation and therefore relatively less room for elastic effects of surface tension.
Although the difference in the viscosity cited in literature for sticky materials and the skin viscosity used here is significant it seems unlikely that increasing skin viscosity will change the observations significantly. The flow would still be laminar - the Reynolds' number is in the range of 0.03 to 0.2 - so it still seems likely that that part of the proportionality remains.
It was impossible to use β-values significantly lower than those used here with the mesh used, because the interfaces got so close that the skin was poorly defined. It is possible that a new model or an improved version of this one could help investigate possible effects of that. It is undeniable that a thinner skin could lead to different phenomena. As

stated previously, there was never any indication that the skin was even close to breaking or thinning significantly, but if the skin was much thinner this could become the case. Whether this ultimately reflects real, wet particles better than the simulations shown here is unknown, but the results of the slow motion videos might suggest so. The surface of the particles that was impacted at very high velocity seemed to deform differently from those impacted at a lower velocity and from the results of these simulations. This is an effect of inertia in the impact, which would decrease for smaller droplets like those inside a spray dryer, which should help mitigate this particular point of confusion.
The dependence on the Reynolds' number has been the focus up until this point because that is more easily explained. The β-dependence however deserves a short discussion as well. A little rewriting of the expression can lead to the following:

$$\frac{1}{1-\beta^3} = \frac{\frac{4}{3}\pi R^3}{\frac{4}{3}\pi R^3 - \frac{4}{3}\pi\left(\beta R\right)^3} = \frac{V_{drop}}{V_{drop} - V_c} = \frac{V_{drop}}{V_s} \tag{23}$$

The first change is simply to multiply with the volume of the droplet. From there it is simply to realize very obvious facts about the expression that appears. The end result is that the β-dependency in figure 41 appear to actually be a relation between the volume of the droplet and the volume of the skin. It is unclear exactly what this signifies.
Finally it will be mentioned that the particle did not come into physical contact with the wall in these simulations. A significant amount of time was spent trying to solve this problem, but to no avail and because of the way COMSOL was used it was impossible for to get helpful support in the time available. It is likely that the problem is a result of the width of the region in which the viscosity changed from the value in the skin to the value in the air. This effectively meant that in this model there was a thin layer of fluid around the particle with a viscosity much higher than the air (η_a), but also lower than that of the skin (η_c). Thus, when the particle came close to the wall, but before coming into contact, this layer with some non-constant viscosity higher than that of air would start to deform and energy would dissipate. Moving this air from between the particle and wall (necessary to establish contact) was thus very difficult and by the time the kinetic energy was spent, the particle had stopped moving. This is as stated the reason why the deformation was determined not by actual spreading. The question thus becomes whether it is a significant problem.
This is considered difficult to answer, but some thoughts on the topic: Any contribution to the problem that would occur at the triple line is lost. Imagine a liquid with highly wetting character (on this specific wall) and it is not at all unlikely that more spreading would occur, even at the short time scales relevant here. The results of the impactor experiments - section 4 - showed that when the droplets had barely been dried they spread easily across the wall, which shows that the liquid does wet the wall material. However, during the high-speed camera experiments with a Teflon surface the sticky particles did not show

any significant difference in their results, suggesting that the wetting does not matter after a certain amount of drying. This could very well be because the time scale for it to matter (traditional wetting is an equilibrium concept) is much longer than the effects that determine spreading and possible even because continued drying 'freezes' the triple line in place shortly after initial spread. If all that is important to the spreading, and therefore the determination of contact area, is internal flow - which seems reasonable from the results in this thesis - it is likely that the deformation modelled here is representative of the phenomena in the real, physical system.
In the general setup paragraph (under section 5.2) the direction of approach for the droplet was mentioned. As was stated there, investigating it would significantly increase the complexity of the model and therefore the computation time - most likely to such a degree that a significant increase in computational resources would be required. A few thoughts to the matter will be given here however. In the results of this simple model a correlation between the Reynolds' number and the spreading parameter r_{spr} was found. If, as was hypothesized above (and will be elaborated below), the important balance is between the initial inertia and viscous dissipation then it is suggested that any velocity component which is parallel to the wall is unimportant. Therefore, an effective velocity could be used in the correlation presented above instead of the actual velocity. This would be $v_{eff} = v_{imp} \cos(\omega)$ where ω is the angle between the direction of approach to the wall and perpendicular to the wall. Thus, the further the impact velocity is from perpendicular to the wall, the less spreading occurs and the less likely the particle is to adhere and stick. It is possible that a different effect could appear if the velocity is very large and close to parallel to the wall. In such a case it is possible to imagine the particle smeared across the wall, which would lead to a very different flow pattern inside the particle and therefore a different dissipation and so the relation presented above would most likely break down.

5.4.1 Analytical Analysis

A scaling rule for the impact of the inhomogeneous droplet with the wall has been obtained and in this section an analytical analysis will be carried out in the hope of lending further credibility to that rule but also some understanding. The analysis will be inspired by a mechanistic model based on viscous dissipation describing the movement of a triple line ([de Gennes et al., 2004] p. 142-144). That model was based on a case with a very small contact angle, which was used to simplify the flow pattern inside the wedge that makes up the fluid close to the triple line. The small contact angle assumption is important in the very first step of their analysis and so we will briefly discuss how they use that.
The slope of the wedge is constant and because it is very small it is $\tan(\theta) \approx \theta$. The velocity of the liquid at the wall is 0 (no-slip) and $1.5v$ at the surface $z = \theta x$ where z is the height, x is the horizontal distance to the triple line and v is the velocity of the triple line (see figure 42).

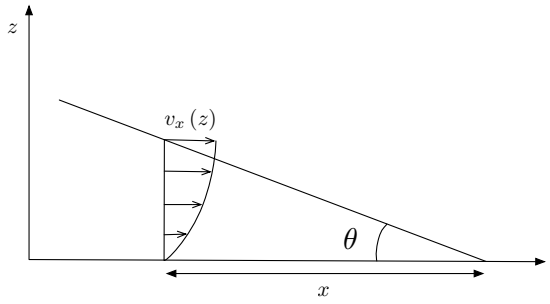

Figure 42: Sketch of the velocity profile near a triple line with a small contact angle - redrawn from figure in [de Gennes et al., 2004]

Because of this simplification the order of magnitude of the velocity gradient is known. This is used to derive a viscous dissipation term as

$$T\dot{S} = \frac{3\eta l}{\theta} v^2 \tag{24}$$

in which l is a dimensionless coefficient in the range of 15 to 20 (otherwise not described). [de Gennes et al., 2004] refers to other sources for further discussion and so I'll list them as well, however they will not be considered here ([Marsh et al., 1993] and [de Gennes, 1985]). In this case the dissipation might be different but it is not inconceivable that a zone exists inside the droplet, near the triple line which has a flow field similar to the flow field in the example described by de Gennes and his colleagues. Because of that, the complexity of the problem when the contact angle is large and because this is but an attempt to describe and understand the problem, this expression for the viscous dissipation will be used throughout.
Consider a droplet approaching a wall. Upon impact there will be a moment when the contact is a point. After this instant the contact line will be a circle, which expands while the net velocity of the droplet is still in the direction towards the wall. As the contact line moves the viscous dissipation will slow the droplet down and the kinetic energy is consumed. A figure which should help visualize the situation and some of the parameters can be seen in the sketch in figure 43.

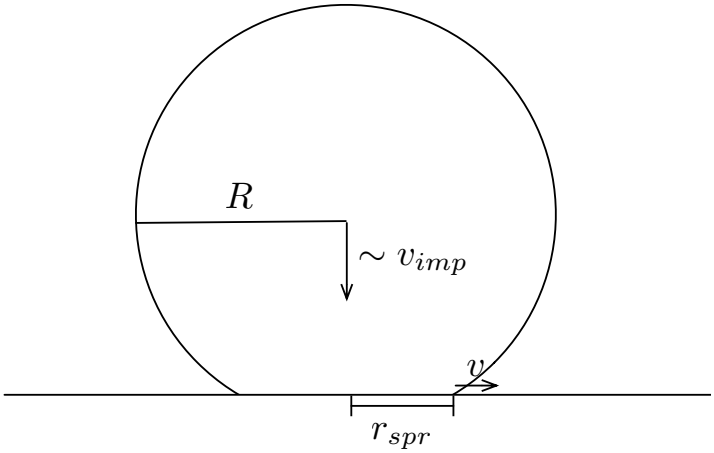

Figure 43: Sketch of the system analysed here, just after the wet particle hits the wall and contact is established including a few key parameters used. Note that the velocity is not exactly v_{imp} because the dissipation has begun, so the velocity is actually lower.

The final position of the line must be

$$r_{spr} = \int_0^\infty v\,(t)\,dt \tag{25}$$

Here, a very simple velocity function for the triple line will be assumed. It is completely unknown how the velocity behaves, but the simplest imaginable would be a constant velocity v_0 for a finite amount of time τ after which the triple line would stop moving completely. Such a velocity function would lead to the following:

$$r_{spr} = \int_0^\tau v_0 dt = v_0 \tau \tag{26}$$

A slightly more complex (although still simple) velocity profile can also be considered. It would make some sense if the movement was largest initially, when the kinetic energy is the largest and when the contact area is smallest. It also makes sense that the rate of decrease in velocity is largest when the approaching velocity is larger compared to later. Because of this the velocity of the contact line can be assumed to be as follows:

$$v = v_0 \exp\left(-\frac{t}{\tau}\right) \tag{27}$$

where v_0 is some characteristic velocity, thought proportional to the so-called impact velocity of the droplet, and τ is some characteristic time. Inserting this into the expression

above the following is obtained:

$$r_{spr} = \int_0^\infty v_0 \exp\left(-\frac{t}{\tau}\right) dt = v_0\tau \tag{28}$$

It can be seen that for these two specific velocity functions the result is the same. For now this result will be left as is, while the dissipation function is considered.
When a droplet impacts the wall the kinetic energy it had before the impact will be consumed in the viscous dissipation at which point it will stop moving (and other effects may take over). Therefore the two will be equated:

$$\frac{1}{2}mv_{imp}^2 = \frac{3\eta l}{\theta} 2\pi \int_0^\infty r \left(\frac{\partial r}{\partial t}\right)^2 dt \tag{29}$$

, in which the prefactor can be recognized from the dissipation term shown in equation 24. First a rearrangement leads to:

$$\int_0^\infty r \left(\frac{\partial r}{\partial t}\right)^2 dt = \frac{\rho R^3 v_{imp}^2}{\eta} \frac{\theta}{9l} \tag{30}$$

Solving this integral is quite difficult because nothing really is known about the contents of it. Once more a crude simplification is made. This is done because the interest is in an order of magnitude analysis, rather than in a perfect description. Assume again that the triple line moves for a period of time τ with a velocity v_0. Note also that r is the position of the triple line, so $\frac{\partial r}{\partial t}$ is actually the velocity. The integral can then be approximated as:

$$\int_0^\tau v_0 t v_0^2 dt = \frac{\rho R^3 v_{imp}^2}{\eta} \frac{\theta}{9l} \tag{31}$$

This integral can be solved easily to obtain:

$$\frac{1}{2}v_0^3\tau^2 = \frac{\rho R^3 v_{imp}^2}{\eta} \frac{\theta}{9l} \;\Rightarrow \tag{32}$$

$$(v_0\tau)^2 = \frac{\rho R^3 v_{imp}^2}{\eta v_0} \frac{2\theta}{9l} \tag{33}$$

Remember from earlier that it was shown that $v_0\tau$ was equal to r_{spr} and the following is obtained:

$$\left(\frac{r_{spr}}{R}\right)^2 = \frac{\rho R v_{imp}}{\eta} \frac{2\theta}{9l} \frac{v_{imp}}{v_0} \;\Rightarrow \tag{34}$$

$$\frac{r_{spr}}{R} = \sqrt{\mathrm{Re}} \sqrt{\frac{2\theta}{9l} \frac{v_{imp}}{v_0}} \tag{35}$$

The proportionality between $\frac{r_{spr}}{R}$ and $\sqrt{\mathrm{Re}}$ reappears here. Note that the term with $\frac{\theta}{l}$ came from an expression of the region in which dissipation occurs, so it is not unlikely that

it could be replaced by a term that includes $\frac{1}{(1-\beta^3)} = \frac{v_{drop}}{v_s}$ but I was unable to determine what this might be in this work. It is very likely that there is a correlation between v_{imp} and v_0 as they are defined here, so that term can be part of a proportionality term - remember that this is an order of magnitude analysis.
Because of this finding it seems very likely that the important phenomenon in the determination of how much contact is established between a droplet and the wall is the dissipation of kinetic energy occurring in a part of the viscous liquid near the moving triple line. It is also of relevance to note, that even though this derivation contains the contact angle between liquid and solid, it is actually not because wetting as such is considered, but merely a way to express the zone in which dissipation was thought to occur. This is important because the interesting parts of the original model ([de Gennes et al., 2004]) remains, while the parts that are dissimilar to the case of a sticky droplet is in a part of the expression that does not fit with the result of the COMSOL simulation.

6 Non-Stickiness Criterion

In this sectio the findings covered in the previous sections will be used to propose a criterion for use in the design and possible operation of spray dryers. First a disclaimer; this model is not a deterministic stickiness model which may be used with just a few material parameters. It is suspected that such a model is far off, if not practically unobtainable. The suggested model will require a drying model of the type described in section 1.2 as characteristic drying curve models. The model used internally at GEA Process Engineering will be used here, but for confidentiality reasons a detailed description of how it works cannot be given. In this section skim milk powder will be used as the example, because of the amount of data available. It is the intention that the method requires very limited experimental work for a new product, but it should be obvious that the more time which can be spent measuring the product, the more accurate the criterion can be.
The criterion will be produced as a simple function, which determines a point during drying after which the particle becomes non-sticky if it hits a wall. This point will be parameter-specific and because drying conditions may vary inside the dryer, the drying time itself will not be the telling parameter. Instead the dry matter content (by percentage of mass) will be used. As will be shown, this gives fairly elegant results.
Imagine a new product is encountered, say because a potential customer wishes to purchase a dryer suitable for it. The first task to perform would be to obtain drying data for the product and fit a suitable model or drying curve. This topic will not be delve into any further, but a single curve will be shown for the drying of skim milk for a specific set of drying conditions and initial solid content. The model used at GEA Process Engineering can account for variations in temperature and relative humidity of the drying gas and in the initial solid content, but it should be obvious that large deviations from the expected values would lead to worse extrapolation of the curve. See figure 44 for an example of such a drying curve.
In this curve, the mass of the droplet is normalized with the initial mass m_0 which eases comparison between materials and droplets. The residual moisture is also defined in a manner that makes it easy to compare across materials and conditions. It is defined as the remaining mass of water divided by the remaining mass of the droplet:

$$RM = \frac{m_d - m_{d,0} \cdot DM_{init}}{m_d} \tag{36}$$

in which RM is the residual moisture, m_d the mass of the droplet and DM_{init} is the initial dry matter content of the droplet.

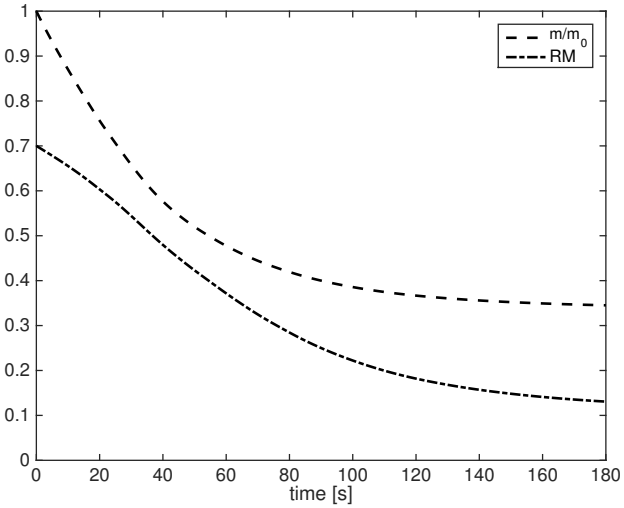

Figure 44: Example of drying curve for skim milk particle with a diameter of 1 mm with change of normalized mass and normalized residual moisture.

A suitably accurate and simple drying curve is established and it is time to turn to the stickiness measurements and their use. The measurement of points where a droplet becomes non-sticky will be carried out as described for a single data point in section 4. That is to say, the experimenter will dry some number of droplets until a sufficiently reliable critical drying time (for which the particle becomes non-sticky) is obtained for a realistic set of drying conditions. This will then be repeated for a different relative humidity but keeping the drying temperature constant. Depending on time availability and accuracy requirements, more data points can be produced, but because very little temperature dependency was found in section 4 and such simple dependence on relative humidity was found a decent fit may be obtained from as little as two stickiness points. As was shown in the results section a linear correlation between the stickiness point and the relative humidity existed, but when implemented with the drying curve shown previously the following is obtained (note that many datapoints are used, because they are available anyway) - see figure 45.

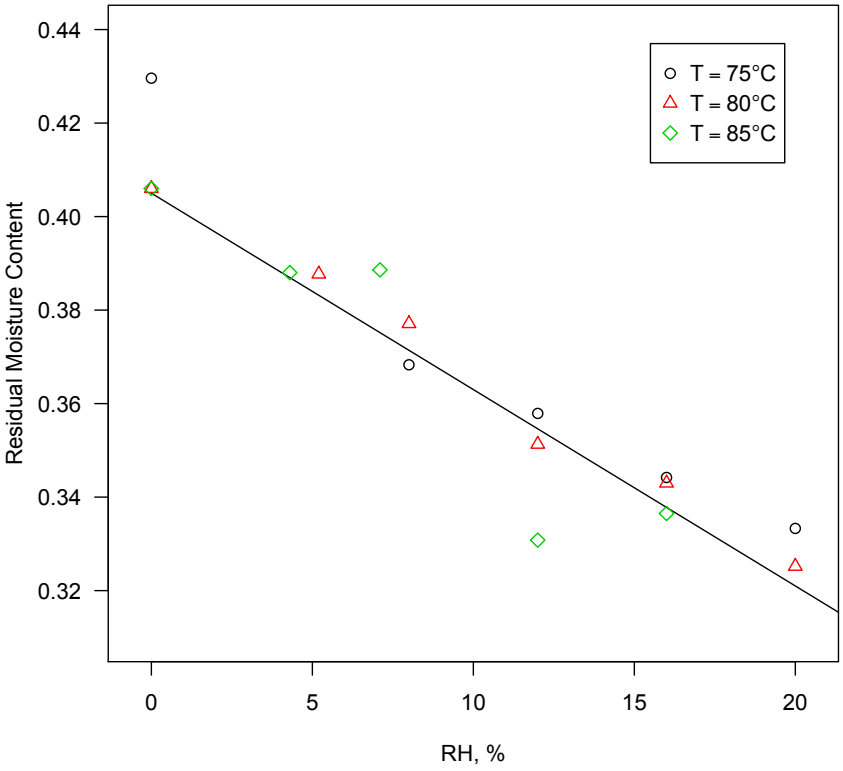

Figure 45: Normalized residual moisture content at the point where the particle becomes non-sticky as dependent on drying conditions.

As mentioned a very small dependence on temperature is observed, while the dependence on relative humidity is linear. This means a linear function can be fitted to the two first stickiness points. These two points would (obviously) be for the same velocity. A third stickiness point is then measured with the same temperature and relative humidity of the drying air as one of the data points used to obtain the humidity correlation. The velocity dependence turned out to be linear as well. This is also evident from figure 46.

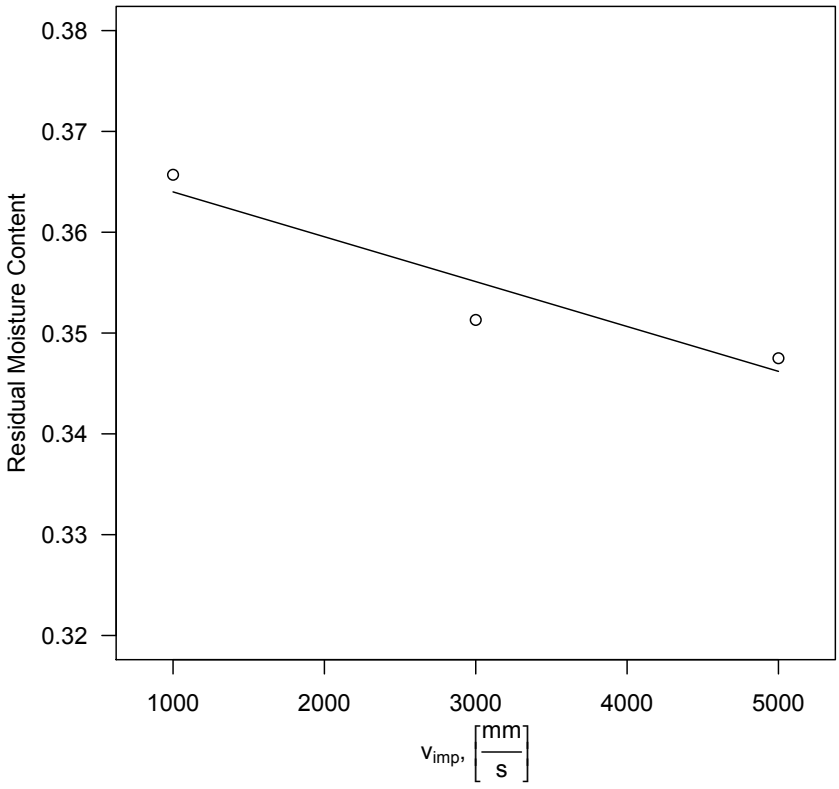

Figure 46: Normalized residual moisture content at the point where the particle becomes non-sticky as dependent on the velocity of impact.

As stated, the dependence is linear. This means that based on as little as three stickiness data points, a function can be obtained that relates the critical residual dry matter where a particle becomes non-sticky to impact velocity and relative humidity of the drying air. This however does not take into consideration the scaling of droplet size in the impact. There is a size dependence hidden in the drying curve (close to a d^2-law) but not in the impact phenomenon. This is where the impact modelling of section 5 comes in.
I have stated - and will discuss why below - that measuring and using material parameters seem inefficient and extraordinarily difficult. Section 5 resulted in a correlation between the Reynolds' number and the spreading. This obviously involves at least two material parameters, namely density and viscosity. Ignoring this for a moment however, it also showed that droplet radius and impact velocity only influenced the impact via the Reynolds' number which means when we know the stickiness dependence upon the impact velocity, we therefore also know the effect of the droplet radius in the impact itself. Therefore instead

of expressing critical dry matter content as a function of impact velocity, we may express it as a function of the product of the impact velocity and the droplet radius. Thus, we have what we need to scale the droplet size included in the non-stickiness function mentioned above.
All that is needed then, is to formalize that into a mathematical equation. Because of the linearities found, this is quite simple. An equation of the following form is proposed:

$$RM_{crit} = RM_{crit,ref} + a\,(RH - RH_{ref}) + b\,(v_{imp}R - v_{imp,ref}R_{ref}) \tag{37}$$

in which reference relative humidity, impact velocity and particle radius are chosen. $RM_{crit,ref}$ is the residual moisture at which a particle becomes non-sticky at the reference conditions and a and b are fitted to data such as that shown above. a is non-dimensional and b has the units of time. The example would look as follows for skim milk powder as measured here:

$$\begin{aligned} RM_{crit} = 3.55 \cdot 10^{-1} &- 4.24 \cdot 10^{-3}\,(RH - 12) \\ &- 8.90\ \mathrm{s}\left(v_{imp}R - 3.0\ \frac{\mathrm{m}}{\mathrm{s}} 5.0 \cdot 10^{-4}\ \mathrm{m}\right) \end{aligned} \tag{38}$$

Imagine then a droplet with a radius of 50 μm dried at a relative humidity of 14% and then hitting a wall at 0.4 $\frac{\mathrm{m}}{\mathrm{s}}$. This droplet would be expected to bounce from the wall if the residual moisture was below 0.360.
A quick comment on the fact that a linear relation between the critical residual moisture and the velocity and droplet radius. In section 5 it was shown that the spreading parameter correlates with the square root of the Reynolds' number. That said, it is unknown exactly how the material parameters change as the droplet dries. Furthermore it is unknown exactly how much spreading is required for a particle to adhere to a surface. Aside from the relative simplicity of this method, it is an advantage that these complex questions need not be answered in detail.
In summary the method is as follows:

- Measure drying kinetics using a SDD technique and fit a drying model to it.
- Measure the point where a droplet becomes non-sticky at one air temperature, but with two different impact velocities and two different relative humidities (three data points total).
- Fit the empirical equation 37 to the data points.

Note that expanding this simple empirical model to encompass temperature dependencies (or other effects), should those be found significant for a given product, is very easily done.

7 Conclusion

The present work covers both experimental and model-based investigation of the problem of stickiness in spray drying. It concludes with a proposed criterion of non-stickiness and a new hypothesis for what happens when a sticky particle hits a wall.

The experimental work consisted of drying a levitated droplet in conditions mimicking a spray dryer. The droplet was impacted with a piston after a specified drying time. Results for drying of skim milk and maltodextrin solutions were reported. It was found that the required time of drying for a particle depended more strongly on relative humidity than the temperature of the drying air, but also that both correlations were linear. Measurements with varying impact velocity showed that when this was increased, the droplet had to be dried longer and once more the correlation appeared linear. This last dependency is opposite of what is reported in literature suggesting the necessity to distinguish between humidifying dry particles and drying of wet droplets.

A high-speed camera was used to investigate the impact between a dried droplet and the piston in the setup described above. Observations with this were mostly qualitative because quantitative analysis was found to be practically impossible. It was found that particles just before and just after the critical point of becoming non-sticky looked quite similar and that very little deformation occurred. Observations showed that for sticky particles only very little apparent wetting occurred and this was independent of the piston surface material used. Furthermore it was seen that the phenomenon was quite similar no matter the impact velocity (although slightly more deformation occurred at the high range) and relative humidity.

Modelling work using multiple level set functions with a finite element method was presented. The model consisted of a droplet with a wet core and a highly viscous skin impacting a wall. It was shown that the conditions of the surrounding air was unimportant and that the material properties of the core was unimportant in almost all cases. A parameter analogous to the radius of the contact area was defined and shown to be proportional with the square root of the Reynolds' number (defined with the material properties of the skin) multiplied with the volume of the droplet and divided by the volume of the skin. A simple analytical model for the movement of a triple line showed that the correlation with the Reynolds' number could be obtained in the dissipation of the kinetic energy in the flow near such a triple line.

Finally the combined observations from experiments and modelling were used to suggest a simple criterion for when a particle can be considered non-sticky. A characteristic drying curve combined with as little as three stickiness data points could be used to produce an empirical function for the critical residual moisture a particle must be below before it is safe for it to impact a wall. This critical residual moisture was a function of the relative humidity of the drying air, the initial size of the droplet and the velocity of the impact with the wall.

The observations also suggests a hypothesis different from the one presented in literature in a few, important ways. A wet particle in the risk of being sticky is inhomogeneous, with the outer parts being more viscous than the core. The particle hits a wall with some kinetic energy and is forced into contact with it. As this happens it starts to deform in a process which dissipated the kinetic energy through viscous flow. The more it deforms, the more energy is dissipated and the larger the contact area becomes. The total deformation required to dissipate all the kinetic energy depends on the viscosity throughout the particle with the more viscous parts being more important. This also means that a large area with a large viscosity leads to very little deformation and therefore very little area of contact. As this deformation ends different forces can contribute to the particle falling off, e.g. drag from air flow or other particles, gravity or possibly small elastic effects. If the contact area established is small, then so is the adhesive energy and the forces listed above are more likely to dislodge the particle. If however the contact area is large enough for the particle to remain adhered it can be said to be sticky. The two most important differences between the current hypothesis in the literature and this one are that this one would lead to a difference between the stickiness of a humidified particle and a dried droplet, i.e. it takes more than the surface properties to assess stickiness, and the contact is forced rather than spontaneous.

7.1 Future Work

The experimental setup presented in this thesis has more variables to investigate than has been covered here. The most obvious would be to investigate how stickiness behaves for a wider range of products. An interesting alternative would be to produce a piston tip with an angled surface. This could be used to investigate how a non-perpendicular angle of approach changes the point of stickiness - this was discussed in the thesis, but no empirics produced.

It would also be interesting to further understand the composition of a droplet as it goes from wet, to sticky and finally to non-sticky. Consider a product with a given set of conditions for which the stickiness is known quite well - measured using the levitator/impactor setup. Then dry droplets to different degrees relative to the critical point and flash freeze them, locking the solvent and product components in their place. It is then possible that the particle could be cut open and the humidity profile determined. This would allow further investigation of the relation between the inhomogeneity of a droplet and its' stickiness properties.

Further work with a numerical model such as the one used here would be helpful if it could lead to a droplet which actually comes into contact with the wall. Given a good model for the triple line this would allow investigation of the importance of wetting and it would allow stronger comparison between the high-speed camera recordings and the simulations.

8 References

[Adhikari et al., 2001] Adhikari, B., Howes, T., Bhandari, B. R., and Truong, V. (2001). Stickiness in Foods: A Review of Mechanisms and Test Methods. *International Journal of Food Properties*, 4(1):1–33.

[Adhikari et al., 2005] Adhikari, B., Howes, T., Lecomte, D., and Bhandari, B. R. (2005). A Glass Transition Temperature Approach for the Prediction of the Surface Stickiness of a Drying Droplet During Spray Drying. *Powder Technology*, 149(2):168–179.

[Amelia et al., 2011] Amelia, R., Wu, W., Cashion, J., Bao, P., Zheng, R., Chen, X. D., and Selomulya, C. (2011). Microfluidic Spray Drying as a Versatile Assembly Route of Functional Particles. *Chemical Engineering Science*, 66(22):5531–5540.

[Angell, 2002] Angell, C. (2002). Liquid Fragility and the Glass Transition in Water and Aqueous Solutions. *Chemal Reviews*, 102(8):2627–2650.

[Annamalai et al., 1993] Annamalai, K., Ryan, W., and Chandra, S. (1993). Evaporation of Multicomponent Drop Arrays. *Journal of Heat Transfer*, 115(3):707–716.

[Bakshi and Smith, 1983] Bakshi, A. and Smith, D. (1983). Effect of Fat Content and Temperature on Viscosity in relation to Pumping Requirements of Fluid Milk Products. *Journal of Dairy Science*, 67(6):1157–1160.

[Balabel, 2012] Balabel, A. (2012). Numerical Simulation of Two-Dimensional Binary Droplets Collision Outcomes Using the Level Set Method. *International Journal of Computational Fluid Dynamics*, 26(1):1–21.

[Balmforth et al., 2010] Balmforth, N. J., Dubash, N., and Slim, A. C. (2010). Extensional Dynamics of Viscoplastic Filaments: II. Drips and Bridges. *Journal of Non-Newtionan Fluid Mechanics*, 165(19-20):1147–1160.

[Bertsch, 1983] Bertsch, A. (1983). Surface Tension of Whole and Skim Milk between 18 and 135 ^{o}C. *Journal of Dairy Research*, 50(3):259–267.

[Bird et al., 1987] Bird, R. B., Armstrong, R., and Hassager, O. (1987). *Dynamics of Polymeric Liquids. Vol. 1. Fluid Dynamics.* Wiley, second edition. ISBN: 978-0-471-80245-7.

[Bird et al., 2007] Bird, R. B., Stewart, W. E., and Lightfoot, E. N. (2007). *Transport Phenomena.* Wiley, second edition. ISBN: 978-0-470-11539-8.

[Boonyai et al., 2003] Boonyai, P., Bhandari, B., and Howes, T. (2003). Stickiness Measurement Techniques for Food Powders: A Review. *Powder Technology*, 145(1):34–46.

[Brask et al., 2007] Brask, A., Ullum, T., Thybo, P., and Andersen, S. J. (2007). High-temperature ultrasonic levitator for investigating drying kinetics of single droplets. In *6th Int. conf. on Multiphase Flow*.

[Brenn, 2005] Brenn, G. (2005). Concentration Fields in Evaporating Droplets. *Heat and Mass Transfer*, 2(48):395–402.

[Brennan et al., 1971] Brennan, J. G., Herrera, J., and Jowitt, R. (1971). A Study of some of the Factors Affecting the Spray Drying of Concentrated Orange Juice, on a Laboratory Scale. *Journal of Food Technology*, 6(3):295–307.

[Brenner and Scott, 2007] Brenner, S. and Scott, L. (2007). *The Mathematical Theory of Finite Element Methods*. Springer, third edition. ISBN: 9780387759333.

[Caviezel et al., 2008] Caviezel, D., Narayanan, C., and Lakehal, D. (2008). Adherence and Bouncing of Liquid Droplets Impacting on Dry Surfaces. *Microfluid Nanofluid*, 5(4):469–478.

[Chen and Hoseney, 1995] Chen, W. Z. and Hoseney, R. C. (1995). Development of an Objective Method for Dough Stickiness. *Food Science and Technology*, 28(5):467–473.

[Chen and Lin, 2005] Chen, X. D. and Lin, S. X. Q. (2005). Air Drying of Milk Droplet under Constant and Time-Dependent Conditions. *AIChE*, 51(6):1790–1799.

[Chuy and Labuza, 1994] Chuy, L. and Labuza, T. P. (1994). Caking and Stickiness of Dairy-Based Food Powders as Related to Glass-Transition. *Journal of Food Science*, 59(1):43–46.

[de Gennes, 1985] de Gennes, P. (1985). Wetting: Statics and Dynamics. *Reviews of Modern Physics*, 57(3):827–863.

[de Gennes et al., 2004] de Gennes, P., Brochard-Wyart, F., and Quéré, D. (2004). *Capillarity and Wetting Phenomena*. Springer.

[de Gennes, 2002] de Gennes, P. G. (2002). Solvent Evaporation of Spin Cast films: "Crust Effects". *Eur. Phys. J. E.*, 7(1):31–34.

[Deganello et al., 2011a] Deganello, D., Croft, T. N., Williams, A. J., Lubansky, A. S., Gethin, D. T., and Claypole, T. C. (2011a). Numerical Simulation of Dynamic Contact Angle Using a Force Based Formulation. *Journal of Non-Newtionan Fluid Mechanics*, 166(16):900–907.

[Deganello et al., 2011b] Deganello, D., Williams, A. J., Croft, T. N., Lubansky, A. S., Gethin, D. T., and Claypole, T. C. (2011b). Level-Set Method for Modelling of Liquid Bridge Formation and Break-Up. *Computers and Fluids*, 40(1):42–51.

[Desai, 2001] Desai, C. (2001). *Introductory Finite Element Method.* CRC Press. ISBN: 9780849302435.

[Downton et al., 1982] Downton, G. E., Flores-Luna, J. L., and King, C. J. (1982). Mechanism of Stickiness in Hygroscopic, Amorphous Powders. *Ind. Eng. Chem. Fundam.*, 21(4):447–451.

[Egholm, 2008] Egholm, R. D. (2008). *Emulsion Design; Analysis of Drop Deformations in Mixed Flows.* PhD thesis, Technical University of Denmark. ISBN: 978-87-91435-73-0.

[El-Sayed et al., 1990] El-Sayed, T. M., Wallack, D. A., and King, C. J. (1990). Changes in Particle Morphology during Drying of Drops of Carbohydrate Solutions and Food Liquids. 1. Effects of Composition and Drying Conditions. *Ind. Chem. Eng. Res.*, 29(12):2346–2354.

[EngineeringToolbox, 2015a] EngineeringToolbox (2015a). Website.
url: http://www.engineeringtoolbox.com/liquids-densities-d_743.html.

[EngineeringToolbox, 2015b] EngineeringToolbox (2015b). Website.
url: http://www.engineeringtoolbox.com/dry-air-properties-d_973.html.

[Foote, 1974] Foote, G. (1974). The Water Drop Rebound Problem: Dynamics of Collision. *Journal of Atmospheric Sciences*, 32(2):390–402.

[Foster et al., 2006] Foster, K. D., Bronlund, J. E., and Paterson, A. H. J. T. (2006). Glass Transition Related Cohesion of Amorphous Sugar Powders. *Journal of Food Engineering*, 77(4):997–1006.

[Fowkes, 1964] Fowkes, F. M. (1964). Attractive Forces at Interfaces. *Industrial and Engineering Chemistry*, 56(12):40–52.

[Frenkel, 1945] Frenkel, J. (1945). Viscous Flow of Crystalline Bodies under Action of Surface Tension. *Journal of Physics*, 9(5):385–391.

[Fu et al., 2012] Fu, N., Woo, M. W., and Chen, X. D. (2012). Single Droplet Drying Technique to Study Drying Kinetics Measurement and Particle Functionality: A Review. *Drying Technology*, 30(15):1771–1785.

[Gerlach et al., 2006] Gerlach, D., Tomar, G., Biswas, G., and Durst, F. (2006). Comparison of Volume-of-Fluid Methods for Surface Tension-Dominated Two-Phase Flows. *International Journal of Heat and Mass Transfer*, 49(3-4):740–759.

[Gianfrancesco et al., 2009] Gianfrancesco, A., Turchiuli, C., Dumoulin, E., and Palzer, S. (2009). Prediction of Powder Stickiness along Spray Drying Process in Relation to Agglomeration. *Particulate Science and Technology*, 27(5):415–427.

[Gordon and Taylor, 1952] Gordon, M. and Taylor, J. S. (1952). Ideal Copolymers and the Second-Order Transitions of Synthetic Rubbers. I. Non-Crystalline Copolymers. *Journal of Applied Chemistry*, 2(9):493–500.

[Goula et al., 2007] Goula, A. M., Karapantsios, T. D., and Adamopoulos, K. G. (2007). An Advanced Centrifugal Technique to Characterize the Sticking Properties of Tomato Pulp during Drying. *Drying Technology*, 25(4–6):599–607.

[Green, 1941] Green, H. (1941). What is Tack? *Paper Trade Journal*, 24(3):309–310.

[Groenewold et al., 2002] Groenewold, C., Möser, C., Groenewold, H., and Tsotsas, E. (2002). Determination of Single-Particle Drying Kinetics in an Acoustic Levitator. *Chemical Engineering Journal*, 86(1-2):217–222.

[Gunn and Kinzer, 1949] Gunn, R. and Kinzer, G. (1949). The Terminal Velocity of Fall for Water Droplets in Stagnant Air. *Journal of Meteorology*, 6(4):243–248.

[Hamawand, 2011] Hamawand, I. (2011). Effect of Colloidal Particles Associated with the Liquid Bridge in Sticking during Drying in Superheated Steam. *International Journal of Engineering, Transactions B: Applications*, 24(2):119–126.

[Hennigs et al., 2001] Hennigs, C., Kockel, T. K., and Langrish, T. A. G. (2001). New Measurements of the Sticky Behavior of Skim Milk Powder. *Drying Technology*, 19(3-4):471–484.

[Hirt and Nichols, 1981] Hirt, C. W. and Nichols, B. D. (1981). Volume of Fluid (VOF) Method for the Dynamics of Free Surfaces. *Journal of Computational Physics*, 39(1):201–225.

[Hogan et al., 2010] Hogan, S. A., Famelart, M. H., O'Callaghan, D. J., and Schuck, P. (2010). A Novel Technique for Determining Glass-Rubber Transition in Dairy Powders. *Journal of Food Engineering*, 99(1):76–82.

[Jenike, 1964] Jenike, A. W. (1964). Storage and Flow of Solids. Work Station Bulletin 123. University of Utah.

[Johnson, 2009] Johnson, C. (2009). *Numerical Solution of Partial Differential Equations by the Finite Element Method*. Dover Publications Incorporated. ISBN: 9780486469003.

[Jonassen, 1998] Jonassen, N. (1998). Human Body Capacitance; Static or Dynamic Concept. In *EOS/EOD Symposium*, pages 111–117.

[Kastner et al., 2001] Kastner, O., Brenn, G., Rensink, D., and Tropea, C. (2001). The Acoustic Tube Levitator - A Novel Device for Determining the Drying Kinetics of Single Droplets. *Chemical Engineering and Technology*, 24(4):335–339.

[Kemp et al., 2001] Kemp, I. C., Fyhr, B. C., Laurent, S., Roques, M. A., Groenewold, C. E., Tsotsas, E., Sereno, A. A., Bonazzi, C. B., Bimbenet, J. J., and Kind, M. (2001). Methods for Processing Experimental Drying Kinetics Data. *Drying Technology*, 19(1):15–34.

[Kentish et al., 2005] Kentish, S., Davidson, M., Hassan, H., and Bloore, C. (2005). Milk Skin Formation during Drying. *Chemical Engineering Science*, 60(3):635–646.

[Kilcast and Roberts, 1998] Kilcast, D. and Roberts, C. (1998). Perception and Measurement of Stickiness in Sugar-Rich Foods. *Journal of Texture Studies*, 29(1):81–100.

[King, 1934] King, L. V. (1934). On the Acoustic Radiation Pressure on Spheres. *Proceedings of the Royal Society of London*, 147A:212–240.

[Kinzer and Gunn, 1951] Kinzer, G. D. and Gunn, R. (1951). The Evaporation, Temperature and Thermal Relaxation-Time of Freely Falling Waterdrops. *Journal of Meteorology*, 8(2):71–83.

[Kudra, 2003] Kudra, T. (2003). Sticky Region in Drying - Definition and Identification. *Drying Technology*, 21(8):1457–1469.

[Kwapinski and Tsotsas, 2006] Kwapinski, W. and Tsotsas, E. (2006). Characterization of Particulate Materials in Respect to Drying. *Drying Technology*, 24(9):1083–1092.

[Langrish, 2007] Langrish, T. A. G. (2007). New Engineered Particles from Spray Dryers: Research Needs in Spray Drying. *Drying Technology*, 25(6):971–983.

[Langrish and Fletcher, 2003] Langrish, T. A. G. and Fletcher, D. F. (2003). Prospects for the Modelling and Design of Spray Dryers in the 21st Century. *Drying Technology*, 21(2):197–215.

[Langrish and Kockel, 2001] Langrish, T. A. G. and Kockel, T. K. (2001). The Assessment of a Characteristic Drying Curve for Milk Powder for Use in Computational Fluid Dynamics Modelling. *Chemical Engineering Journal*, 84(1):69–74.

[Law and Binark, 1979] Law, C. and Binark, M. (1979). Fuel Spray Vaporization in Humid Environment. *International Journal of Mass Transfer*, 22(7):1009–1020.

[Law et al., 1986] Law, C., Xiong, T., and Wang, C. (1986). Alcohol Droplet Vaporation in Humid Air. *International Journal of Mass Transfer*, 30(7):1435–1443.

[Lazar et al., 1956] Lazar, M. E., Brown, A. H., Smith, G. S., Wang, F. F., and Lindquist, F. E. (1956). Experimental Production of Tomato Powder by Spray Drying. *Food Technology*, 10(3):129–134.

[Leaper et al., 2012] Leaper, M. C., Prime, D. C., Taylor, P. M., and Leach, V. (2012). Solid Bridge Formation Between Spray-Dried Sodium Carbonate Particles. *Drying Technology*, 30(9):1008–1013.

[Leung et al., 1981] Leung, E., Jacobi, N., and Wang, T. (1981). Acoustic Radiation Force on a Rigid Sphere in a Resonance Chamber. *J. Acoust. Soc. Am.*, 70(6):1762–1767.

[Lierke, 2002] Lierke, E. G. (2002). Deformation and Displacement of Liquid Drops in an Optimized Acoustic Standing Wave Levitator. *Acta Acustica United with Acustica*, 88(2):206–217.

[Lin and Chen, 2002] Lin, S. X. Q. and Chen, X. D. (2002). Improving the Glass-Filament Method for Accurate Measurement of Drying Kinetics of Liquid Droplets. *Chemical Engineering Research and Design*, 80(4):401–410.

[Liu et al., 2011] Liu, W., Wu, W. D., Selomulya, C., and Chen, X. D. (2011). Facile Spray-Dryer Assembly of Uniform Microencapsulates with Tunable Core-Shell Structures and Controlled Release Properties. *Langmuir*, 27(21):12910–12915.

[Lockemann, 1999] Lockemann, C. A. (1999). A New Laboratory Method to Characterize the Sticking Properties of Free-Flowing Solids. *Chemical Engineering and Processing*, 38(4-6):301–306.

[Marsh et al., 1993] Marsh, J., Garoff, S., and Dussan V., E.B. (1993). Dynamic Contact Angles and Hydronomics Near a Moving Contact Line. *Physical Review Letters*, 70(18):2778–2781.

[Masters, 1996] Masters, K. (1996). Deposit-Free Spray Drying: Dream or Reality? In *96-Proceedings of the 10th International Drying Symposium (IDS'96)*, volume 1, pages 52–60.

[Masters, 2002] Masters, K. (2002). *Spray Drying in Practice*. SprayDryConsult International ApS. ISBN: 87-9866-068-3.

[Men et al., 2009] Men, Y., Zhang, X., and Wang, W. (2009). Capillary Liquid Bridges in Atomic Force Microscopy: Formation, Rupture and Hysteris. *The Journal of Chemical Physics*, 131(18):184702.

[Meng et al., 2014] Meng, F., Doi, M., and Ouyang, Z. (2014). Cavitation in Drying Droplets of Soft Matter Solutions. *Physial Review Letters*, 113(9):098301.

[Mezhericher et al., 2007] Mezhericher, M., Levy, A., and Borde, I. (2007). Theoretical Drying Model of Single Droplets Containing Insoluble or Dissolved Solids. *Drying Technology*, 25(6):1035–1042.

[Mezhericher et al., 2010] Mezhericher, M., Levy, A., and Borde, I. (2010). Theoretical Models of Single Droplet Drying Kinetics: A Review. *Drying Technology*, 28(2):278–293.

[Michalski et al., 1999] Michalski, M. C., Desobry, S., Babak, V., and Hardy, J. (1999). Adhesion of Food Emulsions to Packaging and Equipment Surfaces. *Colloids and Surfaces A: Physicochemical and Engineering Aspects*, 149(1):107–121.

[Michalski et al., 1997] Michalski, M. C., Desobry, S., and Hardy, J. (1997). Food Materials Adhesion: A Review. *Critical Reviews in Food Science and Nutrition*, 37(7):591–619.

[Mont, 1865] Mont, C. L. (1865). Improvements in Preserving Eggs. PAtent.

[Mu and Su, 2007] Mu, F. and Su, X. (2007). Analysis of Liquid Bridge between Spherical Particles. *China Particuology*, 5(6):420–424.

[Mukherjee et al., 2005] Mukherjee, N., Bansal, B., and Chen, X. (2005). Measurement of Surface Tension of Homogenized Milks. *International Journal of Food Engineering*, 1(2):1–6.

[Murti et al., 2010] Murti, R. A., Paterson, A. H. J. T., Pearce, D., and Bronlund, J. E. (2010). The Influence of Particle Velocity on the Stickiness of Milk Powder. *International Dairy Journal*, 20(2):121–127.

[Murti et al., 2009] Murti, R. A., Paterson, A. H. J. T., Pearce, D. L., and Bronlund, J. E. (2009). Stickiness of Skim Milk Powder Using the Particle Gun Technique. *International Dairy Journal*, 19(3):137–141.

[Nikolopoulos et al., 2009] Nikolopoulos, N., Theodorakakos, A., and Bergeles, G. (2009). Off-Centre Binary Collision of Droplets: A Numerical Investigation. *International Journal of Heat and Mass Transfer*, 52(19-20):4160–4174.

[Okuzono et al., 2006] Okuzono, T., Ozawa, K., and Doi, M. (2006). Simple Model of Skin Formation Caused by Solvent Evaporation in Polymer Solution. *Physical Review Letters*, 97(13):136103.

[Osher and Sethian, 1988] Osher, S. and Sethian, J. A. (1988). Fronts Propagating with Curvature-Dependent Speed: Algorithms Based on Hamilton-Jacobi Formulations. *Journal of Computational Physics*, 79(1):12–49.

[Ozawa et al., 2006] Ozawa, K., Okuzono, T., and Doi, M. (2006). Diffusion Process during Drying to Cause the Skin Formation in Polymer Solutions. *Japanese Journal of Applied Physics*, 45(11):8817–8822.

[Özkan et al., 2002] Özkan, N., Walisinghe, N., and Chen, X. D. (2002). Characterization of Stickiness and Cake Formation in Whole and Skim Milk Powders. *Journal of Food Engineering*, 55(4):293–303.

[Ozmen and Langrish, 2002] Ozmen, L. and Langrish, T. A. G. (2002). Comparison of Glass Transition Temperature and Sticky Point Temperature for Skim Milk Powder. *Drying Technology*, 20(6):1177–1192.

[Ozmen and Langrish, 2003] Ozmen, L. and Langrish, T. A. G. (2003). An Experimental Investigation of the Wall Deposition of Milk Powder in a Pilot-Scale Spray Dryer. *Drying Technology*, 21(7):1253–1272.

[Ozmen and Langrish, 2005] Ozmen, L. and Langrish, T. A. G. (2005). Experimental Investigation into the Wall Deposition of Milk Powder in Spray Dryers. *Developments in Chemical Engineering and Mineral Processing*, 13(1-2):91–108.

[Palzer, 2005] Palzer, S. (2005). The Effect of Glass Transition on the Desired and Undesired Agglomeration of Amorphous Food Powders. *Chemical Engineering Science*, 60(14):3959–3968.

[Papadakis and Bahu, 1992] Papadakis, S. E. and Bahu, R. E. (1992). The Sticky Issue of Drying. *Drying Technology*, 10(4):817–837.

[Patel and Chen, 2005] Patel, K. C. and Chen, X. D. (2005). Prediction of Spray-Dried Product Quality Using Two Simple Drying Kinetics Models. *Journal of Food Process Engineering*, 28(6):567–594.

[Paterson et al., 2007] Paterson, A. H. J., Bronlund, J. E., Zuo, J. Y., and Chatterjee, R. (2007). Analysis of Particle-Gun-Derived Dairy Powder Stickiness Curves. *International Dairy Journal*, 17(7):860–865.

[Paterson et al., 2005] Paterson, A. H. J., Brooks, G. F., Bronlund, J. E., and Foster, K. D. (2005). Development of Stickiness in Amorphous Lactose at Constant $T - T_g$ Levels. *International Dairy Journal*, 15(5):513–519.

[Paterson et al., 2001] Paterson, A. H. J. T., Bronlund, J. E., and Brooks, G. F. (2001). The Blow Test for Measuring the Stickiness of Powders. In *Seventh Conference of Food Engineering*, Reno, Nevada, USA.

[Peleg, 1977] Peleg, M. (1977). Flowability of Food Powders and Methods for Its Evaluation - A Review. *Journal of Food Process Engineering*, 1(4):303–328.

[Percy, 1872] Percy, S. (1872). Improvements in Drying and Concentrating Liquid Substances by Atomizing. Patent.

[Peschl, 1989] Peschl, I. A. S. Z. (1989). Quality Control of Powders for Industrial Application. *Powder Handling and Processing*, 1(4):357–364.

[Rabinovich et al., 2005] Rabinovich, Y. I., Esayanur, M. S., and Moudgil, B. M. (2005). Capillary Forces Between Two Spheres with a Fixed Volume Liquid Bridge: Theory and Experiment. *Langmuir*, 21(24):10992–10997.

[Ranz and Marshall, 1952a] Ranz, W. E. and Marshall, W. R. J. (1952a). Evaporation of Drops, Part 1. *Chemical Engineering Progress*, 48(3):141–146.

[Ranz and Marshall, 1952b] Ranz, W. E. and Marshall, W. R. J. (1952b). Evaporation of Drops, Part 2. *Chemical Engineering Progress*, 48(3):173–178.

[Renksizbulut and Bussmann, 1993] Renksizbulut, M. and Bussmann, M. (1993). Multicomponent Droplet Evaporation at Intermediate Reynolds Numbers. *International Journal of Heat and Mass Transfer*, 36(11):2827–2835.

[Rennie et al., 1999] Rennie, P. R., Chen, X. D., Hargreaves, C., and Mackereth, A. R. (1999). A Study of the Cohesion of Dairy Powders. *Journal of Food Engineering*, 39(3):277–284.

[Roos and Karel, 1991] Roos, Y. and Karel, M. (1991). Plasticizing Effect of Water on Thermal Behavior of Crystallization of Amorphous Food Models. *Journal of Food Science*, 56(1):38–43.

[Rumpf et al., 1976] Rumpf, H., Sommer, K., and Steier, K. (1976). Mechanismen der Haftkraftverstärkung bei der Partikelhaftung durch Plastiches Verformen, Sintern und Viskoelastisches Fließen. *Chem. Ing. Tech.*, 48(4):300–307.

[Sano and Keey, 1982] Sano, Y. and Keey, R. B. (1982). The Drying of a Spherical Particle Containing Colloidal Material into a Hollow Sphere. *Chemical Engineering Science*, 37(6):881–889.

[Saunders et al., 1992] Saunders, S. R., Hamann, D. D., and Lineback, D. R. (1992). A Systems Approach to Food Material Adhesion. *Food Science and Technology*, 25(4):309–315.

[Schubert, 1987] Schubert, H. (1987). Food Particle Technology. Part 1: Properties of Particles and Particle Food Systems. *Journal of Food Engineering*, 6(1):1–32.

[Sharma et al., 2012] Sharma, A., Jana, A., and Chavan, R. (2012). Functionality of Milk Powders and Milk-Based Powders for End Use Applications - A Review. *Comprehensive Reviews in Food Science and Food Safety*, 11(6):518–528.

[Shepel and Smith, 2008] Shepel, S. V. and Smith, B. K. (2008). On Surface Tension Modelling Using the Level Set Method. *International Journal for Numerical Methods in Fluids*, 59(2):147–171.

[Shimokawa et al., 2011] Shimokawa, Y., Kajiya, T., Sakai, K., and Doi, M. (2011). Measurement of the Skin Layer in the Drying Process of a Polymer Solution. *Physical Review E*, 84(5):051803.

[Sloth et al., 2006] Sloth, J., Kiil, S., Jensen, A. D., Andersen, S. K., and Jørgensen, K. (2006). Model Based Analysis of the Drying of a Single Droplet in an Ultrasonic Levitator. *Chemical Engineering Science*, 61(8):2701–2709.

[Sperling, 1986] Sperling, L. (1986). *Introduction to Physical Polymer Science*. Wiley. ISBN: 9780471890928.

[Sprittles and Shikhmurzaev, 2012] Sprittles, J. and Shikhmurzaev, Y. (2012). The Dynamics of Liquid Drops and their Interaction with Solids of Varying Wettabilities. *Physics of Fluids*, 24(8):082001.

[Strongin and Borde, 1987] Strongin, V. and Borde, I. (1987). *A Mathematical Model of Convective Drying Incorporating Sorption Isotherms*, volume 4, chapter 5, pages 249–278. CRC Press.

[Sussman et al., 1994] Sussman, M., Smereka, P., and Osher, S. (1994). A Level Set Approach for Computing Solutions to Incompressible Two-Phase Flow. *Journal of Computational Physics*, 114(1):146–159.

[Tsotsas, 2012] Tsotsas, E. (2012). Influence of Drying Kinetics on Particle Formation: A Personal Perspective. *Drying Technology*, 30(11-12):1167–1175.

[Turchiuli et al., 2011] Turchiuli, C., Gianfrancesco, A., Palzer, S., and Dumoulin, E. (2011). Evolution of Particle Properties During Spray Drying in Relation with Stickiness and Agglomeration Control. *Powder Technology*, 208(2):433–440.

[Vehring et al., 2007] Vehring, R., Foss, W. R., and Lechuga-Ballesteros, D. (2007). Particle Formation in Spray Drying. *Journal of Aerosol Science*, 38(7):728–746.

[Wallack and King, 1988] Wallack, D. A. and King, C. J. (1988). Sticking and Agglomeration of Hygroscopic, Amorphous Carbohydrate and Food Powders. *Biotechnology Progress*, 4(1):31–35.

[Walton and Mumford, 1999] Walton, D. E. and Mumford, C. J. (1999). Spray Dried Products - Characterization of Particle Morphology. *Chemical Engineering Research and Design*, 77(1):21–38.

[Wang et al., 2008] Wang, Z., Yang, J., and Stern, F. (2008). Comparison of Particle Level Set and CLSVOF Methods for Interfacial Flows. *AIAA Aerospace Sciences Meeting and Exhibit*, pages 2008–530.

[Werner et al., 2006] Werner, S. R. L., Fanshawe, R. L., Paterson, A. H. J. T., and Jones, J. R. (2006). Stickiness of Corn Syrup Powders by Fluidised Bed Test. *International Journal of Food Engineering*, 2(5). Article 7.

[Williams et al., 1955] Williams, M. L., Landel, R. F., and Ferry, J. D. (1955). The Temperature Dependence of Relaxation Mechanisms in Amorphous Polymers and other Glass-Forming Liquids. *Journal of the American Chemical Society*, 77(14):3701–3707.

[Woo et al., 2008a] Woo, M. W., Daud, W. R. W., Tasirin, S. M., and Talib, M. Z. M. (2008a). Amorphous Particle Deposition and Product Quality under Different Conditions in a Dryer. *Particuology*, 6(4):265–270.

[Woo et al., 2008b] Woo, M. W., Daud, W. R. W., Tasirin, S. M., and Talib, M. Z. M. (2008b). Effect of Wall Surface Properties at Different Drying Kinetics on the Deposition Problem in Spray Drying. *Drying Technology*, 26(1):15–26.

[Woo et al., 2011] Woo, M. W., Fu, N., Che, L., and Chen, X. D. (2011). Evaporation of Pure Droplets in the Convective Regime Under High Mass Flux. *Drying Technology*, 29(14):1771–1785.

[Wu et al., 2011] Wu, W. D., Amelia, R., Hao, N., Selomulya, C., Zhao, D., Chiu, Y. L., and Chen, X. D. (2011). Assembly of Uniform Photoluminescent Microcomposites Using a Novel Micro-Fluidic-Jet-Spray-Dryer. *AIChE Journal*, 57(10):2726–2737.

[Xu et al., 2006] Xu, J., Li, Z., Lowengrub, J., and Zhao, H. (2006). A Level-Set Method for Interfacial Flows with Surfactant. *Journal of Computational Physics*, 212(2):590–616.

[Yarin, 2006] Yarin, A. (2006). Drop Impact Dynamics: Splashing, Spreading, Receding and Bouncing... *Annual Review of Fluid Mechanics*, 38(1):159–192.

[Yarin et al., 2002] Yarin, A. L., Brenn, G., Kastner, O., and Tropea, C. (2002). Drying of Acoustically Levitated Droplets of Liquid-Solid Suspensions: Evaporation and Crust Formation. *Physics of Fluids*, 14(7):2289–2298.

[Yildirim and Basaran, 2001] Yildirim, O. E. and Basaran, O. A. (2001). Deformation and Breakup of Stretching Bridges of Newtonian and Shear-Thinning Liquids: Comparison of One- and Two-Dimensional Models. *Chemical Engineering Science*, 56(1):211–233.

[Zhao et al., 1996] Zhao, H. K., Chan, T., Merriman, B., and Osher, S. (1996). A Variational Level Set Approach to Multiphase Motion. *Journal of Computational Physics*, 127(1):179–196.

[Zuo et al., 2007] Zuo, J. Y., Paterson, A. H., Bronlund, J. E., and Chatterjee, R. (2007). Using a Particle-Gun to Measure Initiation of Stickiness of Dairy Powders. *International Dairy Journal*, 17(3):268–273.

The Danish Polymer Centre
Department of Chemical and Biochemical Engineering
Technical University of Denmark
Søltofts Plads, Building 227
DK – 2800 Kgs. Lyngby
Denmark

Phone: +45 45 25 68 01
Web: kt.dtu.dk/english/Research/DPC